CHAPTER 1: INTRODUCTION

Epstein-Barr virus (EBV) persistently infects more than 90% of the human population. Epstein-Barr virus had been intensively studied over the past years due to its association with a number of malignancies of lymphoid and epithelial origins. EBV is linked to lymphoid malignancies namely classical Hodgkin's disease, non-Hodgkin lymphomas, B-cell lymphomas and nasal NK/T-cell lymphomas (Middeldorp et al., 2003; Saha and Robertson, 2011). EBV is also associated with epithelial malignancies ie. nasopharyngeal carcinoma (NPC) (Chang and Adami, 2006) and EBV-linked gastric carcinoma (GC) (Takada, 2000).

Epstein-Barr virus (EBV) encodes the oncogene LMP1 (Latent Membrane Protein-1) and a candidate oncogene BARF1 (BamH1-A Rightward Frame-1). LMP1 and BARF1 play important roles in cellular gene expression and is thought to be involved in EBV-mediated tumorigenesis (Wei and Ooka, 1989; Wei et al., 1997). Interestingly, BARF1 was expressed in the absence of LMP1 or lytic proteins in primary primate kidney epithelial cells immortalized by EBV infection (Danve et al., 2001).

BARF1 expression had been detected in malignant epithelial cells and B cells. BARF1 expression was demonstrated in B-lymphoma frequent in Malawi (Xue et al., 2002) and in nasal NK/T-cell lymphoma (Zhang et al., 2006). BARF1 was also expressed at high levels consistently in nasopharyngeal carcinoma (NPC) (Decaussin et al., 2000; Seto et al., 2005), in EBV-associated gastric carcinoma (GC) (Zur Hausen et al., 2000) and in EBV-immortalized epithelial cells (Danve et al., 2001).

Several studies have delineated the involvement of BARF1 in oncogenic mechanism. BARF1 had been shown to induce malignant transformation in established rodent fibroblasts (Wei and Ooka, 1989), primary primate epithelial cells (Wei et al., 1997) and in human EBV-negative B cells (Sheng et al., 2001). Furthermore, purified BARF1 from serum showed a powerful mitogenic activity (Houali et al., 2007). BARF1 was also recognized by NK cells in ADCC (Antibody-dependent cellular cytotoxity) test (Tanner et al., 1997). Hence, BARF1 is not only involved in oncogenic mechanism but also in immunomodulation.

The introduction of recombinant EBV carrying the BARF1 gene into EBV-negative cell lines did not alter the expression level of Bcl-2 but induces NPC cell tumorigenicity in nude mice (Seto et al., 2008). Introduction of BARF1 into primary primate kidney epithelial PATAS cells led to morphological changes as well as continuous cell growth (Wei et al., 1997). BARF1 together with H-Ras was reported to be able to transform human epithelial cells (Jiang et al., 2009).

BARF1 has been shown to activate the anti-apoptotic protein Bcl-2 in rodent fibroblasts (Sheng et al., 2001) and in EBV negative human Akata B cells transfected by BARF1 (Sheng et al., 2003), suggesting an anti-apoptotic role of BARF1. Furthermore, BARF1 expression in gastric cancer cells protected the cells from apoptosis (Wang et al., 2006).

Collectively, these findings indicate that besides promoting cell proliferation, BARF1 may function as a survival factor by suppressing apoptosis pathway. However, the exact mechanism of how the anti-apoptotic effect of BARF1 is mediated is not well documented and remains to be clarified. Modulation of the apoptotic machinery in

malignancies is a well established mechanism that promotes the survival of cancer cells. Understanding the involvement of anti-apoptotic genes in cancer cell survival by unravelling the molecular mechanisms by which these genes elicit their effect is pertinent to understand the pathological mechanisms that lead to cancer (Busca et al., 2009).

Hence, this study aimed to investigate the molecular mechanisms by which BARF1 employs in its anti-apoptotic function. I aimed to silence the expression of BARF1 in EBV-positive malignant cells using siRNAs targeting BARF1 mRNA. I hypothesized that BARF1 depletion will induce apoptosis in malignant cell lines associated with EBV.

The specific aims of the current study are as follows:

1. To construct effective siRNA to knockdown BARF1 expression at mRNA and protein levels.
2. To study impacts of BARF1 knockdown on cell proliferation and apoptosis in Epstein-Barr virus-positive malignant cells.
3. To investigate the molecular mechanisms involved in the regulation of apoptosis in BARF1-silenced cells.

CHAPTER 2: LITERATURE REVIEW

2.1. History of Epstein-Barr virus (EBV)

Denis Burkitt described a common cancer primarily affecting the jaws of children in specific regions of Africa (Burkitt, 1958). Burkitt believed a virus might be responsible for the cancer, supported by the climatic and geographic distribution of the cases (Burkitt, 1972). EBV was first identified in 1964 when Anthony Epstein's group identified virus-like particles by electron microscopy in a cell line that had been established from a Burkitt's lymphoma biopsy (Epstein et al., 1964). Later, it was found that sera from patients with the lymphoma that Burkitt had described had much higher antibody titres to EBV than the controls without the lymphoma (Epstein et al., 1965). The subsequent detection of EBV DNA in Burkitt's lymphoma and the experimental production of lymphomas in cotton-top marmosets and owl monkeys established EBV as the first virus clearly implicated in the development of a human tumour (Robertson, 2005).

2.2. Types of EBV

Two subtypes of EBV are known to infect humans: EBV-1 and EBV-2. EBV-1 and EBV-2 differ in the organization of the genes that code for the EBV nuclear antigen (EBNA-2, EBNA-3a, EBNA-3b, and EBNA-3c) (Sample et al., 1990). EBV-2 transforms B cells less efficiently than EBV-1 *in vitro*, and the viability of EBV-2 lymphoblastoid cell lines is less than that of EBV-1 lines (Rickinson et al., 1987).

2.3. Molecular biology of EBV

EBV is a herpesvirus with a 184-kbp long, double-stranded DNA genome that encodes >85 genes (Kieff and Rickinson, 2001). The viral genome consists of a series of 0.5-kb terminal direct repeats at either end and internal repeat sequences that serve to divide the genome into short and long unique sequence domains that have most of the coding capacity. EBV, as with other herpesviruses, has a toroid-shaped protein core wrapped with double-stranded DNA, a nucleocapsid with 162 capsomeres, a protein tegument between the nucleocapsid and envelope, and an outer envelope with external glycoprotein spikes (Kieff and Rickinson, 2001).

2.4. Epstein-Barr virus infection

EBV infection is ubiquitous as over 90% of the population worldwide is infected. Primary EBV infection usually occurs in childhood and is asymptomatic. A clinical syndrome of infectious mononucleosis (IM) may be manifested if the primary infection occurs in adolescence or adulthood, which is a benign lymphoproliferative disorder characterized by an extrafollicular expansion of EBV-infected B lymphoblasts (Young and Rickinson, 2004).

When EBV infects a cell, the DNA becomes a circular episome with a characteristic number of terminal repeats, depending on the number of terminal repeats in the parental genome, with variation introduced during viral replication (Baumforth et al., 1999). If the infection is permissive for latent infection but not replication, future generations will have EBV episomes with the same number of terminal repeats.

Twelve viral genes can be expressed in different combinations during latent viral infection (Figure 2.1), while the remaining 70 major open reading frames are expressed during the replicative, lytic cycle. During latency, EBV genes are expressed in four programs, denoted latency 0, I, II and III. In latency III all 12 latency genes are expressed, including six nuclear proteins, Epstein-Barr nuclear antigen (EBNA)-1-6, three membrane proteins latent membrane proteins (LMP1, LMP2A and LMP2B), BamHI-A rightward transcripts (BARTs) and two small non-translated RNAs (EBER 1 & 2). In latency II, the viral genes for EBNA1, the three membrane proteins and the EBERs are expressed while in latency state 0/I, only LMP2A and variably EBNA-1 are expressed (Amon and Farrell, 2005).

Primary infection is thought to occur in the oropharynx, possibly the epithelial cells, and induces a lytic replication. The virus infects B lymphocytes by binding the CD21 receptor (also known as the C3d or CR2 receptor) on the B cell surface with the viral envelope glycoprotein gp 350. The penetration also requires a complex of three glycoproteins; gH, gL and gp42, in which the binding of gp42 to human leukocyte antigen (HLA) class II molecules functions as a co-receptor (Young and Rickinson, 2004). gH is thought to be critical for cell fusion.

Although many of these virus-infected B cells are removed by the specific primary T cell response, a stable reservoir of memory B cells is thought to harbour EBV genome, in which viral latent gene expression is mostly suppressed. During the latent infection of these memory B cells, EBV replicates once every cell division during S phase as a circular episome (Yates and Guan, 1991).

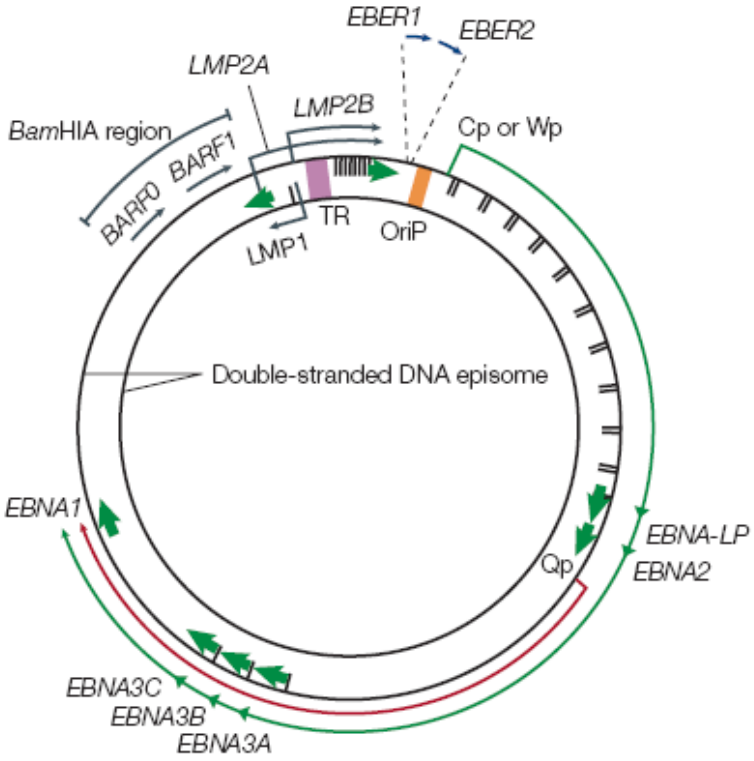

Figure 2.1. The EBV genome. The location and transcription of the EBV latent genes on the double-stranded circular viral DNA episome are shown. The arrows in different colours represent the latent genes and their transcriptional directions.

Latent genes: Nine latent genes include the six EBV-encoded nuclear antigens (*EBNAs 1, 2, 3A, 3B, 3C and EBNA-LP*) and the three latent membrane proteins (*LMPs 1, 2A and 2B*).

EBERs: The transcriptions of non-polyadenylated EBV-encoded RNAs (EBERs) are shown.

BARF1: The exons encoding BARF0 and BARF1 are within BamHI-A region.

TR: The terminal repeat (TR) region formed during the circularization of the linear DNA to become the episome is shown in purple.

*ori*P: The origin of plasmid replication (*ori*P) of EBV genome is shown in orange.

Cp or Wp promoter: The outer green arrow represents transcription of all the EBNAs under the control of either the Cp or Wp promoter during latency III.

Qp promoter: The inner red arrow represents the EBNA1 transcript which is under the control of Qp promoter during latency I and latency II.

EBV binding to CD21 immediately activates tyrosine kinase *lck* and mobilizes calcium. This is followed by an increase in mRNA synthesis, blast transformation, homotypic cell adhesion, surface CD23 expression (a characteristic surface marker for activated B cells), and interleukin (IL)-6 production (Alfieri et al., 1991). The viral genome is then uncoated and delivered to the nucleus where it immediately circularizes. Circularization and W promoter expression launch an ordered cascade of events that leads to the expression of all the EBNA proteins and the two latent membrane proteins (LMPs) (Allday et al., 1989).

The EBV nuclear antigen leader protein (EBNA-LP) and EBNA-2 proteins are the first proteins to be detected upon EBV infection (Hennessy and Kieff, 1985). At 24-48 h after infection, a promoter shift occurs where the C promoter (Cp) is used in favour of the initial promoter W promoter. Initially, it was hypothesized that the switch from the Wp to the Cp promoter coincided with the switch to an expanded pattern of splicing that allows expression of EBNA-3A, EBNA-3B, EBNA-3C, and EBNA-1 (Schlager et al., 1996). It is now known that the expanded pattern of splicing likely precedes the promoter switch.

This is consistent with the data that suggests that the downstream EBNAs regulate promoter Cp activation (Radkov et al., 1997). All of the EBNA transcriptional products are involved in transcriptional control and participate in the activation of the expression of the viral LMP-encoding genes (LMP1 and LMP2) and several cellular genes. The combined action of these viral and cellular proteins serves to initiate cellular S-phase 24-48 h after infection (Rowe, 1999).

After the initial infection, EBV persists in a circulating subset of resting memory B cells in healthy individuals at a frequency of ~1 in 1 x 10^5 to 1 x 10^6 cells. The viral genome is generally episomal and present in low numbers in the host cell's nucleus. Immunosuppressive states permit spontaneous replication of the episomal virus in circulating B cells, as observed in acute infectious mononucleosis (Rowe, 1999).

Immunocompetent carriers control latent EBV infection via cytotoxic T lymphocytes (CTLs). Loss of the EBV-specific CTL may permit the development of lymphoma. Besides its well known tropism for B cells, the targets of EBV infection may also include epithelial cells, T cells, and cells of the macrocytic, granulocytic, and natural killer lineages. These cells may be infected by mechanisms different from the CD21-mediated internalization typical in B cells (Rowe, 1999).

Persistent infection of epithelial cells in nasopharynx is substantially different from B cells, and the mechanisms are still unclear. The virus-positive B cells might be able to activate different latency programmes and undergo the viral lytic cycle in the mucosal sites in the oropharynx (Young and Rickinson, 2004). It is believed that genetic alterations in the epithelial cells confer susceptibility to the EBV infection because EBV genome could not be detected in normal nasopharyngeal epithelial cells (Lo et al., 2004). How persistent and latent infection of nasopharyngeal epithelial cells occurs is a critical aspect for the understanding of carcinogenesis of NPC.

As found in undifferentiated NPC tumours, every NPC cell carries circular and extrachromosomal episomes of EBV genome (Figure 2.1) which is estimated to be 1-30 copies per cell (Spano et al., 2003). The circularization of 172 kb-long EBV episome is formed by joining its terminal repeats regions located at either end of the linear double stranded DNA.

Since cells infected by different EBV particles have different number of terminal repeats in the EBV episomes, the analysis of structure of termini of EBV show that the EBV episomes within an NPC tumour are homogenous and monoclonal (Pathmanathan et al., 1995). This evidence suggests that viral infection may have taken place before the malignant clonal expansion of a single EBV-infected cell.

2.5. EBV genes

2.5.1. Epstein-Barr virus nuclear antigen 1 (EBNA1)

EBNA1 is essential for transformation of B cells by EBV and is expressed during latent and lytic infection. EBNA1 is important in maintaining the replication of the EBV episome in latent infection and is expressed in all types of EBV latency (Kieff and Rickinson, 2001). EBNA1 may also play a role in tumorigenesis. The protein is present in all EBV-associated tumors. EBNA1 is inadequately processed for MHC class I recognition and may play a role in escaping from immune surveillance in infected hosts (Niedobitek and Young, 1994).

2.5.2. Epstein-Barr virus nuclear antigen 2 (EBNA2)

EBNA2 is a transcriptional coactivator that coordinates viral gene expression in latency III and also transactivates many cellular genes. EBNA2 plays a critical role in cell immortalization (Wensing and Farrell, 2000). EBNA2 (and Epstein-Barr virus nuclear antigen leader protein, EBNA-LP) are the first latent proteins detected after EBV infection. There are two distinct types of EBNA2 that are identified serologically, and these two types correspond to EBV-1 and EBV-2 (Rowe and Clarke, 1989).

EBNA2 primarily serves to up-regulate the expression of viral and cellular genes. Among these are CD23 (a surface marker of activated B-cells), *c-myc* (a cellular proto-oncogene), and viral EBNA-C promoter (Weiss and Movahed, 1989). This up-regulation is achieved not by binding DNA directly but by binding other transcription factors (most notably, the viral Cp binding factor 1), consequently bringing the strong transcription domain of EBNA-2 close to the C promoter (Henkel et al., 1994). EBNA-2 is also known to interact with other transcription factors involved in the *Notch* signaling pathway. This pathway is important in cell fate determination in the fruit fly and may play a role in development of T-cell lymphoma in humans. It is likely that many other factors are yet to be discovered that interact with EBNA-2 and aid in transactivating both cellular and viral gene expression (Henkel et al., 1994).

2.5.3. Epstein-Barr virus nuclear antigen 3A, 3B, 3C (EBNA3A, EBNA3B, EBNA3C)

EBNA-3A, EBNA-3B, and EBNA-3C are transcriptional regulators. EBNA-3A and EBNA-3C are crucial for *in vitro* B-cell transformation, whereas EBNA-3B is dispensible (Murray and Young, 2002). EBNA-3 family members are encoded by three genes that are adjacent on the viral genome. Conserved sequences are confined to the NH_2-terminal third of the molecules (Rowe, 1999). Divergence in EBNA-3A, EBNA-3B, and EBNA-3C between the two subtypes of EBV (EBV-1 and EBV-2) is apparent, given that the primary sequences of these genes are only 84, 80, and 72% homologous, respectively (Karlin et al., 1990).

EBNA-3A and EBNA-3C have been shown to both be essential in immortalization. EBNA-3C may overcome the retinoblastoma tumor suppressor gene checkpoint in the G_1 phase of the cell cycle (Parker et al., 1996). EBNA-3C has also been shown to increase the production of LMP-1 in some conditions (Allday and Farrell, 1994). All three EBNA-3s interact with Cp binding factor 1. Cp binding factor 1 is involved in the notch signaling pathway and overexpression of the notch protein has been observed in human T-cell malignancies (Joutel and Tournier-Lasserve, 1998). How each individual EBNA3 proteins regulate Cp binding factor 1-mediated gene expression is not clear.

2.5.4. Epstein-Barr virus nuclear antigen leader protein (EBNA-LP)

EBNA-LP, also known as EBNA-5, is one of the first viral proteins produced during EBV infection of B cells (Wensing and Farrell, 2000). EBNA-LP interacts with EBNA-2 to drive resting B lymphocytes into the G_1 phase of the cell cycle (Sinclair et al., 1994) by binding and inactivating cellular p53 and retinoblastoma protein tumor suppressor gene products (Szekely et al., 1993). It has also been shown that EBNA-LP interacts with other transcription factors involved in the Notch signaling pathway (Henkel et al., 1994). However, more remains to be understood on the function of EBNA-LP in transformation and during the viral life cycle.

2.5.5. Epstein-Barr virus-encoded RNAs (EBERs)

EBERs 1 and 2 are nonpolyadenylated, uncapped, noncoding RNAs of 167 and 172 nucleotides, respectively (Rowe, 1999). They are expressed abundantly in nearly all EBV-infected cells and are expressed in all forms of latency (Murray and Young, 2002). EBERs have been implicated in the induction of autocrine growth factors and in maintaining the malignant phenotype of Burkitt's lymphoma cells, all of which supports a potential role for these RNAs in oncogenesis (Takada and Nanbo, 2001).

Transfection of the EBER genes into the EBV-negative Akata cell line restored the oncogenic potential that was originally present in the EBV-positive Akata cells but was lost in the EBV-negative subclones (Komano et al., 1999). Even so, recombinant EBV with EBER genes deleted can transform lymphocytes, suggesting that EBERs are nonessential

for transformation (Swaminathan et al., 1991). Therefore, the role of EBER in transformation is still unclear.

2.5.6. BamHI-H fragment rightward reading frame 1 (BHRF1)

BHRF1 is an immediate early gene expressed abundantly during EBV lytic replication (Dawson et al., 1995). BHRF1 shows partial (25%) sequence homology to the human BCL-2 proto-oncogene, and both have been shown to protect human B lymphocytes from apoptosis (Henderson et al., 1993). BHRF1 products can also interfere with epithelial cellular differentiation (Dawson et al., 1995). BHRF1 may enhance cell survival, allowing oncogenic mutations to accumulate; it may also permit the production of a maximum number of virions through the inhibition of apoptosis (Oudejans et al., 1995).

2.5.7. BamHI-C fragment rightward reading frame 1 (BCRF1)

EBV BCRF1 protein shows 84% sequence homology to human IL-10. IL-10 is a known growth and activation factor for B cells (Moore et al., 1991). EBV-derived IL-10 is thought to play a role in the establishment of latent infection by suppression of the host immune system (Helminen et al., 1999). BCRF1 is not able to initiate growth transformation or maintaining latent and lytic infection of B cells *in vitro* (Swaminathan et al., 1993).

2.5.8. BamHI-Z leftward reading frame 1 (BZLF1)

BZLF1, or termed Z Epstein-Barr replication activator (ZEBRA) is the major immediate early proteins of EBV. BZLF1 activates transcription of viral early genes. This protein is able to inhibit transcription from the EBNA Cp promoter and may facilitate the switch from latent to lytic infection. BZLF1 inhibits the ability of the viral protein to transactivate viral gene expression by binding to NF-κB or p53 (Sinclair et al., 1992).

2.5.9. Latent Membrane Protein 1 (LMP1)

LMP1 is involved in transformation by acting as a constitutively active receptor (CD40). Hence, this protein mimics the cellular growth signal that normally results from the binding of CD40 ligand. LMP1 has been linked to oncogenesis due to its ability to recruit an array of cellular genes. It also inhibits apoptosis by elevating levels of Bcl-2 (Zimber-Strobl et al., 1996).

LMP1 is an integral membrane protein with six hydrophobic membrane-spanning segments and a COOH-terminal cytoplasmic tail, which contains the effector. LMP1 aggregates in patches on the plasma membrane. Mutational analyses have demonstrated that the NH_2 terminus and the transmembrane segments of LMP1 are responsible for membrane aggregation and that this aggregation is essential for immortalization (Moorthy and Thorley-Lawson, 1993). LMP1 mimics CD40 by associating with the same tumor necrosis factor receptor-associated factors (TRAFs). The COOH-terminal domain of LMP1

interacts TRAF-1 and TRAF-2 and with tumor necrosis factor receptor-associated death domain protein (Izumi and Kieff, 1997).

In the function of LMP1, at least four signaling pathways, namely nuclear factor-κB (NF- κB), c-Jun NH_2-terminal kinase, p38 mitogen-activated protein kinase (MAPK), and Janus kinase/signal transducers and activators of transcription are involved. These molecules affect diverse signaling cascades.

Nuclear factor-κB is a key transcription factor involved in regulation of cell growth and apoptosis. p38/mitogen-activated protein kinase is also a central signaling pathway and activates the ATF2 transcription factor.

Meanwhile, the Janus kinase/signal transducers and activators of transcription cascade integrate with the activator protein-1 transcription factor pathway (Eliopoulos et al., 1999; Gires et al., 1999). The LMP-1 interactions also cause an overexpression of proteins Bcl-2 and A20, which protects the infected cell from p53-mediated apoptosis (Fries et al., 1996).

2.5.10. Latent Membrane Protein 2A and 2B (LMP2A and LMP2B)

The LMP2 gene encodes two proteins: LMP2A and LMP2B. These proteins are both integral membrane proteins that differ in their NH_2-terminal domains. LMP2A carries an extra 118-residue domain encoded in exon 1, whereas the LMP2B exon 1 is noncoding. The NH_2-terminal domain of LMP2A is cytoplasmic and contains an immunoreceptor tyrosine-based activation motif (Rowe, 1999).

A synthesis of the data supports a role for LMP2 in modifying normal B-cell development to favour maintenance of EBV latency in the bone marrow. The expression of LMP2A in Hodgkin's disease and nasopharyngeal carcinoma suggests an important, as yet unknown, function for this protein in oncogenesis (Murray and Young, 2002).

2.5.11. BamHI-A rightward frame 1 (BARF1)

BamHI-A rightward frame 1, BARF1 gene is expressed as a latent gene and transcribed early after EBV infection from the BamHI-A fragment of the EBV genome (Zhang et al., 1988). Another gene encoded by the BamHI-A fragment is BamHI-A rightward transcripts, BARTs. BARTs is located at bp 150,000–161,000 of B95-8 EBV DNA. BARTs has several distinct spliced forms, all of which are 3′-end coterminal (Gilligan et al., 1990).

The BARF1 open reading frame is located within a 40kb fragment of the EBV genome. The BARF1 gene is located downstream of BARTs, encodes 221 amino acids (Sadler et al., 2001) and is translated into a protein of 31–33 kDa (Zhang et al., 1988).

Crystallographic analysis of BARF1 showed that BARF1 froms hexameric rings in which three dimer molecules are interconnected head to tail and arranged in two layers as shown in Figure 2.2.

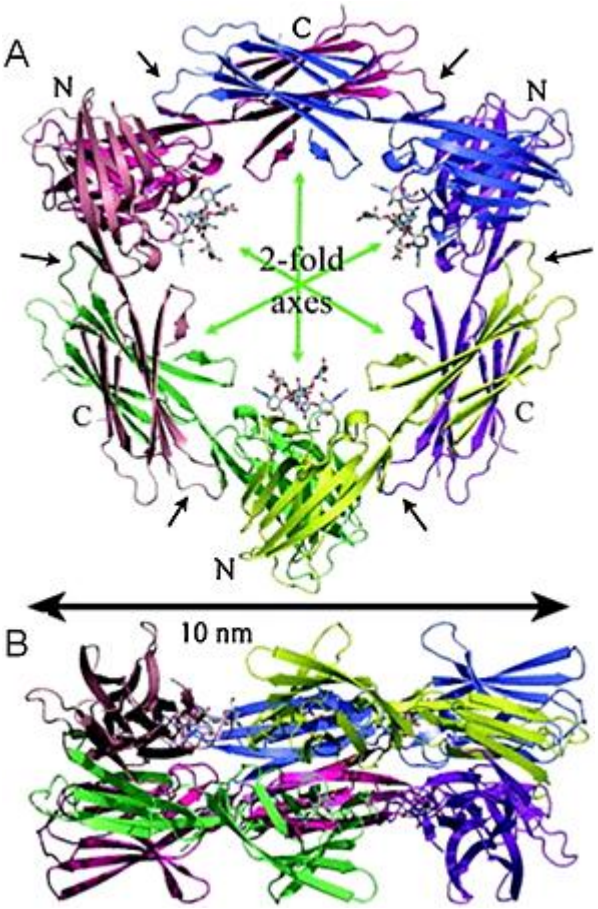

Figure 2.2. The structure of the soluble hexameric molecule BARF1. A) Top view of the BARF1 hexamer. Arrows show the N-linked glycosylation. B) side view of the BARF1 hexamer. Adapted from Hoebe et al., 2013.

Reviewed below are the roles of BARF1 in host cell immortalization and transformation, BARF1 as mitogenic growth factor, BARF1's role in immunomodulation as well as its antiapoptotic function.

Studies have shown that BARF1 modulates the host immune response to EBV infection (Strockbine et al., 1998). BARF1 is a functional homolog of the receptor tyrosine kinase colony-stimulating factor receptor (c-FMS or FMS), competing for its ligand, macrophage colony-stimulating factor (M-CSF, or CSF-1) (Strockbine et al., 1998). M-CSF is a hematopoietic growth factor involved in the proliferation, differentiation, and survival of monocytes, macrophages, and bone marrow progenitor cells (Stanley et al., 1997). It signals through the cell-surface receptor FMS, which is a class III receptor tyrosine kinase featuring five extracellular Ig-like domains, with the membrane-distal domains responsible for ligand recognition and the membrane-proximal domains involved in homotypic interactions (Yuzawa et al., 2007; Chen et al., 2008).

The interaction between BARF1 and M-CSF suggests that BARF1 may work functionally as an immunomodulator. Furthermore, BARF1 inhibits IFN-a production by mononuclear cells, by binding to M-CSF and reducing the effect of M-CSF on the proliferation of macrophages (Cohen and Lekstrom, 1999).

The EBV-encoded BARF1 has been proposed to function as an oncogene. In experiments whereby BARF1 was expressed endogenously, they were found to be secreted (Sall et al., 2004; de Turenne-Tessier et al., 2005; Seto et al., 2005; Wang et al., 2006; Seto et al., 2008; Fiorini and Ooka, 2008; Hoebe et al., 2011; Hoebe et al., 2012; Shim et al., 2012).

BARF1 is expressed in a high proportion of NPC cases and EBV-positive gastric carcinomas (Decaussin et al., 2000; Seto et al., 2005; Takada, 2012) and higher levels of BARF1 antibodies are found in NPC patients (Hoebe et al., 2011).

The N-terminal of BARF1 gene may be essential for the transforming activity; capable of activating expression of the antiapoptotic protein Bcl-2 (Sheng et al., 2001). BARF1 is able to induce malignant transformation in rodent cells (BALB/c3T3 and NIH3T3) as well as in human B cell lines Louckes and Akata (Wei and Ooka, 1989; Wei, et al., 1994; Sheng et al., 2003). Transfection experiments demonstrated the ability of BARF1 to induce cell immortalization or malignant transformation and to activate several cellular genes, including Bcl-2 (de Turenne-Tessier et al., 2005; Ooka, 2005). However, Wei et al in 1997 reported that immortalization can only be achieved in primary monkey epithelial cells. These findings indicate that the function of BARF1 may be cell type specific.

A recent study reported that the introduction of recombinant EBV carrying the BARF1 gene into EBV-negative cell lines did not alter the expression level of *Bcl-2* but induces NPC cell tumorigenicity in nude mice (Seto et al., 2008). Hence, the mechanism of the antiapoptotic effect of BARF1 remains to be clarified.

Introduction of BARF1 gene into primary primate kidney epithelial PATAS cells led to morphological changes, continuous cell growth and the capacity to grow in highly diluted culture condition. However, contact inhibition was conserved in these cells, and no tumor formation was observed after injection into nude mice (Wei et al., 1997). Thus, BARF1 by itself could only immortalize but could not transform the primate primary epithelial cells.

Meanwhile, the cellular function of BARF1 in human nasopharyngeal epithelial cells, which are the natural host cells of EBV infection, remains largely unknown because of the lack of suitable cell model. Therefore, whether BARF1 can transform primate or human epithelial cells remain unclear. However, Jiang and colleagues in 2009 reported that BARF1 together with H-*Ras* could transform human epithelial cells (Jiang et al., 2009). Deregulation of c-myc and/or Bcl-2 expression cannot be the main mechanism of cell transformation by BARF1. Some other signaling pathway might have been disrupted and play an important role in the transformation process by BARF1 (Jiang et al., 2009). Further investigations may help to elucidate the underlying mechanism.

2.6. EBV-associated cancers

Since its discovery as the first human tumor virus, EBV has been implicated in the development of a wide range of cancers.

2.6.1. Burkitt's Lymphoma

Burkitt's lymphoma is a particularly aggressive lymphoma, the hallmark being a chromosomal translocation between chromosome 8 and either chromosomes 14, 2, or 22. Because of this translocation, the oncogene *c-myc* (chromosome 8) is juxtaposed to the immunoglobulin heavy-chain (chromosome 14) or light-chain genes (chromosomes 2 or 22). This aberrant configuration results in the deregulation of *c-myc* expression. The relationship between EBV, Burkitt's lymphoma, and the *c-myc* translocation is complicated by the existence of two types of Burkitt's lymphoma: endemic (EBV present) and nonendemic (EBV generally absent). Although both types of Burkitt's lymphoma exhibit a

c-myc translocation, the breakpoints within the genes involved differ (Baumforth et al., 1999).

Endemic Burkitt's lymphoma occurs primarily in equatorial Africa and Papua New Guinea, with >90% of cases being associated with EBV. The role of EBV in Burkitt's lymphomas is strongly supported by observations of the Akata Burkitt's lymphoma cell line. Akata subcultures that have lost EBV have decreased growth and will not induce tumors in mice (Shimizu et al., 1994). However, reinfection of the Akata cells with EBV reestablishes the malignant phenotype (Komano et al., 1998). Latency I gene expression is observed. It has been theorized that B-cell stimulation caused by continuous reinfection by malaria may contribute to an expanded number of EBV-infected, proliferating B cells, which have a higher probability of harboring cytogenetic abnormalities such as the t(8;14). The breaks in chromosome 8 generally occur outside the *c-myc* locus. Whether there is a direct causal relationship between EBV and the development of the translocation is not known (Lyons and Liebowitz, 1998). There are several other mechanisms by which EBV may mediate lymphomagenesis. For instance, EBV modulates caspase-8 and FLICE-inhibitory protein, which leads to impairment of the Fas-mediated apoptotic pathway. Furthermore, EBV is responsible for increasing levels of the antiapoptotic protein Bcl-2 in lymphoblastiod cell lines that maintain latency I (Tepper and Seldin, 1999).

Nonendemic Burkitt's lymphoma or sporadic lymphoma is found in the West and has been a rare disorder, but its incidence has increased dramatically because of its high prevalence in AIDS patients. Only 15–30% of nonendemic Burkitt's lymphoma cases are associated with EBV in the United States (Subar et al., 1988) but 85% in Brazil (Araujo et al., 1996). As with malaria in endemic Africa, coinfection is thought to increase the

oncogenic potential of the B cell (Araujo et al., 1996). A t(8;14) translocation occurs in nonendemic Burkitt's lymphoma but, unlike the endemic form, the breaks in chromosome 8 appear 5′ to the first noncoding *c-myc* exon within the first exon or within the first intron of *c-myc* (Baumforth et al., 1999).

There are subtle phenotypic differences between endemic and nonendemic Burkitt's lymphoma. In endemic disease, bone marrow is less frequently involved, and patients are more sensitive to chemotherapy (Pagano, 1999). The tumors isolated from nonendemic Burkitt's lymphoma patients are usually from different stages of B-cell development than those isolated from patients with endemic Burkitt's lymphoma (Wensing and Farrell, 2000). The relationship between the phenotypic distinctions and the presence/absence of EBV and/or molecular differences is currently not clear.

2.6.2. Hodgkin's disease

Hodgkin's disease is characterized by an expansion of Reed-Sternberg cells, which are now postulated to be of B-cell lineage. Several lines of evidence link EBV to Hodgkin's disease: (*a*) a 4-fold increase in risk in individuals with a past history of infectious mononucleosis (Muñoz, et al., 1978); (*b*) increased antibody titers to EBV viral capsid antigen (Levine et al., 1971); and (*c*) the detection of monoclonal EBV episomes in Hodgkin's-Reed-Sternberg cells (Herbst et al., 1993).

The role that EBV plays in Hodgkin's disease is still not fully understood. EBV gene expression follows the latency II pattern with EBNA1, LMP-, LMP2A and LMP2B, and the EBERs being expressed. The questionable role of EBNA1 in carcinogenesis and the oncogenic capabilities of LMP1, LMP2A and LMP2B, and the EBERs have been addressed (Khanna et al., 1992).

Not all subtypes of Hodgkin's disease harbor EBV to the same degree. EBV is positive in lymphoma tissue of ~70% of mixed cellularity Hodgkin's disease, >95% of lymphocyte-depleted Hodgkin's disease, and 10–40% of nodular sclerosis; the lymphocyte-predominant Hodgkin's disease subtype is almost always EBV negative (Chapman and Rickinson, 1998). EBV positivity in geographic variations has also been studied. EBV positivity in Hodgkin's disease is found in 65% of cases in Japan, 67% of cases in Mexico, 94% of cases in Peru, 40% of cases in Costa Rica, 92% of cases in Kenya, 41% of cases in Italy, and ~50% of cases in the United States (Tomita et al., 1996; Zarate-Osorno et al., 1995; Monterroso et al., 1998; Leoncini et al., 1996). Strain variation does not seem to be a factor in EBV positivity; however, there is an increased incidence of EBV-2-positive Hodgkin's disease in immunocompromised individuals (Boyle et al., 1993). There is also data that suggests that the incidence of EBV-positive Hodgkin's disease is age-related, with the virus being preferentially associated with tumors from pediatric and older patients (Armstrong et al., 1998).

2.6.3. Non-Hodgkin's Lymphoma in Immunocompetent Individuals

Besides its ability to infect B cells, EBV can also infect other cells. Several types of non-B-cell, non-Hodgkin's lymphoma are associated with EBV (Weiss et al., 1992). Nasal T/natural killer non-Hodgkin's lymphoma cells exhibit several unique genotypic and phenotypic features. These features include an absence of T-cell antigens, expression of natural killer cell marker CD 56, and absence of T-cell receptor gene rearrangement (Tao et al., 1995; Kwong et al., 1997). These tumours occur in the nasal and upper aerodigestion area. EBV is consistently associated with these lymphomas, regardless of geographical location (Tsuchiyama et al., 1998).

Angioimmunoblastic lymphadenopathy is a peculiar T-cell lymphoma in which expanding B-cell clones are often present beside the T-cell clones. EBV infection is mainly in the B lymphocytes and B immunoblasts (Weiss et al., 1992). The presence of EBV in only a subpopulation of cells suggests that EBV infection is secondary to malignancy or that the viral genome has been lost from the malignant cell. EBV-positive B cells have also been observed growing in peripheral T-cell lymphomas (Ho et al., 1998). This raises questions about the possible activation of EBV in latently infected B cells by the neoplastic T cells, and/or the role of the EBV-positive B cells in maintaining the malignant T-cell process (Ho et al., 1999).

2.6.4. Nasopharyngeal Carcinoma (NPC)

Undifferentiated nasopharyngeal carcinoma is associated with EBV and affects mostly individuals in their mid-40s and is more common in men (Vasef et al., 1997). Nearly every undifferentiated nasopharyngeal carcinoma is EBV positive, regardless of geographical origin.

Undifferentiated nasopharyngeal carcinoma is rare in most parts of the world, but there is an exceptionally high prevalence of this cancer in the Chinese province of Canton, Hong Kong, Taiwan, and among the Inuits in Alaska and Greenland. Indeed, in Taiwan, nasopharyngeal carcinoma is the most common cancer in men and the third most common in women (Hsu et al., 1982). The epidemiological pattern may be because of genetic susceptibility correlated with certain Chinese-related HLA antigen profiles and/or to environmental factors (the consumption of salted fish or exposure to fumes, smoke, and chemicals from the occupational environment (Bouvier et al., 1995). NPC is the third most common cancer in males in Peninsular Malaysia (Pua et al., 2008). High prevalence of NPC among the Bidayuhs of Borneo, whose NPC incidence is higher than that of the Cantonese in Southern China has been reported (Devi et al., 2004).

In undifferentiated nasopharyngeal carcinoma, EBV infects the epithelial cells of the posterior nasopharynx in Rosenmuller's fossa in Waldeyer's ring (Prasad et al., 1985). Although an EBV-compatible receptor on epithelial cells has not been found, a surface protein that is antigenically related to the B cell CD21 receptor has been described and could conceivably be used as a point of entry by EBV (Young et al., 1989). Alternatively, it

has been suggested that EBV may gain entry into nasopharyngeal cells through IgA-mediated endocytosis (Lin et al., 1997).

The EBV genomes present in the epithelial cells of the nasopharynx are of clonal origin, and EBV is absent from surrounding tissues and invading T lymphocytes (Pathmanathan et al., 1995). These findings suggest that EBV infection occurs before neoplasia and is necessary for the progression of the malignant phenotype.

EBV-1 and EBV-2 have both been implicated in nasopharyngeal carcinoma. The majority of nasopharyngeal carcinoma cases from peoples in southern China, Southeast Asia, the Mediterranean, Africa, and the United States are associated with EBV-1 infection. Cases involving Alaskan Inuits are almost always EBV-2 related but contain polymorphisms characteristic of Asian EBV-1 (Abdel-Hamid et al., 1992). EBV undergoes latency II expression in undifferentiated nasopharyngeal carcinoma (Niedobitek et al., 1997).

One of the major questions surrounding undifferentiated nasopharyngeal carcinoma is how the EBV-infected cells can escape the immune response. Nasopharyngeal carcinoma cells possess normal antigen processing and are effectively recognized by EBV-specific CTLs, yet they are not destroyed (Bejarano and Masucci, 1998). Overexpression of Bcl-2 may also play a role in oncogenesis by allowing the cell to bypass apoptosis (Lu et al., 1993).

2.6.5. Gastric Carcinoma (GC)

About 10% of gastric carcinoma is associated with EBV. EBV-positive gastric carcinoma is a non-endemic disease distributed throughout the world. EBV DNA is detected in more than 80% of gastric carcinoma of the lymphoepithelioma type by PCR and *in situ* hybridization. In each of the cases, 100% of carcinoma cells are infected with EBV expressing EBNA1, EBER1, EBER2 and BARF0 as well as LMP2A in some cases (Takada, 2000).

EBV exhibits a novel latency pattern in gastric adenocarcinomas that includes the production of BARF1, a homologue to human colony-stimulating factor 1 receptor and intracellular adhesion molecule 1, and the absence of LMP-1 (Kume et al., 1999). Although any mechanism relating EBV to tumorigenesis in gastric malignancies remains highly speculative, it has been demonstrated that there is a delay in apoptosis in EBV-positive gastric carcinomas (associated with up-regulation of BCL-2 and p53) and a decrease in cellular differentiation (associated with decreased E-cadherin expression) (Kume et al., 1999). EBV has been suggested to play an important role in the development of EBV-positive gastric carcinomas.

2.7. Apoptosis

There are two ways for cells to die; apoptosis and necrosis. Necrosis is an accidental death of groups of cells within a tissue. Cell death by apoptosis however, is preprogrammed into the cell or may be induced and results in the death of the individual cells. (Zimmermann and Green 2001).

Apoptosis or programmed cell death is a conserved mechanism to maintain normal cellular homeostasis (Thornberry and Lazebnik, 1998). At the molecular level, apoptosis is tightly regulated (Zimmermann and Green, 2001). Cells undergoing apoptotic cell death exhibit several typical morphological features including cell shrinkage, membrane blebbing, chromatin condensation, nuclear fragmentation and disassembly into membrane-enclosed vesicles (apoptotic bodies) (Okada and Mak, 2004).

2.7.1. Apoptosis pathways

Apoptosis pathways can be initiated through different entry sites, for example, at the plasma membrane by death receptor ligation (receptor/extrinsic pathway) or at the mitochondria (mitochondrial/intrinsic pathway) (Fulda and Debatin, 2006).

Apoptosis via the extrinsic pathway involves activation of death receptors of the TNF receptor family located in the plasma membrane, such as TNF-R, Fas (also called CD95), DR4, and DR5 (Fulda and Debatin, 2006). Despite the fact that each of these receptors is activated by its own ligand, they share a common mechanism.

The stimulation by the ligand results in receptor trimerization to which the protein Fas-associated death domain (FADD) and procaspase-8 can bind. This promotes the formation of the death-inducing signaling complex (DISC) (Peter and Krammer, 2003). Following that, a self-activation of caspase-8 occurs, which leads to activation of effector caspases and completion of apoptosis (Beurel and Jope, 2006).

Apoptosis via the intrinsic pathway involves the loss of integrity of mitochondria with release of cytochrome c (Cyto c) leading to cell destruction. In the cytoplasm, released cytochrome c binds to apoptotic protease-activating factor-1 (Apaf-1), ATP, and procaspase 9, thus forming the apoptosome and leading to activation of caspases which finally induces cell death. The stimuli able to trigger this type of cell death are diverse and they include DNA damage, oxidative stress or endoplasmic reticulum stress (Fulda and Debatin, 2006).

Apoptotic cell death is often mediated by a caspase cascade and although many stimuli exist, the final phases of apoptosis are executed by a few common effector caspases. Mitochondria provide a link between the initiator caspases and the downstream effector caspases. Mitochondria accelerate activation of caspases by releasing proapoptotic molecules, such as cytochrome c and the apoptosis-inducing factor (AIF). The release of these molecules can be stimulated by some caspases and by Bid and BAX, whereas Bcl2 prevents their release (Peter and Krammer, 2003; Fulda and Debatin, 2006).

The release mechanism of signaling molecules from the mitochondria is being intensively studied. These mechanisms may include transport by pore-forming proteins such as Bax (Marzo et al., 1998), opening of the permeability transition pore (PTP) in the inner mitochondrial membrane leading to rupture of the outer mitochondrial membrane

(Zamzami et al., 1996), or cooperation of the PTP and the voltage-dependent anion channel in the outer mitochondrial membrane (Shimizu et al., 1999).

2.7.2. Caspases

Apoptosis is mediated by a family of cysteine proteases known as the caspases (Thornberry and Lazebnik, 1998). Caspases have an absolute requirement for cleavage after aspartic acid and they recognize at least four amino acids N-terminal to the cleavage site. For example, the preferred tetrapeptide recognition motifs of caspase 3 and caspase 9 are DEVD (aspartic acid-glutamic acid-valine-aspartic acid) and LEHD (leucine-glutamic acid-histidine-aspartic acid), respectively. The difference in recognition motifs among caspases likely reflects their diverse substrate specificities. Caspases are all expressed as inactive proenzymes processing an N-terminal prodomain followed by a large and a small subunit (Thornberry and Lazebnik, 1998). Sequential proteolytic processing of the cleavage sites between domains release the large and the small subunits to form a heterodimer in which both the large and the small subunits contribute amino acid residues necessary for substrate binding and catalysis. Two heterodimers associate to form an active tetramer, thereby having two catalytic sites (Thornberry and Lazebnik, 1998).

In response to apoptotic stimuli, initiator caspases, such as caspase 8 and caspase 9, are activated by autocatalytic proteolysis early in the apoptotic process and they are required for the proteolytic activation of downstream effector caspases, such as caspase 3 and caspase 7. Activated caspases are responsible for proteolysis of many substrates which is irreversible, resulting in the apoptotic cell death (Cryns and Yuan, 1998).

Many substrates of activated effector caspases have been found and the relationship of their cleavage to cell death is obvious. For example, caspase-activated deoxyribonuclease (CAD) is kept inactive by inhibitor of CAD (ICAD) (Enari et al., 1998).

During apoptosis, activation of caspase 3 mediates proteolytic cleavage of ICAD, releasing free CAD to function as a nuclease to mediate DNA fragmentation. Besides, anti-apoptotic Bcl-2 proteins are also cleaved by caspases, which may represent a positive feedback mechanism in the activation of apoptosis (Cheng et al., 1997). Caspases also mediate cleavage of lamins which are intermediate filament monomers required for the formation of nuclear lamina (Orth et al., 1996). Destruction of nuclear lamina disrupts the structural organization of chromatin, leading to chromatin condensation. In addition, caspases inactivate proteins involved in DNA repair, such as poly-(ADP-ribose) polymerase (PARP) and DNA-PKcs, and DNA replication, such as replication factor C (Nicholson et al., 1995).

2.7.3. The Bcl-2 family

Activation of caspases is regulated by the Bcl-2 family of proteins which consist of anti-apoptotic and pro-apoptotic proteins (Danial and Korsmeyer, 2004). The Bcl-2 family members share the homology within four conserved regions named Bcl-2 homology (BH) 1-4 domains.

The antiapoptotic proteins Bcl-2 and Bcl-X_L display conservation in all four BH1-4 domains. Structural analysis of antiapoptotic Bcl-2 and Bcl-X_L revealed that their BH1, BH2 and BH3 domains create a hydrophobic pocket which is capable of binding the BH3

domain of pro-apoptotic members, and antagonize their activity (Oltersdorf et al., 2005). Since the hydrophobic pocket is responsible for Bcl-2 antiapoptotic activity, many attempts have been made to develop small molecule inhibitors, such as HA14-1, and ABT-737, which occupy the hydrophobic pocket of Bcl-2 and interfere with its binding activity with Bax (Manero et al., 2006).

Bcl-2 proteins are frequently overexpressed in many cancers which are suggested to contribute to tumorigenesis and chemoresistance. As a result, cancer cells treated with small molecule inhibitors against Bcl-2 undergo apoptosis directly or display synergistic cytotoxicity with chemotherapeutic drugs and γ–irradiation (Oltersdorf et al., 2005). Bcl-2 interacts directly and inhibits BAX activity. Bcl-2 also binds to pro-apoptotic BH3-only proteins, such as Bid, NOXA and PUMA, and sequesters them from activating Bax. Therefore, the ratio of anti- to pro-apoptotic proteins, such as Bcl-2 to Bax, may regulate the threshold to induce apoptosis (Cheng et al., 2001). Besides, the activity of anti-apoptotic Bcl-2 is regulated by transcriptional control or post-translational modifications via phosphorylation. Phosphorylation of Bcl-2 at serine 70 residue inactivates the anti-apoptotic function of Bcl-2. Overexpression of a phosphorylation site mutated form of Bcl-2 (S70A) inhibits apoptosis induced by microtubule inhibitors or DNA damaging agents (Haldar et al., 1995).

Proapoptotic BAX and Bak proteins may constitute a requisite gateway to initiate apoptosis because mouse cells deficient of *Bax* and *Bak* are resistant to all intrinsic death pathway stimuli (Wei et al., 2001). It has been shown that the expression of BAX is trancriptionally upregulated by p53 in response to DNA damaging agents such as cisplatin and γ-rays (Miyashita and Reed, 1995). Besides, DNA damage-induced p53 activation also

increases the transcription of two BH3-only pro-apoptotic genes, *NOXA* and *PUMA* (Nakano and Vousden, 2001; Oda et al., 2000). It has been shown that NOXA or PUMA can bind to Bcl-2 and antagonize its function, which leads to the activation of BAX.

Activated Bax oligomerizes and translocates from cytosol to the mitochondrial outer membrane to induce permeabilization of the mitochondrial outer membrane, resulting in the release of intermembrane space proteins including cytochrome c (Suzuki et al., 2000). Oligomerized Bax may also form pore-like structure on the mitochondrial outer membrane to release cytochrome c as a substantial cytochrome c release occurs before swelling of mitochondrion (Danial and Korsmeyer, 2004). Apoptotic protease-activating factor-1 (Apaf-1) interacts with cytochrome c and becomes competent to recruit procaspase 9 which undergoes self-processing for activation. Subsequent binding of ATP/dATP to Apaf-1 induces its conformational change and facilitates the heptamer assembly, known as the apoptosome. Apoptosome proteolytically activates effector caspases to initiate apoptosis (Bratton and Salvesen, 2010).

Cisplatin treatment upregulates the expression of Fas ligand (FasL) as well as Fas receptor on cell surface, suggesting that cisplatin-induced apoptosis is also mediated via FasL/Fas system (Lacour et al., 2003). Engagement of Fas receptor by FasL binding induces a conformation change of Fas receptor, which is assembled as a trimer on plasma membrane, leading to the assembly of the death-inducing signaling complex (DISC) on its cytoplasmic region (Danial and Korsmeyer, 2004).

The adaptor protein Fas-associated death domain (FADD) which bears both death domain (DD) and death effector domain (DED) binds the DD of Fas and DED of procaspase 8. It is believed that caspase 8 is activated by ‘induced proximity’ where high

local concentration of procaspase 8 promotes its own proteolytic processing and activation (Danial and Korsmeyer, 2004). Subsequently, activated caspase 8 mediates proteolytic activation of effector caspases 3 and 7 to initiate apoptosis. Besides, activated caspase 8 mediates proteolytic processing of pro-apoptotic BH3-only protein Bid. Cleaved Bid translocates to mitochondria and induces conformation change and oligomerization of Bax to release cytochrome c (Lacour et al., 2003). Therefore, caspase 8-mediated cleavage of Bid is required for mitochondria-dependent pathway to amplify the apoptotic signal.

2.7.4. Apoptosis and cell cycle related proteins

The cyclin-dependent kinase (Cdk) inhibitor p27 regulates cell proliferation, cell motility and apoptosis. p21 is the founding member of the Cip/Kip family of CKIs, which also includes p27 and p57. p21 plays an essential role in growth arrest after DNA damage and overexpression leads to G_1 and G_2 or S-phase arrest (Coqueret, 2003). Survivin, the inhibitor of apoptosis protein regulates apoptosis and cell cycle. Its expression is high in a number of malignancies including lymphoma, esophageal, lung, ovarian, central nervous system, breast, colorectal, bladder, gastric, prostate and others. In cancer cells, elevated survivin is commonly associated with enhanced proliferative index, reduced levels of apoptosis, resistance to chemotherapy and increased rate of tumour recurrence (Fukuda and Pelus, 2006). The cellular inhibitor of apoptosis proteins 1 and 2 (cIAP1 and cIAP2) are members of a highly conserved and critically important family of inhibitor of apoptosis proteins (IAPs) that function to regulate both intrinsic and extrinsic death signalling (Graber and Holcik, 2011).

Six well-characterized insulin-like growth factor binding proteins (IGFBP-1 to IGFBP-6) have been found and characterized from a variety of vertebrate species, including humans. IGFBPs exert their role by association with insulin-like growth factor-I (IGF-I) and insulin-like growth factor-II (IGF-II) and the regulation of a key signaling pathway triggered by these IGFs (Akkiprik et al., 2008). IGFBP-2 is overexpressed in a wide variety of human malignancies, including glioma, prostate cancer, lung cancer, colorectal cancer, ovarian cancer, breast cancer and leukemia. IGFBP-2 is frequently overexpressed in advanced cancers and is suggested to be involved in the metastatic process (Migita et al., 2010). IGFBP-2 expression correlates with grade of malignancy. The level of IGFBP2 appears to be low in well-differentiated tumours but high in poorly differentiated tumours (Schutt et al., 2004). IGFBP-2 has a multitude of effects that are mediated either by its IGF-dependent or by its IGF-independent actions. IGF-dependent actions are considered to be due to any type of modulation of IGF activity, whereas IGF-independent actions are those mediated by other mechanisms in which IGFs are not involved (Frommer et al., 2006). The IGF-independent function of IGFBP-2 in cellular signalling has been suggested due to its cytosolic or perinuclear localization, which may inhibit cellular growth and modulate proapoptotic signals. Therefore, the function of IGFBP-2 could be complex depending on the cell type and cellular microenvironment (Fukushima and Kataoka, 2007).

Insulin-like growth factor binding protein-3 (IGFBP-3) is a member of a family of high-affinity binding proteins known to regulate the function of insulin-like growth factors (IGF-I and IGF-II) through modulating interactions with the signalling receptor IGF-I receptor (IGF-IR) (Williams et al., 2006).

IGFBP-3 can modulate cell proliferation by adjusting levels of p53, preventing DNA damage, and modulating NF-κB activities. These cumulative reports have suggested that IGFBP-3 has important biological significance in controlling cell growth, transformation and survival, independent of its actions on IGF-1 regulation. Recent studies suggest that IGFBP-3 is involved in the induction of apoptosis (Grimberg, 2000; Zhang et al., 2013). IGFBP-4 primarily functions as an inhibitory protein for cancer cell lines by binding to both IGF-I and IGF-II with equal affinity. IGFBP4 exerts pro-apoptotic effects by inhibiting the activity of IGF-I (Ryan et al., 2009; Durai et al., 2007).

2.7.5. Modulation of apoptosis by Epstein-Barr virus

EBV replicates in epithelial cells, *in vivo* and establish long term latency in lymphocytes. Wild-type EBV has not been reported to induce apoptosis on infection of resting human B lymphocytes or of Burkitt's tumor B lymphoblasts, *in vitro,* or in marmoset B lymphocytes, *in vivo.* This is partly because EBV upregulates the expression of Bcl-2 in B lymphocytes (Mancao et al., 2005).

The anti-apoptotic cell protein Bcl-2 plays important role in normal B lymphocyte development. Burkitt's tumor cells are germinal center B lymphocytes and Bcl-2 is not normally expressed in germinal center B lymphocytes. Bcl-2 is turned on later in B cell maturation and enables antigen-stimulated B lymphoblasts to survive apoptosis as the normal B lymphocyte moves beyond the germinal center. As mature lymphocytes go into a resting state, Bcl-2 expression is downregulated. EBV infection of resting B lymphocytes

then transforms them into immortalized lymphoblasts that are partially protected from apoptosis by upregulated Bcl-2 expression (Mancao et al., 2005).

2.8. RNA interference

2.8.1. Introduction

RNA interference (RNAi), an ancient defense pathway, is a common denominator for the posttranscriptional gene silencing (PTGS) phenomenon observed in a variety of species such as plants, fungi and animals (Fire et al., 1998). The introduction of long dsRNA into cells can effectively and specifically lead to the degradation of cognate mRNAs in a gene-dependent manner. This powerful technology has been widely employed to manipulate gene expression, elucidate signal pathways and to identify gene functions in a whole-genome scale. Researchers worldwide have used RNAi for basic research, and are now developing RNAi-based drugs for the prevention and treatment of human diseases such as viral infection, tumours and metabolic disorders (Plasterk, 2002; Yin and Wan, 2002; Dave and Pomerantz, 2003).

Despite significant advances that have been made in the therapy of viral diseases, current drugs and vaccines are restricted with many factors such as toxicity, complexity, cost and resistance. RNAi is a self-defense mechanism of eukaryotic cells, which specially prevent infection evoked by viruses (Plasterk, 2002). It can inhibit the expression of crucial viral proteins by targeting viral mRNA for degradation through cellular enzymes. In fact, RNAi does work effectively as an antiviral agent in plants. This breakthrough technology emerges as a powerful tool to protect human cells from viral infection (Gitlin et al., 2002).

2.8.2. RNAi machinery

Biochemical and genetic studies have revealed the molecular mechanisms by which dsRNA causes the degradation of target messenger RNA (Dykxhoorn et al., 2003). RNAi includes two steps: initiation step and effector step. In the initiation step, Dicer, a member of the RNase III family of ATP-dependent ribonucleases, binds with high affinity to dsRNA containing 2 nucleotide (nt) 3' overhangs and chops long dsRNA (introduced directly or via a transgene or virus) into small interfering RNAs (siRNAs) duplexes.

Generally, Dicer enzymes contain an N-terminal DEXH-box RNA helicase domain, a domain of unknown function (DUF283), a PAZ (PIWI–Argonaute–Zwille) domain, two RIII domains and a dsRNA-binding domain (dsRBD) (Carmell and Hannon, 2004). Dicer can cleave dsRNA into siRNAs or microRNAs (miRNAs) from endogenous stem loop precursors (Lee et al., 2004).

Biochemical studies show that siRNAs are 21-23 nt dsRNA duplexes with 2-nt 3' overhangs, a 5'-monophosphate and a 3'-hydroxyl group (Elbashir et al., 2001). In the effector step, the siRNA duplexes are incorporated into RNA induced silencing complex (RISC). The phosphorylation of siRNA 5'-terminal is required to entry into RISC (Khvorova et al., 2003).

A helicase domain of RISC binds to one end of the duplex and unwinds the double-strand in an ATP-dependent manner. The thermodynamic stability of the first few base pairs of siRNA can affect the ratio of RISC containing the antisense or sense strands of siRNAs (Dorsett and Tuschl, 2004).

Dicer with R2D2 (Dcr-2-associated protein) binds siRNA and facilitates its loading onto RISC. The active RISC then targets the homologous transcript by base pairing interactions and cleaves the mRNA between the 10^{th} and 11^{th} nucleotide from the 5' terminus of the siRNAs (Khvorova et al., 2003).

MicroRNAs (miRNAs) are endogenous ~22 nt RNAs that play important roles in regulatory by targeting mRNAs for degradation or translational repression in animals and plants. Since miRNAs and endogenous siRNAs share central biogenesis and can perform interchangeable biochemical functions, these silencing RNAs cannot be distinguished by either their chemical composition or mechanism of action (Bartel, 2004). These short RNA species are produced by Dicer cleavage of long (~70 nt) endogenous precursors with imperfect hairpin RNA structure in animals. Mature miRNAs repress translation by partial base-pairing with 5' or 3' ends of mRNAs while complete complementary of miRNA to its target mRNA (endogenous siRNA) can result in cognate mRNA degradation (Bartel, 2004).

In addition, many other proteins such as eukaryotic translation initiation factor 2C2 (eIF2C2) and Argonaute proteins are likely to function in both pathways. Argonaute proteins are the key components of RISC. They are evolutionarily conserved with two distinguishing domains, PAZ and PIWI. The PIWI domain is restricted to Argonautes while the PAZ domain is shared with Dicer family proteins (Song et al., 2003).

2.8.3. Silencing mechanism of RNAi

Long dsRNA enables the effectively silencing of gene expression by presenting various siRNA sequences to target mRNA. Cells infected by viruses invariably produce dsRNA, but viruses can escape a profound cellular response. The dsRNA binds to dsRNA-binding proteins (dsRBPs), which have been shown to counteract the effects of Interferon (IFN) and the resultant dsRNA-activated protein kinase (PKR) activation, and to suppress RNAi. Recently, it has become clear that 21-nucleotide siRNAs are so short that they cannot induce an interferon response in mammalian cells (Lichner et al., 2003). So, the antiviral effects of siRNAs have attracted a great number of scientists to channel their interests into this field.

The inhibition of viral infection can be mediated by siRNA molecules that target viral mRNA for degradation. In comparison with other conventional drugs, siRNA have many advantages. First, it is much easier and more flexible to select target sites because target mRNA and siRNA are sequences-specific and complementary. For a given mRNA molecule, the inhibitory effects of siRNAs can be achieved by targeting different regions of target mRNA. Second, for gene silencing, only substoichiometric amount of siRNA is enough to drastically decrease homologous mRNA within 24 h. Third, siRNAs can result in the degradation of cognate mRNA in cells of different species (Lichner et al., 2003). Today, researchers are developing efficient siRNA delivery systems, which can help siRNAs enter efficiently into cells in nearly all organs. Fourth, siRNAs do not seem to adversely affect cell control mechanisms.

The high homology of siRNA to the target region of cognate transcription provides selective destruction of only interested transcript. siRNAs that do not have targets will remain inert within cells. This exclusive specificity without adverse side effects is the most attractive feature of RNAi as an antiviral approach. Fifth, siRNAs can silence gene stably. With the application of plasmid vectors and viral vectors, siRNAs can display their long-term biological effects (Li et al., 2002). Taken together, siRNAs synthesis *in vivo* or *in vitro* transfected into cultured cells or animals could result in the sequence-specific silencing of mRNA molecules. With the proof-of-concept studies, siRNAs have been widely used as an alternate therapeutic strategy.

2.8.4. RNAi application to viral infection

Researchers strongly believe that RNAi will finally be used as a viable therapeutic alternative for various diseases in the near future. The inhibitory action of siRNAs has been documented for numerous viruses.

Synthetic siRNAs are able to inhibit viral production. This was determined by introducing siRNAs into the cells before viral infection and then assaying virus titres in the culture supernatants at different times after infection (Ge et al., 2003). Scientists, in the first application of RNAi technology to prevent disease, revealed that siRNA-directed inhibition of *Fas* gene expression could protect mice from antibody or concanavalin A-induced hepatitis (Song et al., 2003). In addition, siRNA inhibitory effects also occurred in cells that have been infected with virus prior to siRNA introduction. Introducing siRNAs into cultured cells and chicken embryos before virus infection was able to inhibit influenza virus

production. Influenza virus usually infects epithelial cells in the upper airway and the lungs. Hence, siRNAs can be administered by inhalation.

This mode of administration is very convenient and high local siRNA concentration is easily achieved to enable epithelial cells to uptake sufficient siRNA, resulting in the prevention of influenza infection (Ge et al., 2003). In other studies, Gitlin et al. (2002) showed that RNAi effectively prevented viral infection in mammalian cells by using siRNAs against the poliovirus genome. Hepatitis C virus (HCV) infection is a major cause of chronic liver disease, which can lead to the development of liver cirrhosis and hepatocellular carcinoma. In 2003, Kapadia et al. revealed that siRNAs could specifically inhibit HCV RNA replication and protein expression in Huh-7 cells. In their experiments, HCV RNA replication was inhibited within 2 days of siRNA transfection, and the effect lasted at least 6 days. The stability of the siRNAs, combined with the efficient transfection observed in these experiments may demonstrate the application potential of RNAi to the prevention of viral infection (Kapadia et al., 2003).

In the research of viral diseases, RNAi has been widely used in the inhibition of the expression of viral antigens. Viral proteins play roles in pre- or post-transcriptional aspects of the viral life cycle instead of being involved in viral RNA or protein synthesis. Many cellular membrane molecules act as receptors for viruses. In a study by Novina and colleagues, CD4 molecule, the main receptor for HIV-1 in a HeLa-derived cell line was knocked down by specific siRNAs. The investigations suggested that siRNA-directed CD4 silencing specifically inhibited HIV-1 infection (Novina et al., 2002). CCR5, a human chemokine receptor protein, is a necessary coreceptor for infection by most strains of HIV-

1. The inhibition of CCR5 expression by siRNAs was found to protect lymphocytes from HIV-1 virus infection (Qin et al., 2003).

SARS-CoV (the SARS-associated coronavirus) has been classified as a novel member of the coronavirus family with a spike protein, which plays an important role in viral entry and pathogenesis. In 2004, Zhang et al. showed that the DNA vector-driven siRNA against this spike protein could specifically silence gene expression of the spike protein in SARS-infected 293T cells (Zhang et al., 2004). The above examples strongly suggest that the suppression of expression of viral antigens by RNAi will be effective strategies for the therapy of viral infection.

RNAi can be employed to suppress the transcription of viral genome. Viruses need to transcribe its genome after entering the host cells. Besides using cellular factors, viruses can generate their transcriptional activators such as E6 and E7 proteins of human papillomaviruses (HPVs). HPV are small DNA viruses with a genome of approximately 8 kb and many subtypes. HPV16 is a main causative agent of cervical cancers and encodes the *E6* and *E7* oncogenes, which are essential for malignant transformation as well as maintenance of the tumour's malignant phenotype. Experiments demonstrated that E6 siRNAs were potent in the suppression of viral oncogene expression when E6 siRNAs were transfected into HPV16-related cervical cancer cells. E6 siRNAs exhibited a potent growth inhibitory activity too. Thus, anti-*E6* siRNA may be used as a gene-specific therapy for HPV-related cancers (Yoshinouchi et al., 2003).

For RNA viruses, especially in retroviruses, *gag*, *env* and *pol* are essential for genome transcription. Avian Sarcoma Leucosis Virus (ASLV) is a positive-RNA virus. When siRNAs matching two sequences in the *gag* gene of ASLV were introduced into

cultured chicken DF-1 cells, provirus formation analysis showed that the anti-*gag* siRNAs could inhibit the transcription of the retrovirus (Hu et al., 2004).

Silencing the many accessory genes in viruses is thought to be good therapeutic strategies for the treatment of viral diseases. Viral RNA is introduced into the host cell cytoplasm in the form of a nucleoprotein complex upon HIV-1 infection. siRNA duplexes against several regions of the HIV-1 genome, including the viral long terminal repeat (LTR) and the accessory genes were introduced into CD4-positive HeLa (Magi) cells. Virus production was reduced 30-fold to 50-fold when compared with cells not transfected with siRNA duplexes. These results provided a therapeutic alternative for AIDS by siRNA-mediated degradation (Jacque et al., 2002).

Epstein-Barr virus (EBV) is a prototype gamma herpes virus with a dsDNA genome. It is the first human virus identified and is related to the pathogenesis of several malignancies, including Burkitt's and T cell lymphomas, Hodgkin's disease, breast and gastric carcinomas, and some AIDS-related lymphomas. Latent membrane protein-1 (LMP-1), encoded by EBV, is an oncoprotein playing an essential role in cell transformation as well as nasopharyngeal carcinoma (NPC) metastasis. Li *et al* showed that the stable suppression of LMP-1 by shRNA plasmid significantly altered EBV-positive NPC cell (C666) motility, substratum adhesion, and transmembrane invasion ability (Li et al., 2004). Application of RNAi to the study of accessory genes tells us more about molecular mechanisms underlying viral infection so that more effective drugs to treat viral diseases could be developed.

RNAi has been used in large-scale, genome-wide screens. Scientists have developed many RNAi libraries to study the function of genes in nematodes and human, which can greatly facilitate the identification of drug targets against viral infection. With the advent of RNAi library in mammals and the refinement of techniques to silence gene, siRNA-based drugs will surely make great advances in the prevention and treatment of viral diseases.

CHAPTER 3: METHODOLOGY

3.1. Cell lines and cell culture conditions

AG876, Hone-Akata and B95-8 cell lines were grown in RPMI-1640 (Roswell Park Memorial Institute medium) (GIBCO/BRL, USA) supplemented with 2mM L-glutamine and 10% (v/v) fetal bovine serum (GIBCO/BRL, USA) at 37°C under a humidified atmosphere of 95% air and 5% CO_2. AG876 and B95.8 were obtained from ATCC®, USA. AG876 are EBV-positive malignant cells (EBV type 2) derived from a patient with endemic Burkitt's lymphoma (Pizzo et al., 1978). B95.8 is the EBV-producing marmoset cell line (Miller and Lipman, 1973). Hone Akata (a gift from Prof Sam Choon Kook) is an NPC epithelial cell line that is superinfected with the Akata strain of EBV (EBV type 1) (Glaser et al., 1989).

3.2. Detection of BARF1 gene expression in EBV-positive malignant cells

3.2.1. Total RNA extraction

RNA was extracted from cells using the RNeasy Mini Kit® (Qiagen, Germany) according to the manufacturer's protocol. For pelleted cells, 350 µl (for $<5 \times 10^6$ cells) or 600 µl (for $5 \times 10^6 - 1 \times 10^7$ cells) of Buffer RLT (RNeasy lysis buffer) was added to the cell pellet in a microcentifuge tube and vortexed to mix. For direct lysis of cells grown in a monolayer, 350 µl (for dish diameter <5 cm) or 600 µl (for dish diameter 6-10 cm) of

Buffer RLT was added to the cell culture dish and lysate was collected with a rubber policeman. Lysate was transferred into a microcentrifuge tube and vortexed to mix.

After the lysis step, lysate was homogenized by passing through the QIAshredder spin column. To the homogenized lysate, 1 volume (350 µl or 600 µl) of 70% ethanol was added and mixed well by pipetting. Sample was then transferred to an RNeasy mini column placed in a collection tube and centrifuged at 8000 × g for 15 s. The flow-through was discarded and followed by washing in 700 µl of Buffer RW1 (stringent buffer for washing membrane-bound RNA to remove carbohydrates, proteins and fatty acids) and 500 µl of Buffer RPE (washing buffer to remove salt traces).

The washing steps involved centrifugation at 8000 × g and flow-through was discarded after each washing step. The RNeasy column was placed in a new collection tube and eluted by adding 50 µl RNase-free water to the RNeasy silica-gel membrane. The eluate was collected by centrifugation at 8000 × g for 1 min. The extracted RNA was checked by electrophoresis on a 1% w/v agarose gel stained with ethidium bromide and quantified with NanoDrop 2100 UV-vis Spectrophotometer (Thermo-Scientific).

3.2.2. DNase treatment of total RNA

For 1µg of total RNA, DNase treatment was performed in a 10 µl reaction containing 1 µl (1U) DNase I (Invitrogen, USA), 1 µl 10× DNase I Reaction Buffer (Invitrogen, USA) and DEPC-treated water. After incubation at room temperature for 15 min, DNase I was inactivated by adding 1 µl of 25 mM EDTA solution (pH 8.0) to the

reaction mixture. The tube was then heated at 65°C for 10 min. The RNA sample was ready to be used in reverse transcription, prior to amplification.

3.2.3. Reverse Transcription PCR (RT-PCR)

Reverse transcription (RT) was used to generate amplified cDNAs of BARF1 gene. RT was performed using the SuperScript™ III One-Step RT-PCR System with Platinum® *Taq* (Invitrogen, USA) according to the manufacturer's recommendations. BARF1 specific primers (forward: 5'-ATGGCCAGGTTCATCGCTCAG-3' and reverse: 5'-TTATTGCGACAAGTATCCAGAAAC-3') with the concentration of 10µM were used in a total reaction volume of 50 µl. The components of the RT-PCR reaction as well as the amplification conditions are listed in Table 3.1. Amplified products were analyzed by agarose gel electrophoresis. Fragment of the correct size was cloned into the pCR4 vector as described in Section 3.2.4.

Table 3.1: Components of RT-PCR and amplification conditions

RT-PCR Components	Volume	Amplification Conditions
2× Reaction Mix	25 µl	I. cDNA synthesis and pre-denaturation (one cycle) 50°C for 30 min 94°C for 2 min II. PCR Amplification (40 cycles) 94°C for 15 s 55°C for 30 s 72°C for 2 min III. Final Extension (one cycle) 72°C for 10 min
Template RNA	1 µg	
Sense primer (10 µM)	1 µl	
Anti-sense primer (10 µM)	1 µl	
SuperScript III RT/Platinum *Taq* Mix	2 µl	
Milli-Q® water	Added up to 50 µl	

3.2.4. Cloning of the full length BARF1 into pCR4 sequencing vector

BARF1 that was amplified as described in Section 3.2.3 was cloned into the pCR®4-TOPO plasmid (Invitrogen, USA). The plasmid is a linearized vector with single 3'-thymidine overhangs that facilitates efficient TA-cloning of PCR products which normally have one overhanging adenosine residue at the 3' ends. Amplified BARF1 (1 µg) was mixed with 10 ng of pCR®4-TOPO vector in a total volume of 6 µl reaction mix containing 0.2 M NaCl and 0.01 M $MgCl_2$. The cloning reaction was incubated for 5 min at room temperature and placed on ice prior to transformation into *E. coli.*

3.2.5. Transformation of TOP10 competent *E. coli* cells

The cloning reaction solution (containing ligated pCR4-BARF1 plasmids) was introduced into the TOP10 competent *E. coli* cells by heat shock. Fifty µl competent cells were first thawed on ice. Two µl of the ligation reaction solution was added into the competent cells and incubated on ice for 30 min. The tube was then incubated at 42°C water bath for 90 s and then immediately transferred on ice for 2 min. The cells were transferred to 250 µl S.O.C. medium in a 15 ml tube and incubated at 37°C for 1 h with shaking at 150 rpm. One hundred µl of the cells was spread onto a Luria Bertani (LB) agar plate [1% (w/v) tryptone, 0.5% (w/v) yeast extract, 1% (w/v) NaCl, 1.5% (w/v) agar, pH 7.0, autoclaved] containing 100 µg/ml ampicillin. The plate was inverted and incubated at 37°C overnight. Bacterial clones were analyzed for the presence and the correct orientation of the insert using colony PCR using cycling conditions described in Table 3.1 (Pre-denaturation, PCR amplification and final extension conditions). Colonies harbouring the positive clones were selected and grown in 5 ml LB medium [1% (w/v) tryptone, 0.5% (w/v) yeast extract, 1% (w/v) NaCl, pH 7.0, autoclaved] containing 100 µg/ml ampicillin in 15 ml tubes at 37°C for 16h with shaking at 225 rpm.

3.2.6. Extraction of plasmid DNA from bacterial culture

Extraction of plasmid DNA was carried out at room temperature with QIAprep® Miniprep according to the manufacturer's instructions (QIAGEN, Hilden, Germany). The 5 ml overnight culture of *E. coli* in LB medium was centrifuged at 18000 × g for 30 s to obtain the pellet and the supernatant was discarded.

Pelleted bacterial cells were resuspended in 250 µl buffer P1 and transferred to a 1.5 ml centrifuge tube. Two hundred and fifty µl of buffer P2 was added and mixed by inverting the tube gently five times.

Three hundred and fifty µl buffer N3 was then added and mixed by inverting the tube gently five times. The lysed cells were centrifuged at 18000 × g for 10 min. The supernatant was transferred to the QIAprep Spin Column and centrifuged at 18000 × g for 30 s. The flow-through was discarded by decanting. The Spin Column was washed with 0.75 ml of buffer PE and centrifuged at 18000 × g for 1 min. The Spin Column was then placed in a clean 1.5 ml centrifuge tube and 50 µl of water was added to the center of the column. After 1 min incubation, the tube was centrifuged at 18000 × g for 1 min and the eluate containing the plasmid DNA was collected in the 1.5 ml centrifuge tube.

3.2.7. Purity of the extracted plasmid

The purity and concentration of the plasmids were assessed by UV spectrophotometry. One hundred µl of water was used as blank control. Two µl of sample DNA was diluted in 98 µl of water. The absorbance at 260 nm (A260) and 280 nm (A280) was measured using a cuvette. The A260 indicated the concentration of the plasmid DNA. The concentration of plasmid DNA was calculated based on the equation below;

DNA concentration (µg/ml) = (A260) × (dilution factor) × (50 µg DNA/ml)

The purity of the plasmids is indicated by the ratio of A260/A280 which is ~1.8-2.0 if the quality is high.

3.2.8. DNA sequencing of pCR4-BARF1 plasmid

DNA sequencing of the cloned BARF1 in pCR®-TOPO vector was performed using the M13 forward and reverse primers;

M13 forward (5'-GTAAAACGACGGCCAG-3')

M13 reverse (5'-CAGGAAACAGCTATGAC-3').

Sequencing was performed by Advanced Interactive Technologies (AIT) Pte Ltd, Singapore. The resulting DNA sequence for each BARF1 clone was aligned with the BARF1 sequence of AG876 and Akata strains using the CLC Sequence Viewer 5.1.2.0.

3.3. Designing siRNA targeting the BARF1 mRNA

Three siRNA sequences against the different positions of BARF1 open reading frame (ORF) (GenBank accession no. V01555) were designed using Ambion's online siRNA finder (http://www.ambion.com/techlib/misc/siRNA_finder.html). siRNAs were chemically synthesized and purified by Ambion Inc. (USA). The siRNA sequences against BARF1 are listed in Table 3.2. The locations of the siRNAs in BARF1 mRNA are depicted in Figure 3.1. A control siRNA which had no significant homology to any coding sequences in human and EBV genome was also synthesized and used.

Several recommendations for designing siRNA sequences were taken into consideration: (1) 19-29 nucleotides in length; (2) no significant homology to other genes;

(3) no runs of more than three same nucleotides; (4) low GC content (~30-50%); (5) no known site for RNA-protein interaction.

Table 3.2: siRNA sequences against BARF1 open reading frame

BARF1 siRNA	Positions in BARF1 ORF	siRNA sequence
siBARF1-1	189-207	Sense: 5'-GCACCACGAUGUCAUCUUUtt-3' Antisense: 5'-AAAGAUGACAUCGUGGUGCat-3'
siBARF1-2	409-427	Sense: 5'-CCAGACUUCUCUGUCCUUAtt-3' Antisense: 5'-UAAGGACAGAGAAGUCUGGga-3'
siBARF1-3	545-563	Sense: 5'- GCCUCUCUGUUGCUGUUGAtt-3' Antisense: 5'-UCAACAGCAACAGAGAGGCtc-3'

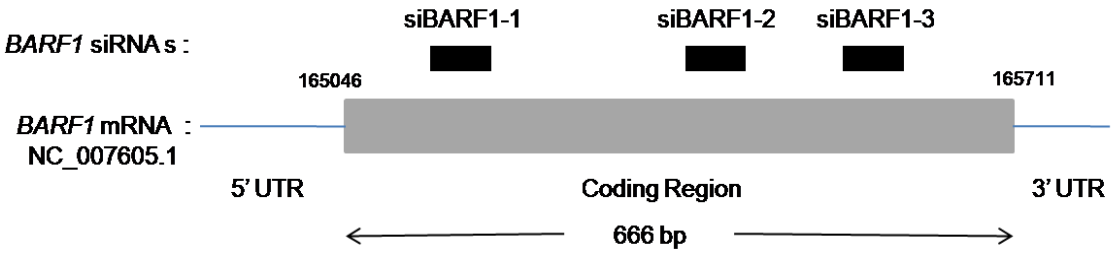

Figure 3.1. Locations of the siRNAs in BARF1 mRNA. The BARF1 mRNA is depicted as a line that is divided into 5' UTR, coding region, and 3' UTR.

3.4. siRNA transfection

The reverse transfection method was employed to deliver siRNA molecules into cell lines. In the reverse transfection method, cells are in suspension compared to the traditional pre-plating method. Because cells are in suspension, a larger amount of cell surface is exposed to transfection agent/siRNA complexes, and this contributes to the improved transfection efficiency.

Cells were harvested and the number of cells was determined as described in Section 3.6.1. Cells were resuspended in normal growth medium to 1×10^5 cells/ml and kept at 37°C until needed in subsequent steps. For a 6 well culture plate, 2.4 ml cells/well were used whereas 400 µl cells/well were used for a 24 well plate.

Transfection agent siPORT *NeoFX* (Ambion Inc., USA) was diluted in Opti-MEM I medium (GIBCO/BRL, USA) in a sterile conical tube and incubated for 10 min at room temperature. The volumes of siPORT *NeoFX* used were according to the manufacturer's recommendations. A range of siRNA concentration (5-50 nM) was prepared in Opti-MEM I medium. Diluted siRNA was mixed gently with diluted siPORT *NeoFX* by pipetting and incubated at room temperature for 10 min to allow for the formation of transfection agent/siRNA complexes. After incubation, transfection complexes (100 µl and 600 µl/well for 24 well and 6 well plates respectively) were dispensed into the empty wells of a culture plate. Nontransfected control wells were also set up. Next, cells suspension prepared earlier were added to the culture plate containing the transfection agent/siRNA complexes and mixed by rocking the plate gently back and forth. The plate was incubated at 37°C in

normal cell culture conditions for 24 h. The culture medium was then replaced with fresh normal medium and incubated.

3.5. Analysis of gene expression in siRNA-treated cells

3.5.1. Total RNA extraction

RNA was extracted from cells using the RNeasy Mini Kit® (Qiagen, Germany) according to the manufacturer's protocol. (Refer Section 3.2.1).

3.5.2. DNase treatment of total RNA

Total RNA was treated with DNase I (Invitrogen, USA) as explained in Section 3.2.2. The quality and integrity of the treated RNA was then assayed using the Agilent RNA 6000 Nano kit. The assay was run on the Agilent 2100 Bioanalyzer instrument and data was analyzed using the Agilent 2100 Expert Software. An RNA Integrity Number (RIN score) was generated for each sample on a scale of 1-10 (1=lowest; 10=highest) as an indication of RNA quality.

3.5.3. cDNA synthesis

For first strand cDNA synthesis, SuperScript™ III First-Strand Synthesis System (Invitrogen, USA) was used. Five µg of total RNA was mixed with 1 µl of 50 µM oligo $(dT)_{20}$ and 1 µl of 10 mM dNTP mix in a total reaction volume of 10 µl.

The RNA/primer mixture was incubated at 65°C for 5 min and placed on ice for at least 1 min. Next, 10 µl of cDNA Synthesis Mix (Refer Table 3.3) was added to the mixture, mixed gently and incubated at 50°C for 50 min. The reaction was terminated by heating at 85°C for 5 min and then chilled on ice. Reaction was collected by centrifugation and 1 µl of RNase H was added to each tube. Tube was incubated at 37°C for 20 min. Synthesized first strand cDNA was stored at -20°C or used immediately in real time quantitative PCR assay.

Table 3.3: Components of the cDNA Synthesis Mix

Component	Volume/reaction
10× RT buffer	2 µl
25 mM $MgCl_2$	4 µl
M DTT	2 µl
RNaseOUT™ (40 U/µl)	1 µl
SuperScript™ III RT (200 U/µl)	1 µl

3.5.4. Real Time Quantitative PCR Assay

Real time quantitative PCR using absolute quantification approach was used to quantify the copy number of BARF1 molecules within cDNA samples. An internal reference standard in the form of a plasmid containing only the target gene (pCR-TOPO-BARF1) was employed. Purified plasmid clones were quantified using spectrophotometer

(Shimadzu, Japan). A known amount of plasmid was used to construct a calibration curve and then the copy numbers of unknown samples were identified from this. Results were expressed in absolute terms as the number of copies of BARF1 gene.

With the molecular weight of the plasmid and insert known, the copy number was calculated as follows;

Weight in daltons (g/mol) = (bp size of ds product)(330 Da × 2nt/bp)

Hence: (g/mol)/Avogadro's number = g/molecule = copy number

(where: bp = base pairs, ds = double-stranded, nt = nucleotides).

Knowing the copy number and concentration of plasmid DNA, the precise number of molecules added to subsequent real-time PCR runs was calculated.

Real-time PCR runs were performed using Rotor-Gene™ 6000 (Qiagen, Germany). Each reaction contained 1× TaqMan® Universal PCR Master Mix, No AmpErase® UNG (Applied Biosystems), 1× target primers and TaqMan® probes mix and template DNA (either cDNA diluted in RNase-free water or plasmid DNA dilutions ranging from 1×10^3 to 1×10^9) in a final volume of 20 µl. Cycling conditions were as follows; 10 min at 95 °C followed by 40 cycles of 15 s at 95°C and 1 min at 60°C.

A standard curve was drawn by plotting the natural log of the threshold cycle (C_T) against the natural log of the number of molecules. The C_T was defined as the cycle at which a statistically significant increase in the magnitude of the signal generated by the PCR reaction was first detected. C_T was calculated under default settings for the Rotor-Gene 6000 Series Software 1.7 (Applied Biosystems, USA).

The equation drawn from the graph was used to calculate the precise number of specific BARF1 cDNA molecules present per microgram of total oligo-dT primed cDNA, tested in the same reaction plate as the standard.

3.5.5. Semi-quantitative Reverse Transcription PCR (RT-PCR)

Semi-quantitative RT-PCR was performed to identify expression levels of genes in cells treated with BARF1 siRNA. Total RNA was extracted and treated with DNase (as described in Sections 3.2.1 and 3.2.2 respectively). First strand cDNA was then synthesized as described in Section 3.5.3. PCR amplification was performed using gene-specific primers (Table 3.4) with the concentration of 10µM and used in a total reaction volume of 50 µl.

For comparison of the expression levels of genes among different cell populations, the number of PCR cycles was optimized for each primer set so as to visualize PCR products at their linear range. Aliquots were removed and examined from each PCR reaction every three or five additional cycles after 15 cycles of PCR reaction. Relative levels of GAPDH expression were detected and normalized as loading control.

PCR amplifications of GAPDH gene were performed as independent reactions. The amplification conditions were 30 cycles at 94°C for 30 s, 53°C for 30 s, and 72°C for 30 s. The PCR products were visualized by agarose gel electrophoresis and the intensity of the bands was quantified by densitometry using Image J software.

Table 3.4: Oligonucleotide primers used in RT-PCR analysis

Transcript	Primer sequence (5'-3')	Product size	GenBank No.
Bcl-2	CCTGTGGATGACTGAGTACC GAGACAGCCAGGAGAAATCA	128 bp	NM_000633
BAX	GTTTCATCCAGGATCGAGCAG CATCTTCTTCCAGATGGTGA	537 bp	NM_004324
GAPDH	TGCCTCCTGCACCACCAACT CGCCTGCTTCACCACCTTC	349 bp	NM_001289746.1

3.6. Cell proliferation assay

3.6.1. Trypan blue exclusion assay

The dye exclusion test is used to determine the number of viable cells present in a cell suspension. It is based on the principle that live cells possess intact cell membranes that exclude certain dyes, such as trypan blue, whereas dead cells do not. In this test, a cell suspension is simply mixed with dye and then visually examined to determine whether cells take up or exclude dye. A viable cell will have a clear cytoplasm whereas a nonviable cell will have a blue cytoplasm.

Cell pellet was resuspended thoroughly in 1 ml of 1× PBS to disperse any clumps. Fifty µl cell suspension was added to 450 µl of 0.4% trypan blue in a microcentrifuge tube and mixed gently. Ten µl of cell suspension was then transferred immediately to the edge of a hemocytometer (Improved Neubauer) chamber. The suspension was expelled and let to be drawn under the coverslip by capillarity. The slide was then transferred to the microscope stage and cells lying within the 1 mm^2 area in the central area of the grid were counted manually using a tally counter. The concentration of cells was calculated using the formula below;

$$c = n \times \text{dilution factor} \times 10^4$$

where c is the cell concentration (cells/ml) and n is the number of cells counted.

3.6.2. WST-1 assay

Cells were seeded in microplates (tissue culture grade, 96 wells, flat bottom) at a concentration of 4×10^3 cells/well. Cells were incubated for 48h, 72h, and 96h at 37°C and 5% CO_2. For each incubation time, different plates were used. On the day of the assay, 10 µl/well of Cell Proliferation Reagent WST-1 (Roche, Germany) was added and incubated for 4h at 37°C and 5% CO_2. Plates were shaken thoroughly for 1 min on a shaker. Absorbance of the samples was measured against a background control as blank using a microplate (ELISA) reader. The wavelength for measuring the formazan product is between 420 – 480 nm (maximum absorption at about 440 nm).

3.7. Detection of apoptotic cells

3.7.1. Annexin V staining

The analysis of phosphatidylserine on the outer leaflet of apoptotic cell membranes was performed using Annexin-V-Fluorescein and propidium iodide (PI) for the differentiation from necrotic cells. Staining was performed using the Annexin-V-FLUOS Staining Kit (Roche, Germany) according to the manufacturer's instructions. For positive control, apoptosis was induced using 1µM staurosporine (Cell Signaling Technology, USA).

For staining of cell suspensions, 10^6 cells were washed with PBS and centrifuged at 200 × g for 5 min. Cell pellet was resuspended in 100 µl of Annexin-V-FLUOS labeling solution and incubated at 15-25°C for 10-15 min. For adherent cells grown in 96-well plate, medium was removed and 100 µl of Annexin-V-FLUOS labeling solution was added to each well. Plate was incubated at 15-25°C for 10-15 min. Stained cells were analyzed on a flow cytometer.

For each 10^6 stained cells, 0.5 ml Incubation buffer was added and analyzed on a flow cytometer using 488 nm excitation and a 515 nm bandpass filter for fluorescein detection and a filter >600 nm for PI detection. Electronic compensation of the instrument was carried out to exclude overlapping of the two emission spectra. Gating was performed on the FSC (forward scatter) vs SSC (side scatter) plot that encompasses >90% of the whole cell population.

3.7.2 Mitochondrial membrane potential

The loss of mitochondrial membrane potential (ΔΨ) is a hallmark for apoptosis. To measure the mitochondrial potential in cells, the APO LOGIX JC-1 Mitochondrial Membrane Potential Assay Kit (Cell Technology Inc, USA) was used according to the manufacturer's instructions. About 0.5 ml cell suspension was transferred into a sterile centrifuge tube and centrifuged for 5 min at room temperature at 400 × g. Supernatant was removed and cells were resuspended in 0.5 ml 1× JC-1 reagent. Cells were then incubated at 37°C in a 5% CO_2 incubator for 15 min. This was followed by centrifugation for 5 min at 400 × g and the supernatant was removed. The cell pellet was resuspended in 2 ml 1× Assay Buffer, centrifuged and supernatant was removed. Stained cells were analyzed on a flow cytometer.

Cell pellet was resuspended in 0.5 ml 1× Assay Buffer and analyzed immediately by flow cytometry. Mitochondria containing red JC-1 aggregates in healthy cells are detectable in the FL2 channel and green JC-1 monomers in apoptotic cells are detectable in the FITC channel (FL1). Electronic compensation of the instrument was carried out to exclude overlapping of the two emission spectra. Gating was performed on the FSC (forward scatter) vs SSC (side scatter) plot that encompasses >90% of the whole cell population.

3.8. Western blot analysis

3.8.1. Preparation of cell lysates

For adherent cells, culture medium was carefully removed by decanting. Appropriate amount of M-PER reagent (Thermo Scientific, USA) was then added to the plate/flask (Refer Table 3.5) and shaken gently for 5 min. The lysate was collected and transferred to a microcentrifuge tube. Samples were centrifuged at ~14000 × g for 5-10 min to pellet the cell debris. Supernatant was then transferred to a new tube for analysis.

Suspension cells were pelleted by centrifugation at 2500 × g for 10 min. Supernatant was discarded and M-PER reagent was added to the cell pellet. At least 1 ml of M-PER reagent was used for each 100 mg (~ 100 µl) of wet cell pellet. The mixture was pipetted up and down to resuspend the pellet. Cell debris was removed by centrifugation at ~ 14000 × g for 15 min. Supernatant was then transferred to a new tube for analysis.

Table 3.5: Volume of M-PER used for different sizes of standard culture plates

Plate size/Surface area	M-PER reagent volume
100mm*	500-1000 µl
60 mm	250-500 µl
6-well plate	200-400 µl per well
24-well plate	100-200 µl per well
96-well plate	50-100 µl per well

*Cells grown in 100 mm plates typically contain 10^7 cells (50 mg) and yield ~3 mg total protein depending on cell type.

3.8.2. Preparation of mitochondria and cytosolic fractions

For extraction of mitochondria and cytosolic fractions, the Mitochondria Isolation Kit for cultured cells (Thermo-Scientific, USA) was used according to the manufacturer's protocols. Briefly, 800 µl of Mitochondria Isolation Reagent A was added to pelleted cells. Tube was vortexed at medium speed for 5 s and incubated on ice for exactly 2 min. Next, 10 µl of Mitochondria Isolation Reagent B was added and tube was vortexed at maximum speed for 5 s. Tube was incubated on ice for 5 min, and vortexed at maximum speed every minute. Next, 800 µl of Mitochondria Isolation Reagent C was added and tube was inverted several times to mix. Tube was centrifuged at 700 × *g* for 10 min at 4°C. The supernatant was transferred to a new 2 ml tube and centrifuged at 3000 × g for 15 min at 4°C.

The supernatant (cytosol fraction) was transferred to a new tube. The pellet contained the isolated mitochondria. Five hundred μl Mitochondria Isolation Reagent C was added to the pellet, and centrifuged at 12000 × *g* for 5 min. Supernatant was discarded. The mitochondrial pellet was maintained on ice before immunoblot analysis due to the fact that freezing and thawing may compromise mitochondria integrity. For analysis by Western blotting, mitochondrial pellet was boiled with SDS-PAGE sample buffer and applied to the gel.

3.8.3. Concentration of secreted protein

Culture media was collected and centrifuged at 3000 × *g* for 10 min to eliminate cellular debris. Following clearing, 10 ml culture media were concentrated to 10 μl with centrifugal filter Vivaspin 15R. Examination of secreted BARF1 expression was performed using this concentrated fraction.

3.8.4. Measurement of protein concentration

Protein concentration was measured on a 96-well plate using Bio-Rad dye reagent. A two-fold serial dilution of bovine serum albumin (BSA) (Bio-Rad, USA) protein in M-PER reagent was used as the protein standards (0.5, 1, 2, 4, 8 μg/μl in M-PER reagent). Ten μl of protein standards or samples was added into each well of a 96-well plate. Two

hundred μl of Bio-Rad dye reagent were added and mixed gently. After incubation at room temperature for 5 min, the absorbance at 590 nm was measured using MRX microplate

reader (Dynex Technologies Inc, USA). The standard curve was generated by plotting standard protein concentrations against absorbance at 590 nm. The corresponding protein concentration of the sample was determined from the standard curve using the equation of the slope of the straight line:

y = ……. x, where x = absorbance, y = protein concentration (µg/µl).

3.8.5. SDS-polyacrylamide gel electrophoresis (PAGE)

3.8.5.1. Gel set-up

Vertical SDS-PAGE slab gels were prepared using mini-PROTEAN® 3 electrophoresis system (Bio-Rad, USA). Tables 3.6 and 3.7 list the volume of each reagents required for setting up resolving and stacking gels of two 0.75-mm thick acrylamide gels. A resolving gel [7.5, 10 or 12.5% (w/v) acrylamide (depending on the size of protein examined), 125mM Tris-HCl (pH 8.8), 0.1% (w/v) SDS, 0.12% (w/v) ammonium persulfate and 0.2% (v/v) TEMED] was prepared by adding freshly prepared ammonium persulfate and TEMED to the earlier mixed resolving gel solution in a 25-ml beaker. The resolving gel was allowed to set in the gel system for 30 min at room temperature. A stacking gel [4% (w/v) acrylamide, 37.5 mM Tris-HCl (pH 6.8), 0.1% (w/v) SDS, 0.12% (w/v) ammonium persulfate and 0.2% (v/v) TEMED] was set on the top of a resolving gel and let to polymerize for 30 min at room temperature.

Table 3.6: List of components for setting two 0.75-mm thick resolving gels

Reagent	Volume		
	12.5%	10%	7.5%
Water	4.36 ml	4.86 ml	5.485 ml
40% (w/v) acrylamide/bis-acrylamide (19:1)	3 ml	2.5 ml	1.875 ml
4× resolving buffer	2.5 ml	2.5 ml	2.5 ml
*10% (w/v) ammonium persulfate (in water)	120 µl	120 µl	120 µl
*TEMED	20 µl	20 µl	20 µl
Total volume	10 ml	10 ml	10 ml

4× resolving buffer contains 500 mM Tris-HCl (pH 8.8), 0.4% (w/v) SDS.

* 10% (w/v) ammonium persulfate and TEMED were added just before setting the gel.

Table 3.7: List of components for setting stacking gels

Reagent	Volume
Water	3.18 ml
40% (w/v) acrylamide/bis-acrylamide (19:1)	0.5 ml
4× stacking buffer	1.25 ml
*10% (w/v) ammonium persulfate (in water)	60 µl
*TEMED	10 µl
Total volume	5 ml

4× stacking buffer contains 150 mM Tris-HCl (pH 6.8), 0.4% (w/v) SDS.
* 10% (w/v) ammonium persulfate and TEMED were added just before setting the gel.

3.8.5.2. Protein preparation and gel electrophoresis

Each protein sample was prepared to have equal volume and equal amount of protein. Each protein sample was prepared by adding equal amount of protein (i.e., 20 μg), 2 μl of 6× sample buffer [350mM Tris-HCl (pH 6.8), 30% (v/v) glycerol, 21.4% (v/v) β-mercaptoethanol, 10% (w/v) SDS, 0.01% (w/v) bromophenol blue] and appropriate M-PER reagent to have equal volume of 12 μl. After boiling at 100°C for 5 min, the denatured protein samples were immediately cooled down on ice and centrifuged briefly at 4°C. Equal volume of the samples (10 μl) was loaded onto the SDS-polyacrylamide gel and electrophoresis was carried out with running buffer [25mM Tris-HCl, 192mM glycine, 0.1% (w/v) SDS] at a constant current (20 mA per gel) for ~ 1 hr at room temperature until the bromophenol blue (in the sample buffer) reached the bottom of the gel. Five μl Fermentas Page Ruler (Fermentas, USA) was also run to indicate the molecular weight of the proteins.

3.8.5.3. Transfer of proteins onto a polyvinylidene difluoride membrane

After electrophoresis, the proteins were transferred onto a polyvinylidene difluoride (PVDF) membrane (PALL Corporations, Pensacola). The transfer was carried out in a semi-dry transblot (Bio-Rad, USA) with ice-cold transfer buffer [25mM Tris, 192mM glycine, 20% (v/v) methanol] at a constant voltage of 20 V for 50min.

3.8.6. Protein signal detection

3.8.6.1. Antibody incubation

The membrane was blocked with 10% blocking solution (KPL Inc, USA) in Tris-buffered saline-Tween 20 [TBST; 20mM Tris-HCl (pH 7.5), 137 mM NaCl, 0.1% (v/v) Tween 20] for 1 hr at room temperature with gentle agitation. The membrane was washed in TBST for 15 min once and then 5 min twice. The membrane was then incubated with primary antibody in 5% (w/v) blocking solution in TBST for 1 hr at room temperature with gentle shaking on a belly dancer. The details of the antibodies used and their immunoblotting conditions are listed in Table 3.8.

After washing several times in TBST, the membrane was incubated with appropriate secondary antibody conjugated with alkaline phosphatase in 3% (w/v) blocking solution in TBST for 1 hr at room temperature with gentle shaking on a belly dancer. Membrane was washed in TBST for 15 min once and 5 min thrice on a belly dancer. After the final wash, excess TBST was drained and the blot was placed on a clean container with the protein side up for protein signal detection.

3.8.6.2. Signal detection

Signals were visualized by either enhanced chemiluminescent detection system using LumiGLO® Reagent (Cell Signaling Technology, Danvers, MA) or colorimetry using the BCIP/NBT phosphatase substrate system.

For enhanced chemiluminescent detection system, substrate was prepared by diluting 20× LumiGLO and 20× Peroxide to 1× in water. The mixture was applied onto the surface of the membrane (bound with horse radish peroxidase-conjugated antibodies) with the protein side up and incubated in the dark for 1 min at room temperature. Excess solution was removed, and then the membrane was wrapped with the saran wrap and placed in an X-ray film cassette with protein side up. In the dark room, an X-ray film (Kodak) was placed onto the protein side of the membrane and exposed for 1-5 min to obtain the signals.

To develop the film, the X-ray film was immersed in developer (Kodak) for 5 min with gentle shaking at room temperature. The film was then rinsed in water and fixed in a fixer (Kodak) for 5 min with gentle shaking. Next, the film was rinsed in water and air-dried. Signals were analyzed using a gel documentation system. Expressions of GAPDH, β-actin or α-tubulin were also assessed on the same membrane as an internal loading control using specific antibodies.

For the colorimetry method, alkaline phosphatase-conjugated IgG was added to the membrane and detected with the BCIP/NBT phosphatase substrate system (KPL, USA) according to the manufacturer's protocol.

Table 3.8: List of antibodies used in Western blotting and immunoprecipitation (IP)

Antibody	Protein size (kDa)	Species	Antibody dilution	Source
Primary antibody				
GAPDH	40	Mouse	1:1000	Abcam
β-actin	42	Mouse	1:1000	Abcam
Cleaved PARP	89	Rabbit	1:1000	Cell Signaling Technology
Cleaved Caspase-3	19	Rabbit	1:1000	Cell Signaling Technology
Cleaved Caspase-9	37	Rabbit	1:1000 1:100 (IP)	Cell Signaling Technology
Cytochrome c	14	Rabbit	1:1000	Cell Signaling Technology
COX IV	17	Rabbit	1:1000	Cell Signaling Technology
Apaf-1	135	Rabbit	1:1000 1:100 (IP)	Cell Signaling Technology
BARF1	26	Rabbit	1:100	A gift from Dr. Middeldorp
Bcl2	28	Rabbit	1:1000	Cell Signaling Technology
BAX	20	Rabbit	1:1000	Cell Signaling Technology
Secondary antibody				
Anti-mouse IgG, AP-linked		Goat	1:5000	Sigma-Aldrich
Anti-rabbit IgG, AP-linked		Goat	1:5000	Santa Cruz Biotechnology
Normal IgG		Rabbit	1:100 (IP)	Santa Cruz Biotechnology

3.9. Apoptosis antibody array

Detection of apoptotic proteins was done using the RayBio® Human Apoptosis Antibody Array kit with the glass-slide array format AAH-APO-G1 (RayBioTech, USA). This kit detects 43 different apoptotic proteins as well as GAPDH (Glyceraldehyde 3 phosphate dehydrogenase) as a loading control indicator for protein samples (Table 3.9) with picogram-per-milliliter (pg/ml) sensitivity.

Briefly, glass chip was taken out from the box and air-dried for 60 minutes. Glass chip was then assembled into incubation chamber and incubation frame. One hundred µl of 1X Blocking Buffer was added into each well printed with antibodies and incubated at room temperature for 30 min to block slides. Blocking Buffer was then decanted from each well. One hundred µl of protein sample (500 µg/ml) was added to array wells and array was incubated at 4°C overnight. Samples were decanted from each well and array was washed five times (2 min per wash) with 150 µl of 1X Wash Buffer I followed by washing twice with 150 µl of 1X Wash Buffer II (2 min per wash). Wash step was done at room temperature with gentle shaking and Wash Buffer I and II were completely removed in each wash step.

Next, 70 µl of diluted biotin-conjugated antibodies was added to each well and array was incubated at room temperature for 2h. This was followed by wash steps using 1X Wash Buffer I and II as described above. Then, 70 µl of 1,500 fold diluted HiLyte Plus™-conjugated streptavidin was added to each array well and the incubation chamber was sealed with adhesive film. The incubation plate was covered with aluminum foil to avoid exposure to light and incubated at room temperature for 2h. Array slide was then washed twice with Wash Buffer I as described above and excess wash buffer was decanted from wells.

The slide was disassembled out of the incubation frame and chamber and the whole slide was placed in a 50 ml centrifuge tube. About 30 ml Wash Buffer I was added to cover the whole slide and the tube was gently shaken at room temperature for 10 minutes. Wash Buffer I was then decanted and the wash step was repeated once. The slide was then washed with Wash Buffer II (about 30 ml) with gentle shake at room temperature for 10 minutes. The slide was then rinsed with distilled H_2O. Water droplets were removed by centrifuging at 1000 rpm for 3 min and slide was air dried completely for at least 20 min, protected from light.

The array slide was scanned with G2505C microarray scanner (Agilent Technologies) using the cy3 (green) channel. The image extraction and data analyses were done using GenePix® Pro Microarray Acquisition and Analysis software version 6.1.0.4 (Agilent Technologies). The background corrected raw intensity values were used for analysis.

The biotin-conjugated proteins produce fluorescence signals, which were used to identify the orientation and to compare the relative expression levels among the different wells. The positive controls are biotinylated antibody. Standardized amounts of biotinylated IgG are printed directly onto each array and if all other variables are the same, the positive control intensities will be equal. The positive controls monitor the detection process and were used for normalization.

Table 3.9: RayBio® Human Apoptosis Antibody Array G series

	A	B	C	D	E	F	G	H	I	J	K	L	M
1	Pos	Pos	Pos	Neg	Neg	bad	bax	bcl-2	bcl-w	BID	BIM	Caspase 3	Caspase 8
2	Pos	Pos	Pos	Neg	Neg	bad	bax	bcl-2	bcl-w	BID	BIM	Caspase 3	Caspase 8
3	CD40	CD40L	cIAP-2	cytoC	DR6	Fas	FasL	neg	HSP27	HSP60	HSP70	HTRA	IGF-I
4	CD40	CD40L	cIAP-2	cytoC	DR6	Fas	FasL	neg	HSP27	HSP60	HSP70	HTRA	IGF-I
5	IGF-II	IGFBP-1	IGFBP-2	IGFBP-3	IGFBP-4	IGFBP-5	IGFBP-6	IGF-1sR	livin	p21	p27	p53	SMAC
6	IGF-II	IGFBP-1	IGFBP-2	IGFBP-3	IGFBP-4	IGFBP-5	IGFBP-6	IGF-1sR	livin	p21	p27	p53	SMAC
7	Survivin	sTNF-R1	sTNF-R2	TNFalpha	TNF-beta	TRAILR-1	TRAILR-2	TRAILR-3	TRAILR-4	XIAP	Neg	Neg	Neg
8	Survivin	sTNF-R1	sTNF-R2	TNFalpha	TNF-beta	TRAILR-1	TRAILR-2	TRAILR-3	TRAILR-4	XIAP	Neg	Neg	Neg

3.10. Immunoprecipitation

Immunoprecipitation of caspase 9 from total protein was done by incubating 1 μg anti-caspase 9 antibody (Cell Signaling Technology, USA) with 400 μg of total protein for 1 h at 4°C. Next, 20 μl of protein A agarose beads (Santa Cruz Biotechnology, USA) was added and incubated at 4°C overnight on a rocker platform. Immunoprecipitates were collected by centrifugation at 1000 × g for 5 min at 4°C.

Precipitates were washed five times with M-PER Mammalian Protein Extraction Reagent (Thermo-Scientific, USA) and once with PBS. The pellet was resuspended in 1× sample buffer [50 mM Tris (pH 6.8), 100 mM bromophenol blue and 10% glycerol]. This solution was incubated at 90°C for 10 min, electrophoresed and immunoblotted with anti-Apaf-1 (Cell Signaling Technology, USA).

3.11. Statistical analysis

Statistical analyses were done using Microsoft Office Excel 2007. Student's t-tests were performed to determine significance level of statistical data. *P* value was used to gauge the significant difference between samples. Two levels of *p* value were used to discern samples that are statistically significant from samples that are statistically highly significant. $p<0.05$ was considered to be statistically significant and a more stringent threshold $p<0.001$ was considered to be statistically highly significant.

CHAPTER 4: RESULTS

4.1. BARF1 mRNA expression in EBV-positive malignant cells

4.1.1 BARF1 is expressed in AG876 and Hone-Akata cells

To assess BARF1 silencing in EBV-positive malignant cells, I first sought to detect the expression of BARF1 in AG876 and Hone-Akata cells. AG876 are EBV-positive malignant cells (EBV type 2) derived from a patient with Burkitt's lymphoma (Pizzo et al., 1978) whereas Hone-Akata is an NPC epithelial cell line that is superinfected with the Akata strain of EBV (EBV type 1) (Glaser et al., 1989).

Total RNA was extracted from these cells and subjected to RT-PCR amplification. Figure 4.1(a) shows the electrophoregram of the total RNA from AG876 and Hone-Akata cells. The total RNA is shown to have sharp and clear 28S and 18S rRNA bands. Partially degraded RNA will have a smeared appearance when electrophoresed. The 28S rRNA band is approximately twice as intense as the 18S rRNA band. This 2:1 ratio (28S:18S) indicates that the extracted RNA is intact.

Using primers BARF1-F and BARF1-R, the 666 bp amplicon of BARF1 was amplified from AG876 and Hone-Akata cells as shown in Figure 4.1(b). The full length BARF1 was then cloned into pCR4 sequencing vector and sequenced. DNA sequencing analysis (Appendix 1) revealed that the BARF1 sequence from both AG876 and Hone-Akata cell lines matched the BARF1 sequence of AG876 and Akata EBV strains respectively. This confirmed that there were no mutations on BARF1 genes in both AG876 and Hone-Akata cell lines.

As shown in Figure 4.1(b), it was confirmed that AG876 and Hone-Akata cell lines express BARF1 gene. These cell lines were therefore chosen to evaluate the knockdown effect of BARF1-specific siRNA.

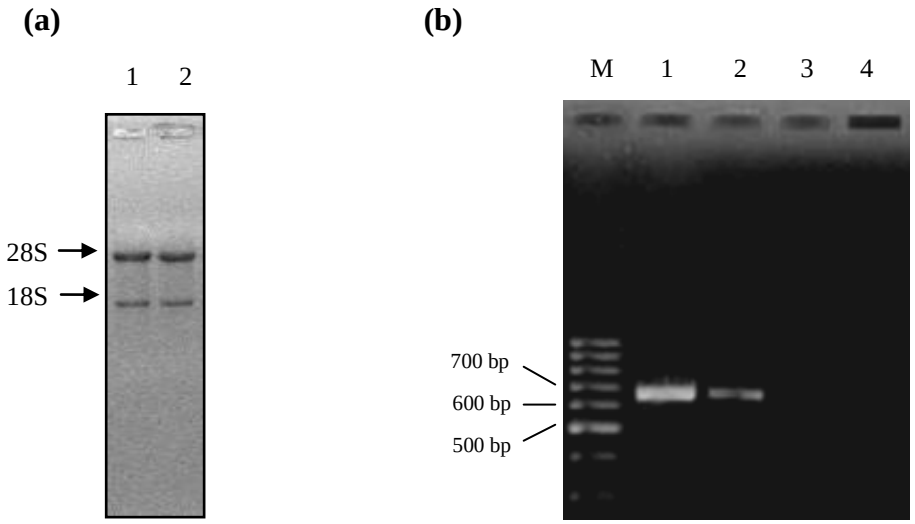

Figure 4.1. RT-PCR amplification of BARF1 from AG876 and Hone-Akata cell lines. (a) Total RNA extracted from AG876 (Lane 1) and Hone-Akata (Lane 2) cells. (b) Amplification of BARF1 (~666 bp). Lane M: 100 bp molecular marker. Lane 1: BARF1 from AG876 cells. Lane 2: BARF1 from Hone-Akata cells. Lane 3: Negative control for AG876 cells. Lane 4: Negative control for Hone-Akata cells.

4.2. BARF1 siRNA suppresses the expression of BARF1 at the mRNA level

4.2.1. RNA quality and integrity analysis

Extracted RNA is rapidly digested in the presence of the nearly ubiquitous RNase enzymes. As a result, shorter fragments of RNA commonly occur in a sample, which can potentially compromise results of downstream applications (Auer et al., 2003; Imbeaud et al., 2005).

Because of the critical influence of RNA integrity on downstream experiments, prior to qRT-PCR analysis, total RNA that was extracted from untreated and siRNA-treated AG876 and Hone-Akata cells were treated with DNase I and subjected to RNA quality and integrity analysis. Figure 4.2 shows the quality of RNA analyzed on Agilent 2100 Bioanalyzer. The microcapillary electrophoresis image shows two bands comprising the 28S and 18S ribosomal RNA (rRNA).

RIN values range from 1 (totally degraded) to 10 (intact). The representative RIN scores of RNA in this study are shown in Figures 4.3 and 4.4. The RNA used in this study have RIN values ranging from 9.60 to 10, indicating that the RNA are intact and are of high quality.

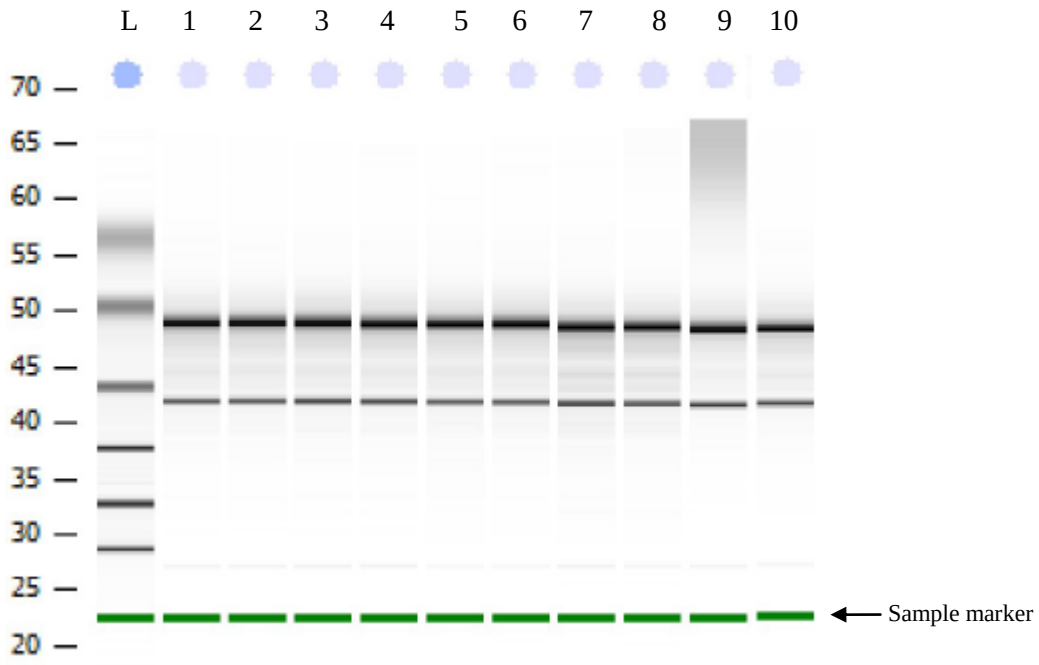

Figure 4.2. Quality of RNA extracted from control and siBARF1-treated AG876 and Hone-Akata cells. RNA was analyzed using Agilent 2100 Bioanalyzer. Lane L: RNA ladder; lanes 1-5: AG876 untreated, siNEG, siBARF1-1, siBARF1-2, siBARF1-3; lanes 6-10: Hone-Akata untreated, siNEG, siBARF1-1, siBARF1-2, siBARF1-3.

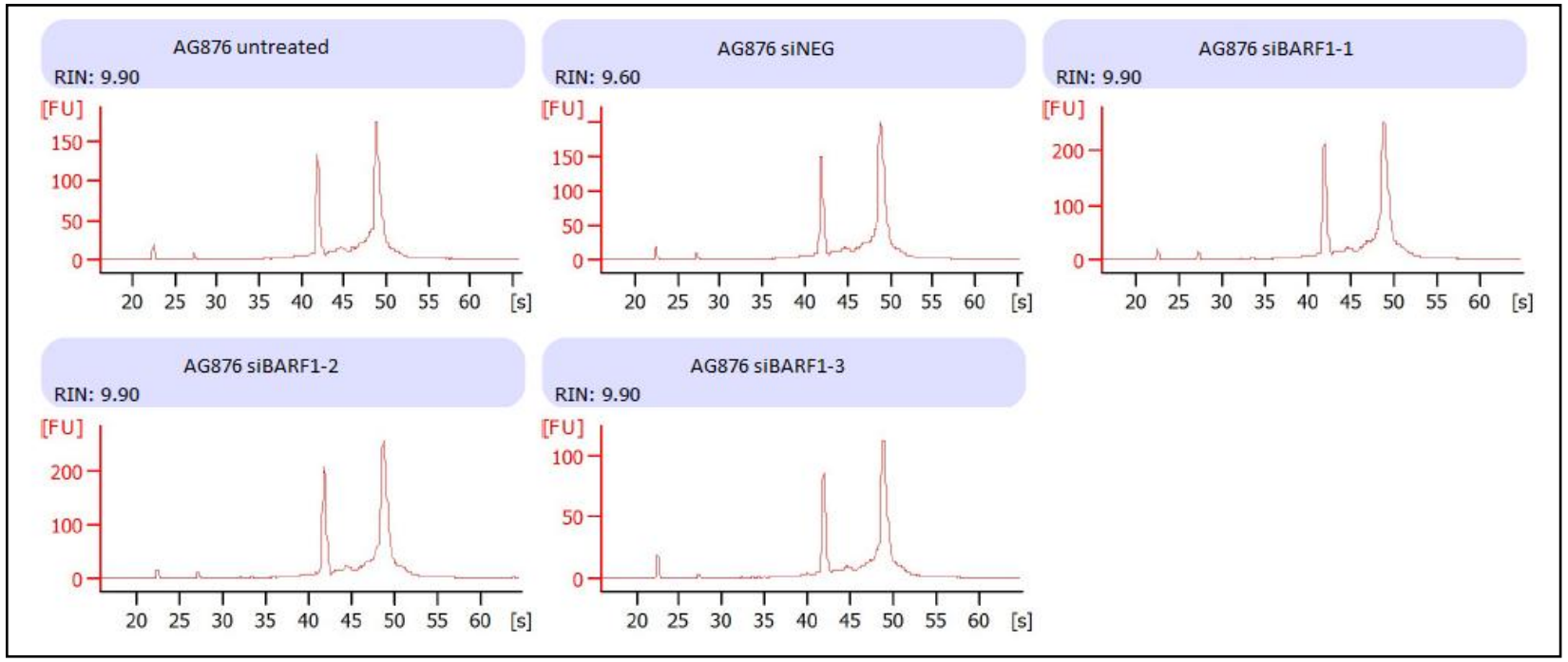

Figure 4.3. RIN values of RNA extracted from control and siBARF1-treated AG876 cells. RNA was analyzed using Agilent 2100 Bioanalyzer.

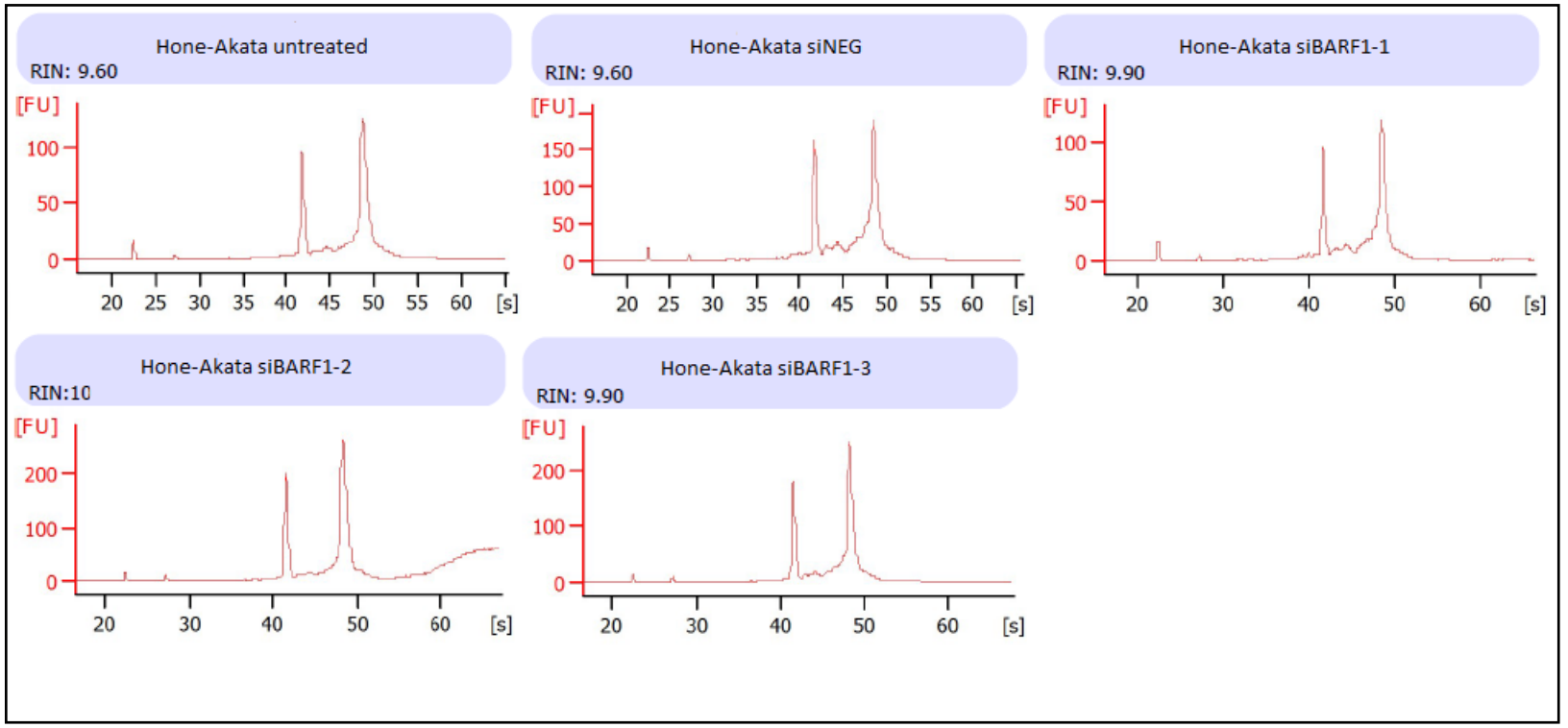

Figure 4.4. RIN values of RNA extracted from control and siBARF1-treated Hone-Akata cells. RNA was analyzed using Agilent 2100 Bioanalyzer.

4.2.2. Single transfection of BARF1 siRNA

To silence the expression of BARF1 mRNA specifically, siRNAs targeting BARF1 were designed according to the cDNA sequenced in AG876 and Hone-Akata cells. Three siRNA sequences against the open reading frame of BARF1 mRNA (named siBARF1-1, siBARF1-2 and siBARF1-3) as well as a control siRNA (named siNEG) which had no significant homology to any coding sequences in human and EBV genome were synthesized.

All three siRNAs (siBARF1-1, siBARF1-2 and siBARF1-3) were tested for the most effective BARF1 gene knockdown ability. siRNA molecules in a range of siRNA concentration (5-50 nM) were delivered transiently into AG876 and Hone-Akata cells using the reverse transfection method. In the reverse transfection method, cells are in suspension compared to the traditional pre-plating method. In suspension form, a larger amount of cell surface is exposed to transfection agent/siRNA complexes, and this contributes to the improved transfection efficiency.

To assess the efficiency of BARF1 silencing, total RNA from siRNA-treated and control cells was isolated. After cDNA synthesis, quantitative real-time (qRT)-PCR (using Taqman probes) targeting BARF1-specific sequence was used to determine BARF1 mRNA expression levels. Results were expressed in absolute terms as the number of copies of BARF1 gene.

In AG876 and Hone-Akata cells, 48 h post-transfection with siRNAs (5-50 nM) targeting BARF1 gene caused a dose-dependent downregulation of BARF1 gene expression (Figure 4.5).

After 48 h of transfection with 35 nM siBARF1-1, siBARF1-2 and siBARF1-3, BARF1 mRNA expression was downregulated to 54%, 27% and 50% residual level compared to untreated cells in AG876 cells and 67%, 43% and ~57% residual level in Hone-Akata cells respectively (Figure 4.5). The negative control siRNA had no significant effect on BARF1 expression (Figure 4.5).

Using 50 nM siRNA concentration, we noticed a further but minimal downregulation of BARF1 when compared with 35 nM siRNA (Figure 4.5). In AG876 cells, siBARF1-1, siBARF1-2 and siBARF1-3 downregulated BARF1 expression to 52%, 24% and 47% residual level respectively. In Hone-Akata cells, siBARF1-1, siBARF1-2 and siBARF1-3 downregulated BARF1 expression to 64%, 40% and 53% residual level respectively (Figure 4.5).

However, in cells treated with 50 nM siNEG, a considerably high amount of cell detachment was noticed when compared with cells transfected with 35 nM siNEG, suggesting cell cytotoxicity. This effect may be due to the use of high amount of transfection agent in order to deliver high amount of siRNA (50 nM).

.

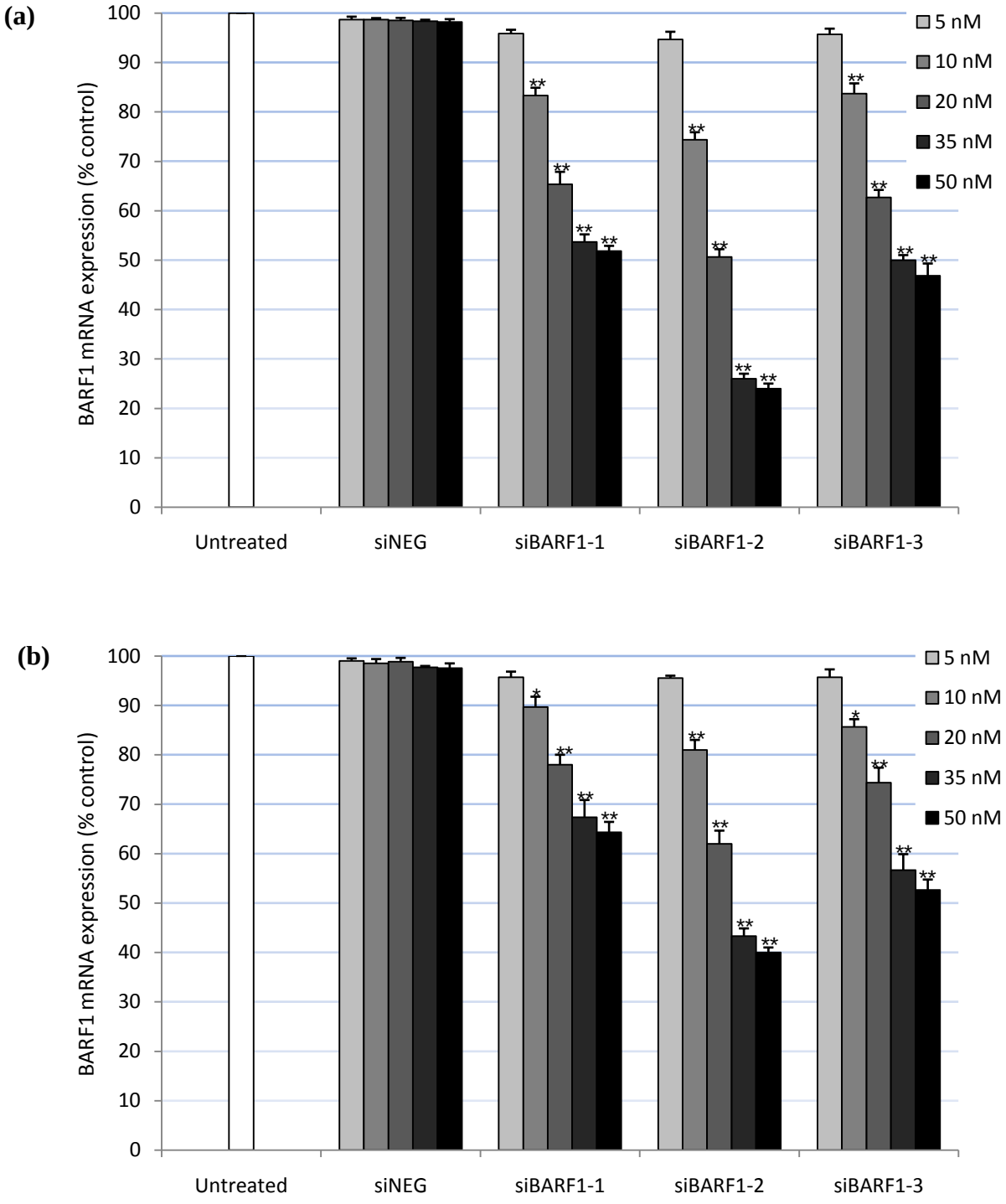

Figure 4.5. qRT-PCR analysis of BARF1 mRNA expression in (a) AG876 and (b) Hone-Akata cells after single transfection with siNEG and siBARF1. Representative results from three independent experiments are shown as mean ± SD ($^{*}p<0.05$, $^{**}p<0.001$, significant difference from untreated and siNEG-treated controls).

4.2.3. Double transfection of BARF1 siRNA

Initial attempt to increase BARF1 knockdown using 50 nM siRNA resulted in detachment of cells in siNEG-treated cells which may indicate cell cytotoxicity. Alternatively, a double transfection method was tested with initial transfection (5-35 nM siBARF1) of cell suspensions followed by re-transfection of adherent cells (5-35 nM siBARF1) on the following day.

In AG876 and Hone-Akata cells, double transfection with siRNAs (5-35 nM) targeting BARF1 gene also caused a dose-dependent downregulation of BARF1 gene expression (Figure 4.6).

In AG876 and Hone-Akata cells, double transfection with 35 nM siBARF1-1 downregulated BARF1 mRNA to 45% and 46% residual level respectively 48 h post the initial transfection (Figure 4.6). Double transfection with siBARF1-2 suppressed BARF1 expression to 10% and 15% residual levels in AG876 and Hone-Akata cells respectively. siBARF1-3 downregulated BARF1 mRNA to 26% and 29% residual level in AG876 and Hone-Akata cells respectively. In double transfection experiments, no significant difference in knockdown efficiency was observed using siNEG when compared with untreated control (Figure 4.6).

Our results demonstrate that using double transfection method, siBARF1-2 (35 nM) targeting the position 409-427 reduced the BARF1 mRNA level most significantly followed by siBARF1-3 and siBARF1-1.

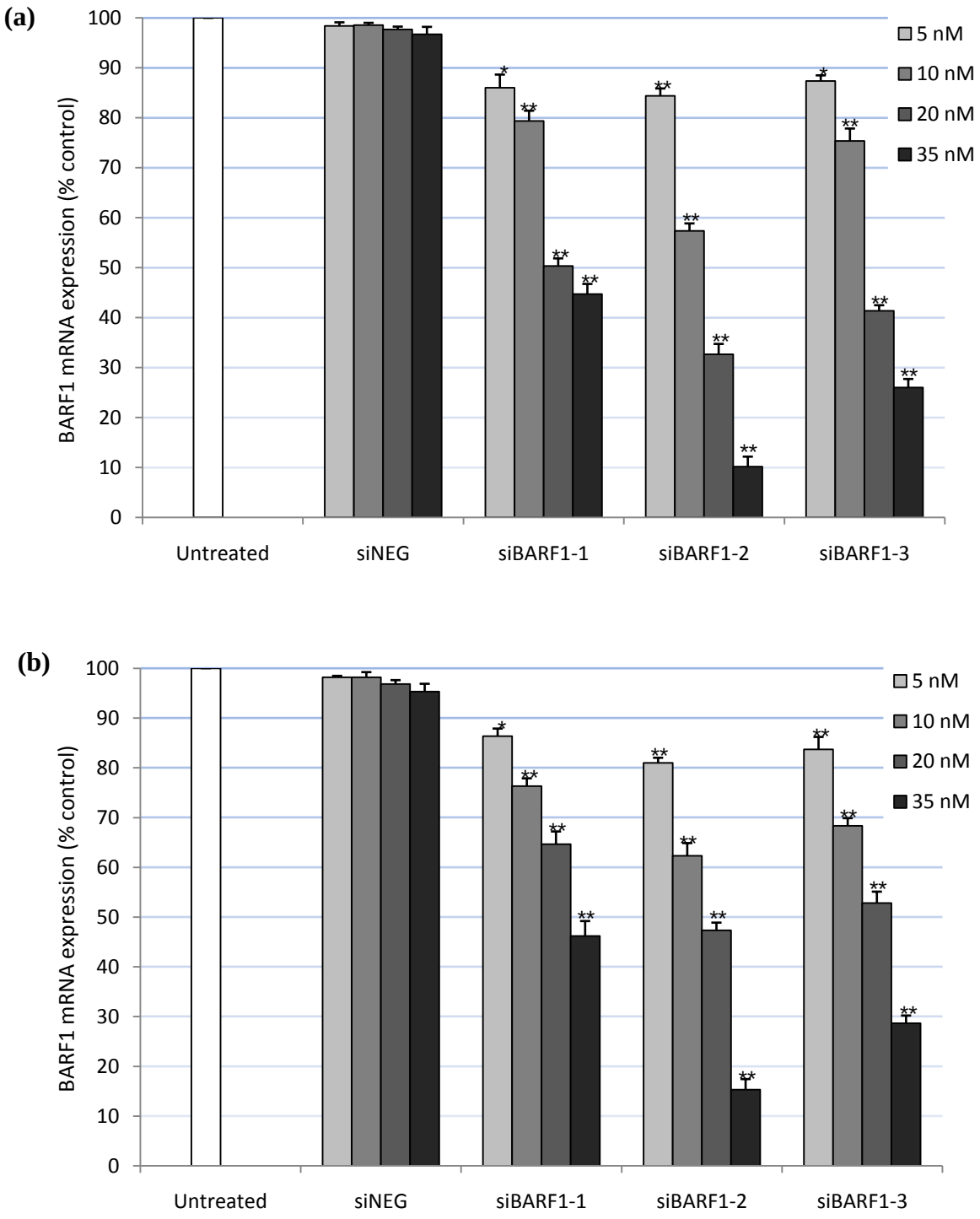

Figure 4.6. qRT-PCR analysis of BARF1 mRNA expression in (a) AG876 and (b) Hone-Akata cells after double transfection with siNEG and siBARF1. Representative results from three independent experiments are shown as mean ± SD ($^{*}p<0.05$, $^{**}p<0.001$, significant difference from untreated and siNEG-treated controls).

4.3. siBARF1 suppresses the expression of BARF1 protein

Next, the effect of BARF1 mRNA knockdown was examined at the protein level. To substantiate the qRT-PCR data, immunoblotting using anti-BARF1 monoclonal antibody was performed to detect the BARF1 protein expression in both the culture media as well as the cell lysate.

Western blot analysis (Figure 4.7a) of cell lysate at 72 h post-transfection shows a decrease in BARF1 protein band intensity in siBARF1-2 treated cells when compared with control (untreated and siNEG-treated) cells. BARF1 protein was detected as ~ 26 kDa band on Western blots using the MoAb 4A6 anti-BARF1 antibody. GAPDH was used as loading control. However, attempts to detect the secreted form of BARF1 protein from the concentrated culture media using Western blot failed (data not shown).

Densitometry analysis (Figure 4.7b) reveals that treatment with siBARF1-2 caused ~80% and ~62% depletion of BARF1 protein in AG876 and Hone-Akata cell lysates respectively when compared with untreated controls.

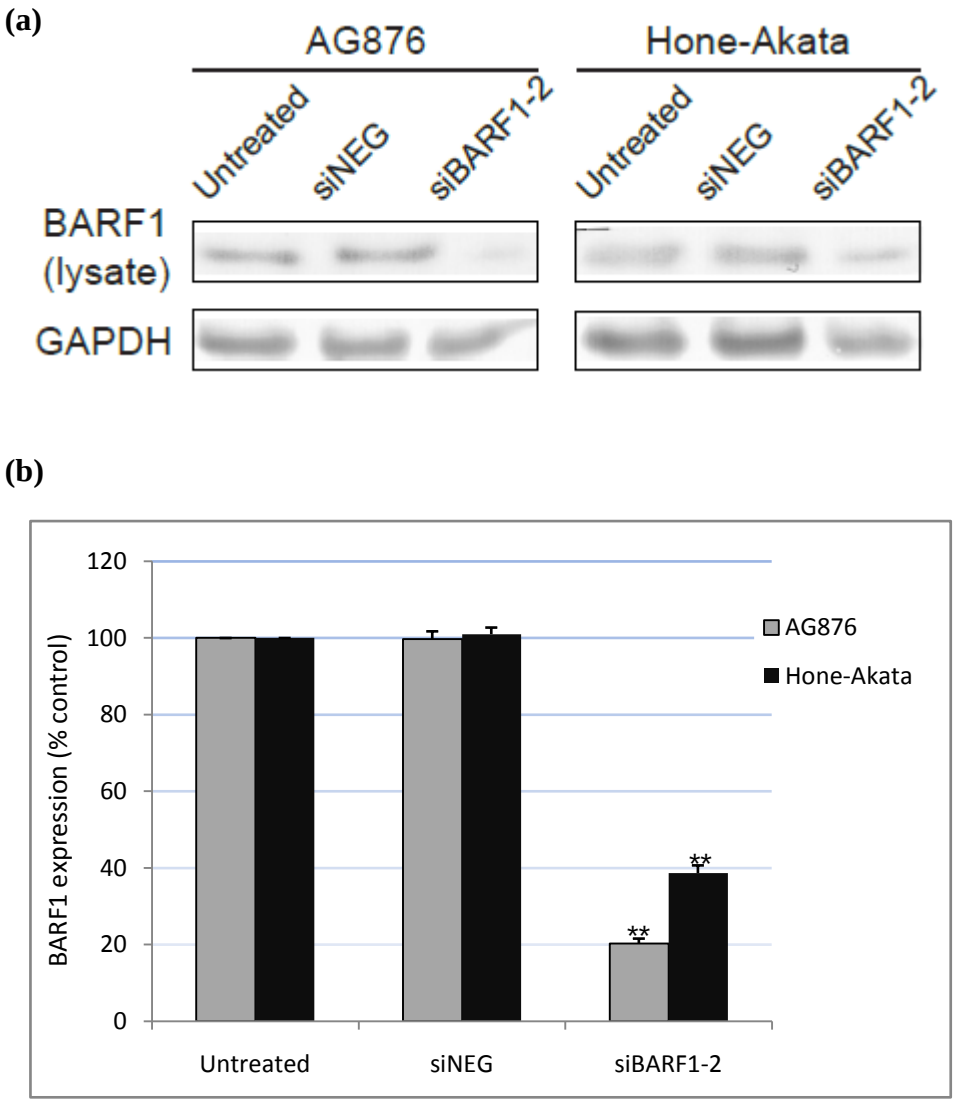

Figure 4.7. BARF1 knockdown in AG876 and Hone-Akata cells using siBARF1-2. (a) Representative western blot showing decrease in BARF1 protein signal in cells transfected with siBARF1-2 compared with control cells. (b) BARF1 expression analyzed by densitometry. Representative results from three independent experiments are shown as mean ± SD ($^{**}p<0.001$ significant difference from untreated and siNEG-treated controls).

4.4. Silencing of BARF1 expression inhibits cell proliferation

4.4.1. Trypan blue exclusion assay

The effect of BARF1 depletion using siBARF1-1, siBARF1-2 and siBARF1-3 on the viability of AG876 and Hone-Akata cells was determined using the trypan blue exclusion test. BARF1 siRNAs were transfected using both the single and double transfection methods.

When the harvested cells were counted, the number of control cells (untreated and siNEG-treated) continued to increase in a time-dependent manner (Figures 4.8 and 4.9). No significant changes were observed in the pattern of cell growth 48 h post-transfection. However, cell proliferation was significantly inhibited 72 h post-transfection in BARF1-depleted cells when compared with the untreated and siNEG-treated controls.

Inhibition of cell proliferation was most significant in AG876 and Hone-Akata cells that were double transfected with siBARF1-2, followed by siBARF1-3- and siBARF1-1-transfected cells, when compared with untreated and siNEG-treated controls.

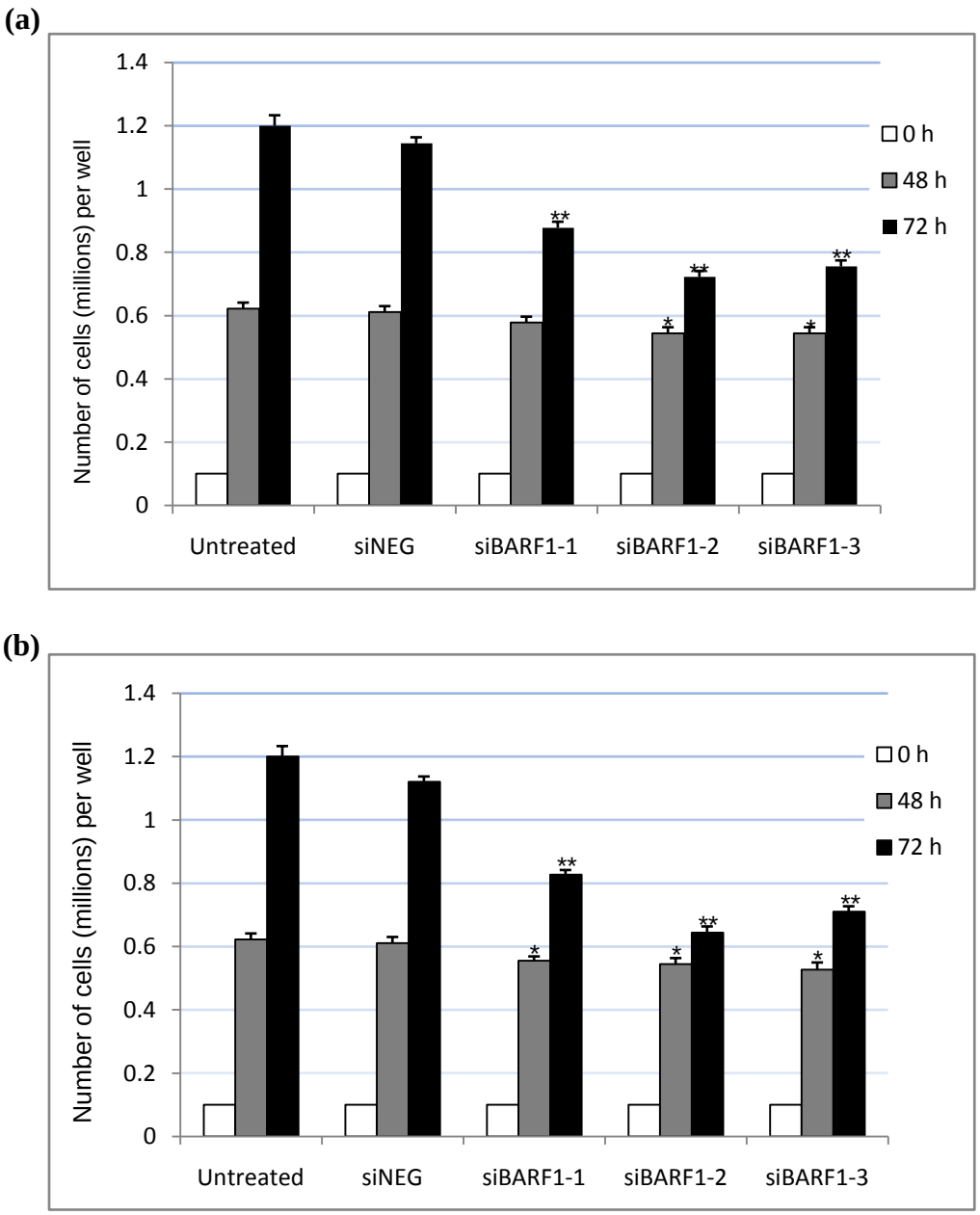

Figure 4.8. Number of viable AG876 cells after (a) single and (b) double transfection of siRNAs determined using the trypan blue exclusion assay. Representative results from three independent experiments are shown as mean ± SD ($^{*}p<0.05$, $^{**}p<0.001$, significant difference from untreated and siNEG-treated controls).

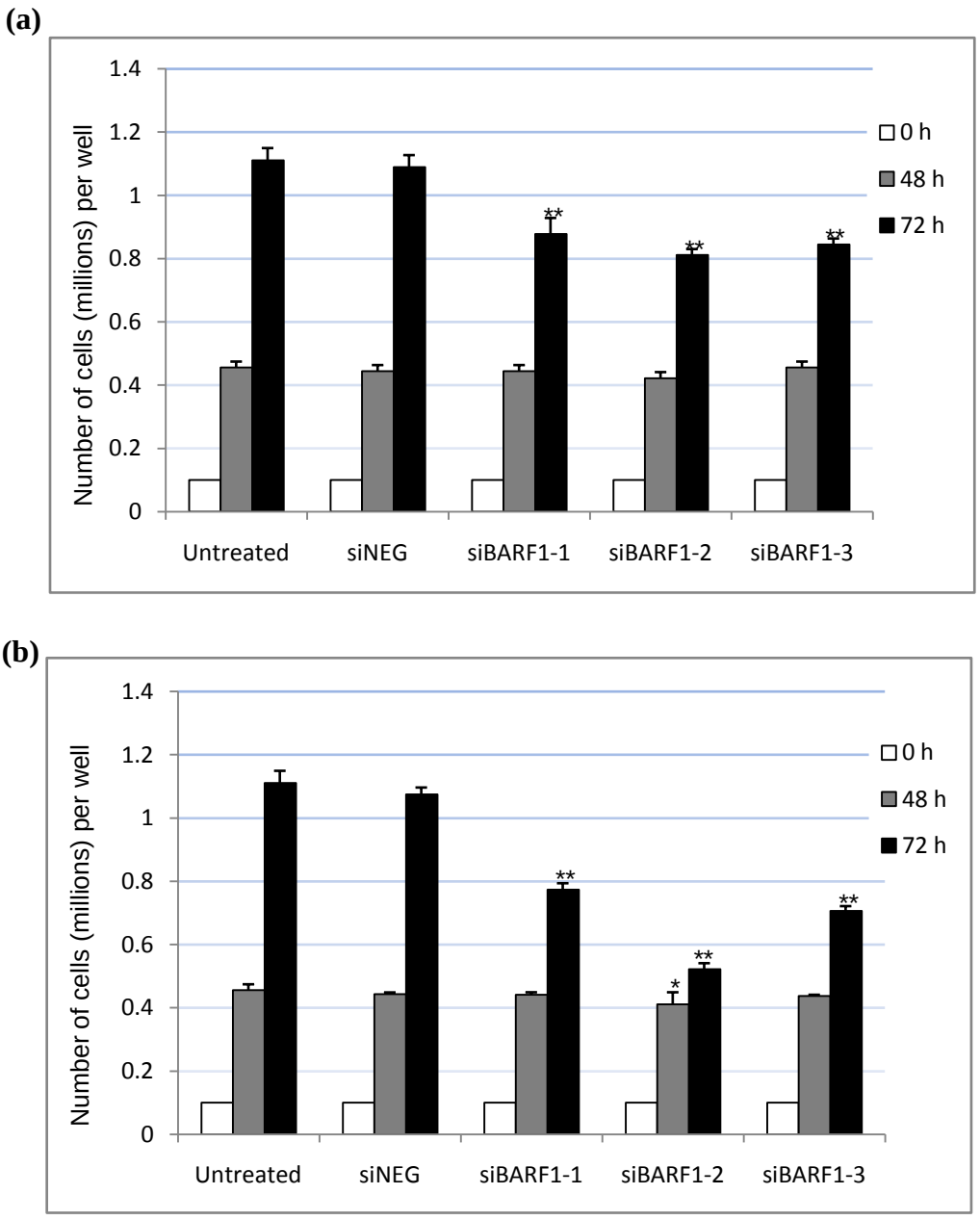

Figure 4.9. Number of viable Hone-Akata cells after (a) single and (b) double transfection of siRNAs determined using the trypan blue exclusion assay. Representative results from three independent experiments are shown as mean ± SD ($^{*}p<0.05$, $^{**}p<0.001$, significant difference from untreated and siNEG-treated controls).

4.4.2. WST-1 assay

To confirm the effect of BARF1 knockdown on cell proliferation, the WST-1 cell proliferation assay was used. The anti-proliferative effects in AG876 and Hone-Akata cells were validated by double transfection using siBARF1-2 or siBARF1-3. Double transfection was employed for this assay as we found that this method downregulated BARF1 gene expression more effectively than the single transfection method (Figures 4.5 and 4.6). Moreover, double transfection method using siBARF1-2 or siBARF1-3 inhibited cell proliferation more significantly compared with siBARF1-1 (Figures 4.8 and 4.9).

The results indicate that at 72 h post-transfection, the growth of siBARF1-transfected cells was inhibited substantially in both AG876 and Hone-Akata cells when compared with the untreated and siNEG controls (Figures 4.10 and 4.11). The anti-proliferative effect of BARF1 silencing was found to be higher in cells transfected with siBARF1-2 (Figure 4.10) compared with cells treated with siBARF1-3 (Figure 4.11). At any indicated time point, no obvious anti-proliferative effect was exhibited in untreated and siNEG control cells.

These results indicate that cell proliferation is inhibited in BARF1-silenced AG876 and Hone-Akata cells. All downstream experiments were carried out using double transfection of siBARF1-2.

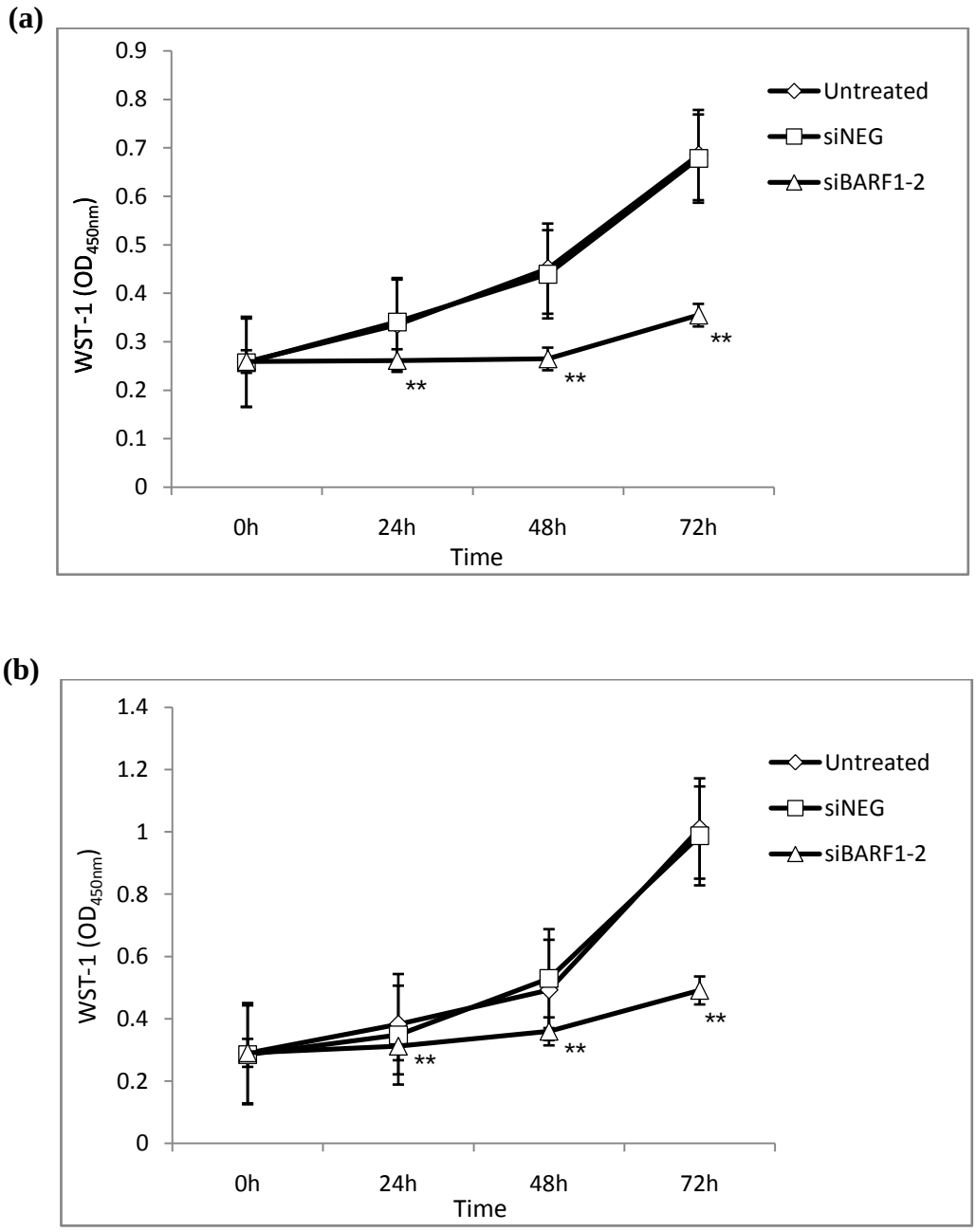

Figure 4.10. WST-1 analysis of the growth of (a) AG876 and (b) Hone-Akata cells after transfection with siNEG and siBARF1-2. Representative results from three independent experiments are shown as mean ± SD ($^{*}p<0.05$, $^{**}p<0.001$, significant difference from untreated and siNEG-treated controls).

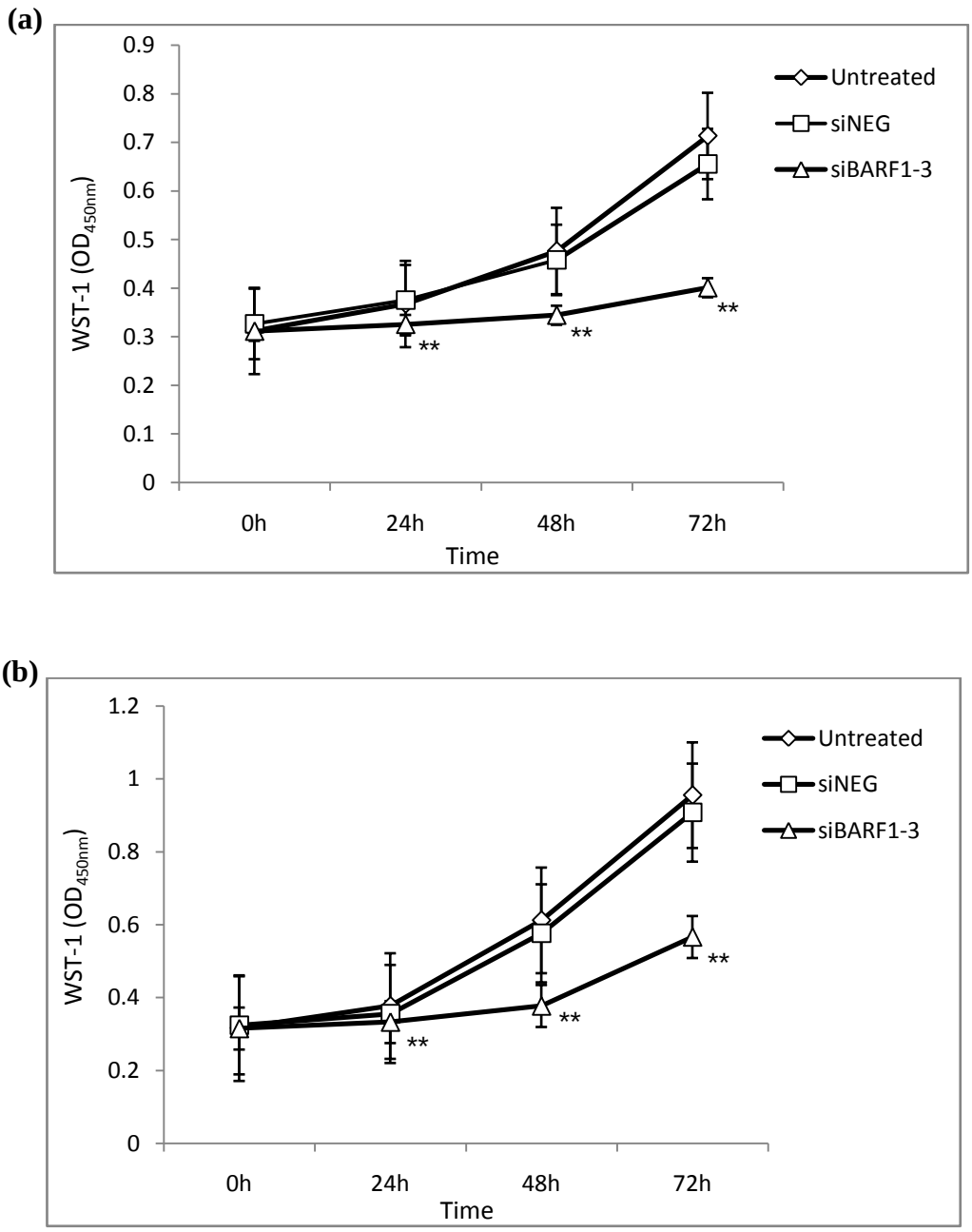

Figure 4.11. WST-1 analysis of the growth of (a) AG876 and (b) Hone-Akata cells after transfection with siNEG and siBARF1-3. Representative results from three independent experiments are shown as mean ± SD ($^{*}p<0.05$, $^{**}p<0.001$, significant difference from untreated and siNEG-treated controls).

4.5. BARF1 downregulation induces apoptosis-mediated cell death

4.5.1. Annexin V

Due to the growth inhibitory effects of BARF1 silencing in the EBV-positive malignant cells; AG876 and Hone-Akata, the induction of cell death in these cells was next examined. The apoptosis-mediated cell death was examined by flow cytometry analysis using the Annexin V-FITC/PI double fluorescence staining, 72 h post-transfection. Simultaneous staining of FITC-conjugated annexin-V with PI discerns early apoptotic cells (annexin-V positive, PI negative) from late apoptotic/dead cells (annexin-V positive, PI positive).

Data from flow cytometry analysis revealed that BARF1 silencing using siBARF1-2 significantly increased the apoptotic cell population in both AG876 and Hone-Akata cells when compared with untreated and siNEG-treated controls. In AG876 cells, the percentage of early and late apoptotic cell population increased to 37% and 14% respectively following BARF1 depletion. In Hone-Akata cells, BARF1 knockdown increased the early and late apoptotic cell population to 30% and 14% (Figure 4.12a).

Results from flow cytometry analysis indicate that 51% of BARF1-depleted AG876 cells and 44% of BARF1-depleted Hone-Akata cells die through apoptosis (Figure 4.12b).

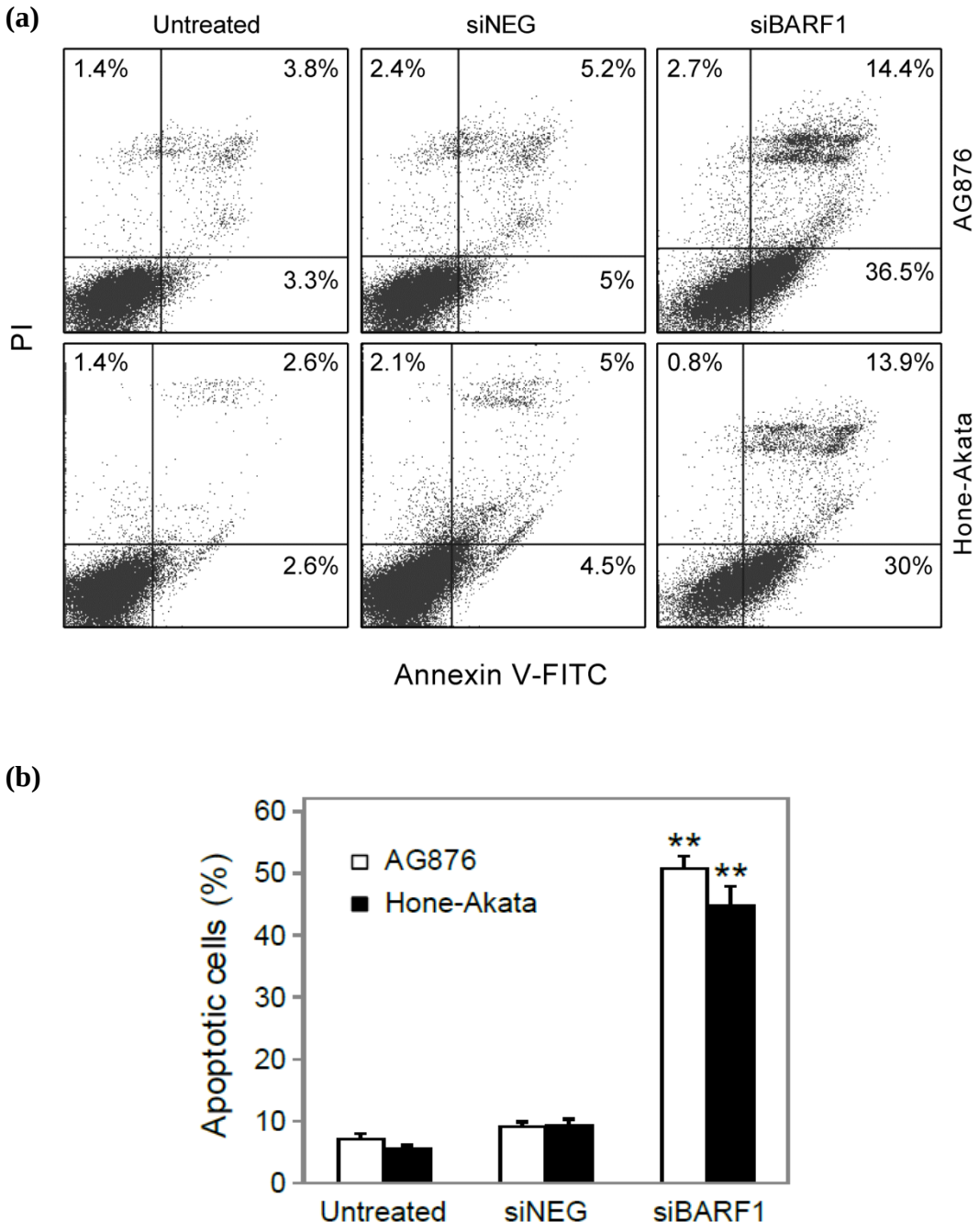

Figure 4.12. Silencing of BARF1 induced apoptosis-mediated cell death in AG876 and Hone-Akata cells. (a) Detection of apoptosis 72 h after transfection with siNEG and siBARF1-2 using flow cytometry analysis following annexin V-FITC/propidium iodide (PI) dual fluorescence staining. Cells in lower left quadrant correspond to viable cells, lower right correspond to early apoptotic cells, upper right correspond to late apoptotic cells and upper left correspond to secondary necrotic cells. (B) Histograms represent the percentage of apoptotic cells (annexin V-FITC-positive) in control (untreated and siNEG-treated) and siBARF1-2-transfected cells. Representative data from three independent experiments are shown. Values are mean ± SD ($^{**}p<0.001$, significant difference from untreated and siNEG-treated controls).

4.5.2. PARP cleavage

The apoptosis-inducing effect of BARF1 downregulation using siBARF1-2 was further examined by Western blot analysis for the proteolytic cleavage of PARP, a typical marker for the onset of apoptosis. Cells were harvested 72 h post-transfection and total protein was extracted. As shown in Figure 4.13, the native 116kDa PARP protein was found to be cleaved to an 89kDa fragment in BARF1-silenced AG876 and Hone-Akata cells. GAPDH was used as loading control.

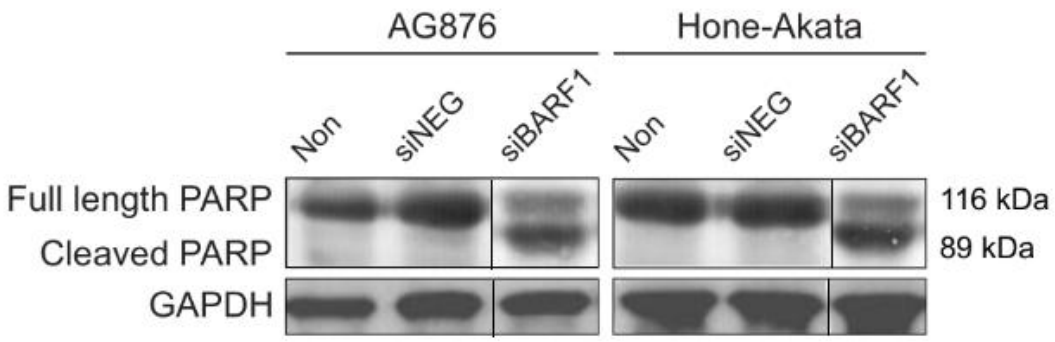

Figure 4.13. Detection of PARP cleavage in AG876 and Hone-Akata cells. Immunoblot shows degradation of PARP from its 116kDa native form to the 89kDa cleaved form, confirming the apoptosis-mediated cell death. The experiments were repeated three times and representative blots are shown.

4.6. Downregulation of BARF1 induces depolarization of mitochondrial membrane potential (MMP)

4.6.1. Flow cytometry analysis of MMP

The involvement of mitochondria in initiation of apoptosis in cells was evaluated by recording changes in its membrane potential. Analysis of mitochondrial membrane potential ($\Delta\Psi m$) by flow cytometry was done 72 h post-transfection using the APO LOGIX JC-1 Mitochondrial Membrane Potential Assay Kit. The cationic dye (JC-1) forms red aggregates in mitochondria and exists as green monomers in the cytosol of live, non-apoptotic cells. Upon collapse of the mitochondrial membrane potential in apoptotic cells, JC-1 remains in the cytoplasm as green monomers.

Figure 4.14a shows that treatment of AG876 and Hone Akata with siBARF1-2 resulted in a significant decrease of the red aggregates of JC-1, indicating loss of mitochondrial membrane potential. Transfection with siBARF1-2 increased the percentage of cells with only JC-1 monomers to 84% and 77% in AG876 and Hone-Akata cells respectively when compared with untreated and siNEG controls (Figure 4.14b).

Knockdown of BARF1 collapsed the mitochondrial membrane potential of EBV-positive malignant cells significantly, confirming the induction of apoptosis in these cells.

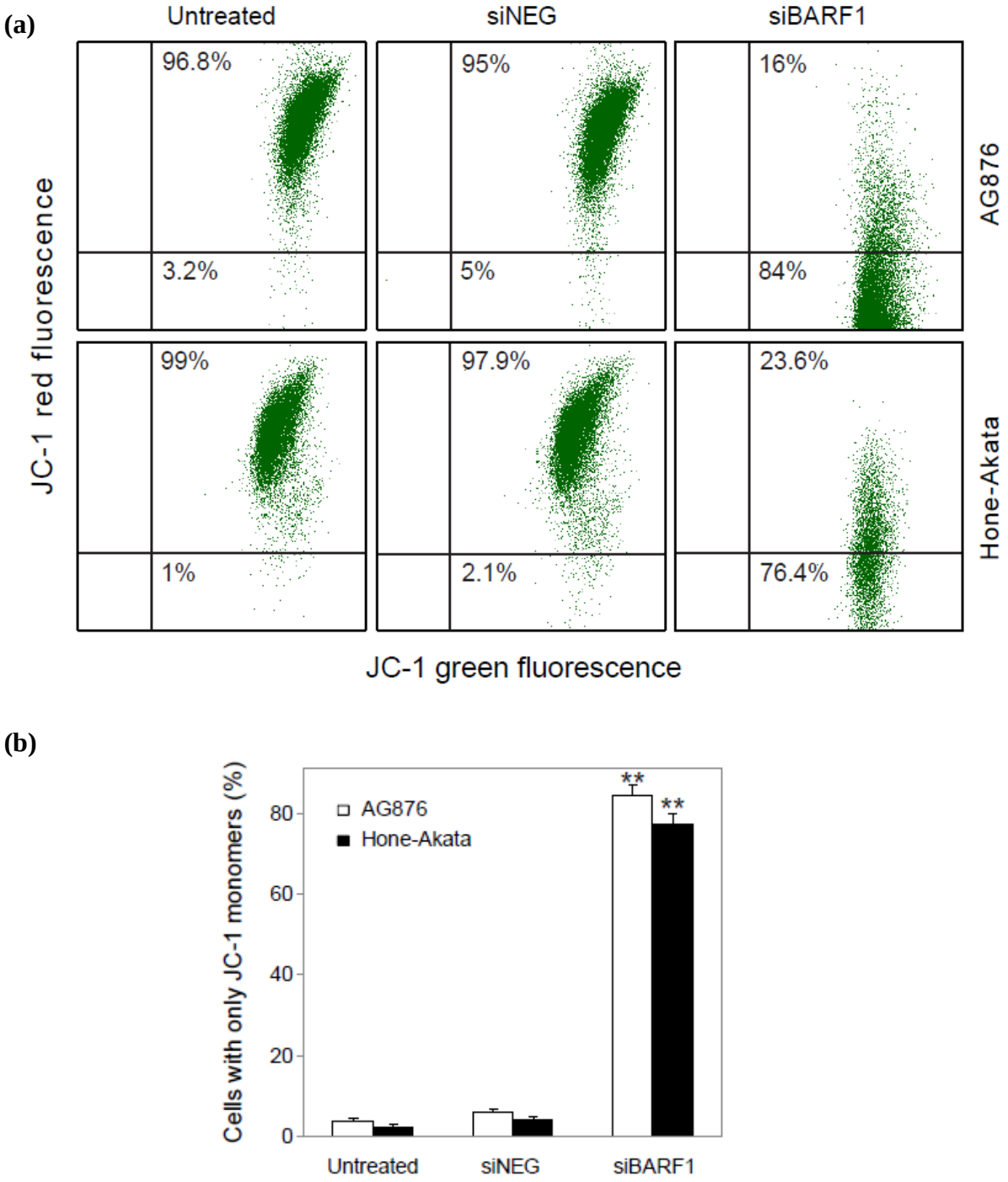

Figure 4.14. Depletion of BARF1 induced depolarization of MMP in AG876 and Hone Akata cells. MMP was determined by flow cytometry after staining the control and siBARF1-treated cells with JC-1 fluorescent dye. (a) Dot plots show the MMP of cells. (b) Histograms represent percentage of cells with only JC-1 monomers indicating apoptotic cells with depolarized MMP. The experiments were repeated three times and representative data are shown. Values are mean ± SD ($^{**}p<0.001$, significant difference from untreated and siNEG-treated controls).

4.7. BARF1 silencing upregulates the expression of pro-apoptotic proteins and downregulates the expression of anti-apoptotic proteins

4.7.1. Antibody array analysis of apoptosis-related proteins expression

To evaluate the expression of apoptosis-related proteins, control and siBARF1-transfected AG876 and Hone-Akata cell lysates were analyzed using RayBio Human Apoptosis Antibody Array G Series. Cells were harvested 72 h post-transfection and total protein was extracted from the cell lysates.

Quantification of protein signals from the antibody array data revealed that following BARF1 silencing in AG876 cells, expression of BAX and caspase 3 increased 2-fold and 4.2-fold respectively whereas p21 and p27 increased 1-fold when compared with siNEG-treated control. Expression of IGFBP-2, IGFBP-3 and IGFBP-4 increased 2.6-fold, 2.3-fold and 2.9-fold respectively following BARF1 depletion in AG876 cells. In Hone-Akata cells, expression of BAX, caspase 3, p21 and p27 increased 1.8-fold, 4.7-fold, 1-fold and 3.2-fold respectively following BARF1 depletion when compared with siNEG-treated control. Expression of IGFBP-2, IGFBP-3 and IGFBP-4 increased 1.1-fold, 2.5-fold and 2.3-fold respectively following BARF1 depletion in Hone-Akata cells (Figure 4.16).

In AG876, BARF1 depletion resulted in a 1.5-fold decrease in Bcl-2 and 2.2-fold decrease in cIAP-2 and survivin expressions when compared with siNEG-treated control. In Hone-Akata cells, expression of Bcl-2, cIAP-2 and survivin decreased 2.5-fold, 2-fold, and 2.5-fold respectively following BARF1 depletion when compared with siNEG-treated control (Figure 4.16).

Antibody array analysis indicated that expression of BAX, caspase 3, p21, p27, IGFBP-2, IGFBP-3 and IGFBP-4 increased while expression of Bcl-2, cIAP-2 and survivin decreased in both AG876 and Hone-Akata cells that were treated with siBARF1-2 (Figures 4.15 and 4.16).

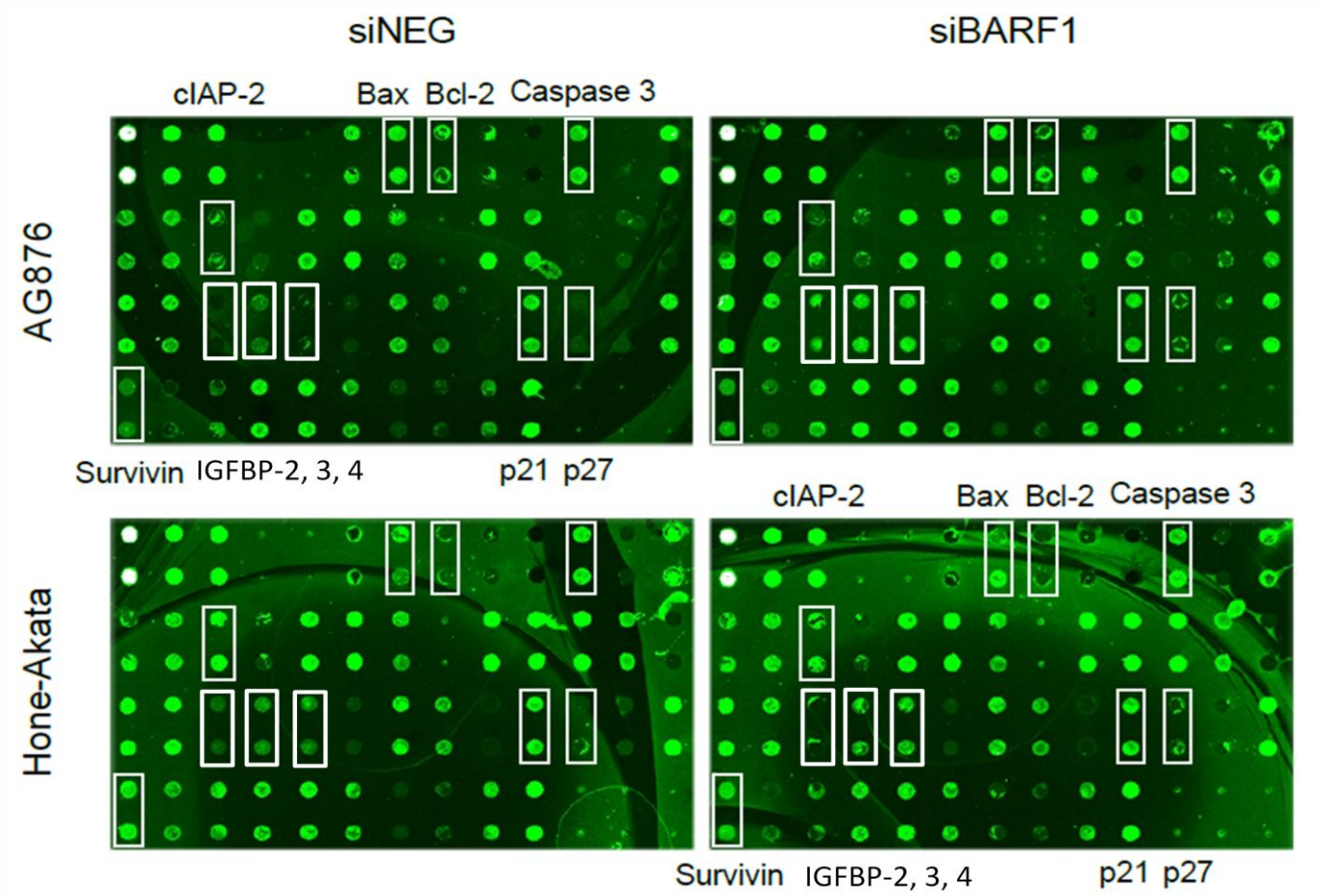

Figure 4.15. Expression of pro- and anti- apoptotic proteins in AG876 and Hone-Akata cells after transfection with siNEG and siBARF1-2, analyzed using human apoptosis antibody arrays.

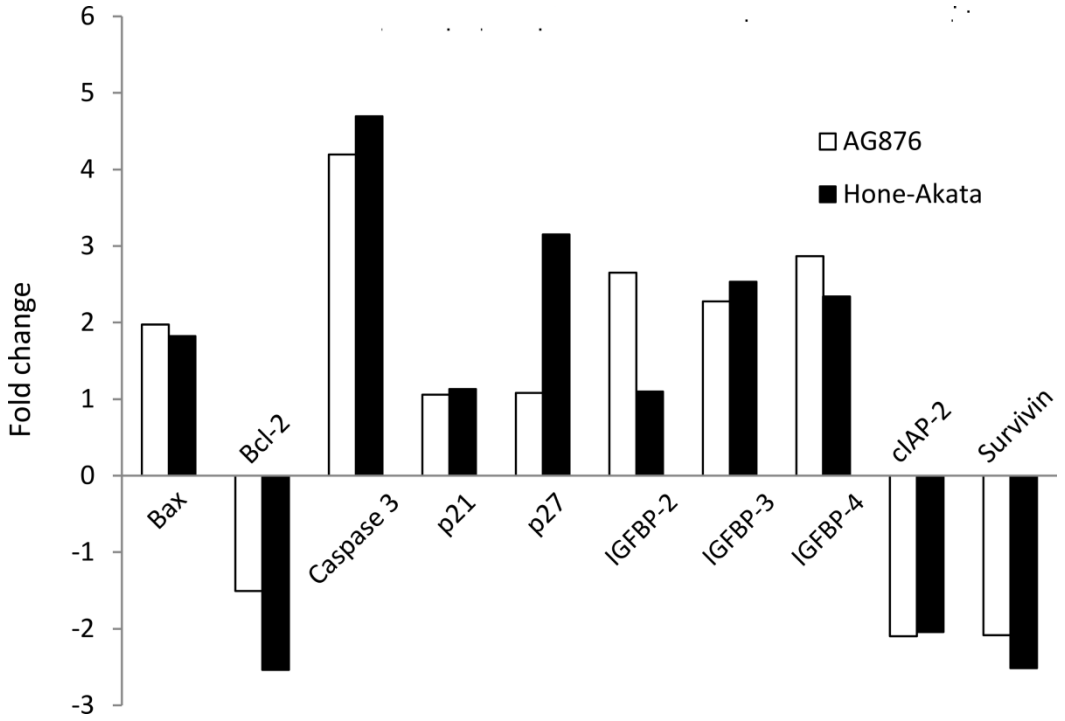

Figure 4.16. Histograms represent the fold change of apoptotic proteins derived from the fluorescence signal intensities of the arrays.

4.7.2. Analysis of Bcl-2/BAX ratio in BARF1-silenced cells

The implications of BARF1 silencing were further explored by analyzing the Bcl-2/BAX ratio in BARF1-depleted cells. Quantification of protein signals from the antibody array data revealed that BAX increased 2-fold in AG876 and 1.8-fold and Hone-Akata cells while Bcl-2 decreased 1.5-fold and 2.5-fold in AG876 and Hone-Akata cells respectively (Figure 4.16).

In siBARF1-2-transfected cells, Bcl-2/BAX ratio decreased by 71% in AG876 and by 79% in Hone-Akata cells as compared to siNEG controls (Figure 4.17).

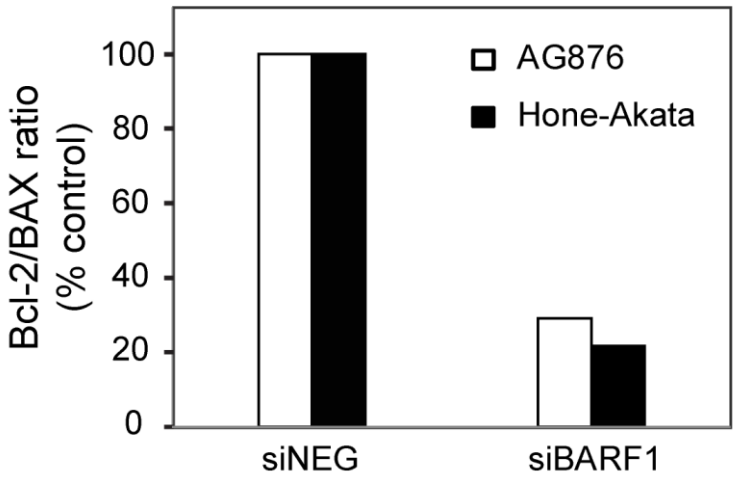

Figure 4.17. Bcl-2/BAX ratio of control and siBARF1-transfected cells. Bcl-2/BAX ratio was deduced from the fluorescence signal intensities of the apoptosis antibody array.

To ascertain if the decreased Bcl-2 expression and increased BAX expression were caused by gene transcription, the transcript levels of Bcl-2 and BAX was examined using semi-quantitative RT-PCR. The results revealed that expression of Bcl-2 mRNA was decreased by siBARF1-2 in both AG876 and Hone-Akata cells whereas the expression of BAX mRNA was increased by siBARF1-2 in both AG876 and Hone-Akata cells (Figure 4.18a). Quantification by densitometry showed that with siBARF1-2 treatment, the Bcl-2/BAX ratio at the mRNA level decreased significantly by 87% in AG876 and 78% in Hone-Akata when compared with the untreated controls and by 81% and 74% in AG876 and Hone-Akata respectively when compared with siNEG control (Figure 4.18b).

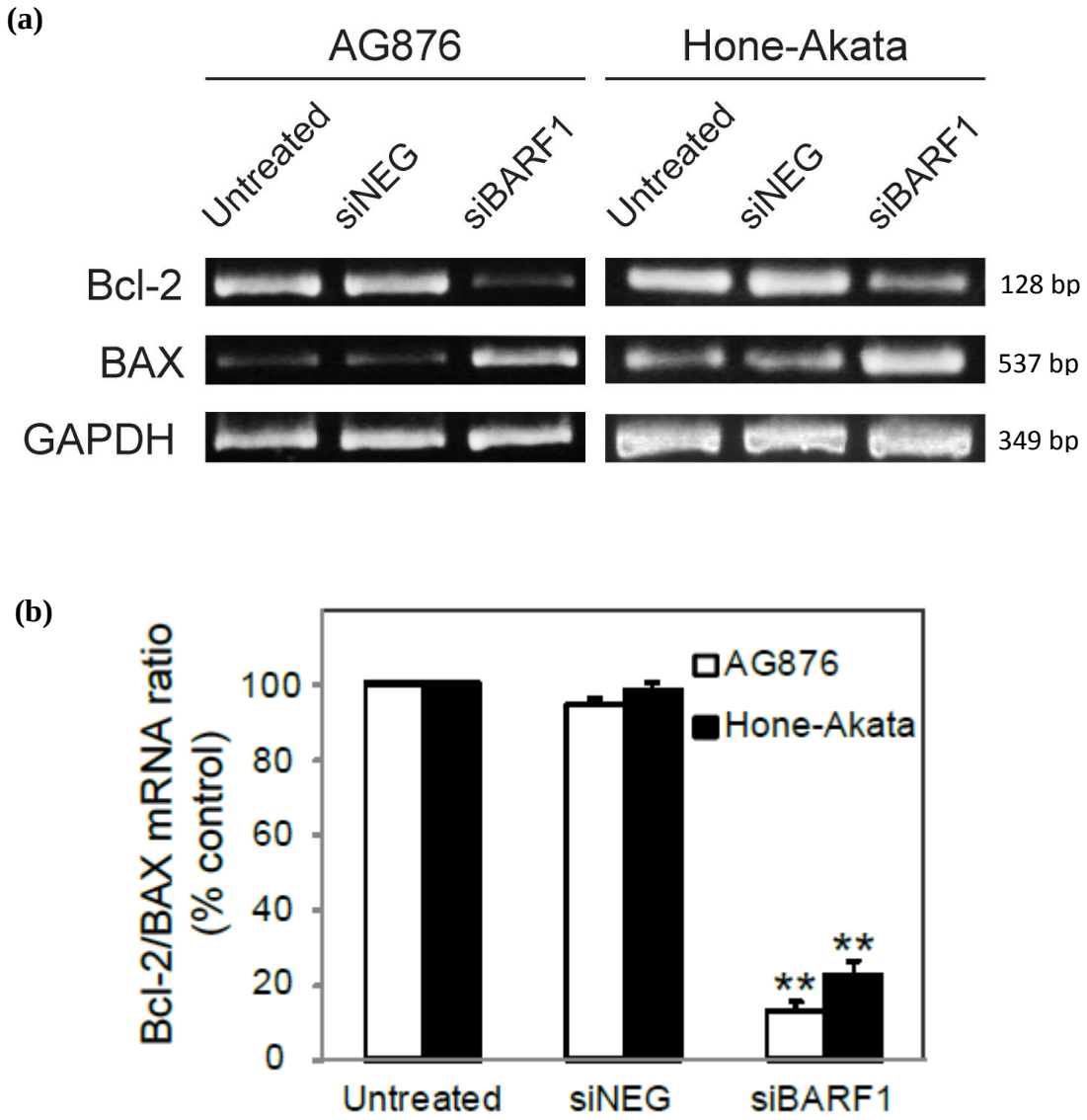

Figure 4.18. Analysis of Bcl-2 and BAX mRNA expression in control and siBARF1-transfected AG876 and Hone-Akata cells. (a) Semi-quantitative RT-PCR analysis of Bcl-2 and BAX mRNA expression. (b) Bcl-2/BAX mRNA ratio analyzed by densitometry. Representative data from three independent experiments are shown as mean ± SD ($^{**}p<0.001$, significant difference from untreated and siNEG-treated controls).

The protein levels of Bcl-2 and BAX were checked using Western blotting. The results revealed that expression of Bcl-2 was upregulated whereas BAX expression was downregulated following BARF1 depletion in both AG876 and Hone-Akata cells (Figure 4.19a).

Quantification by densitometry showed that with siBARF1-2 treatment, the Bcl-2/BAX ratio at the protein level decreased significantly by 63% in AG876 and 82% in Hone-Akata as compared to the untreated controls and by 59% and 78% in AG876 and Hone-Akata respectively when compared with siNEG control (Figure 4.19b).

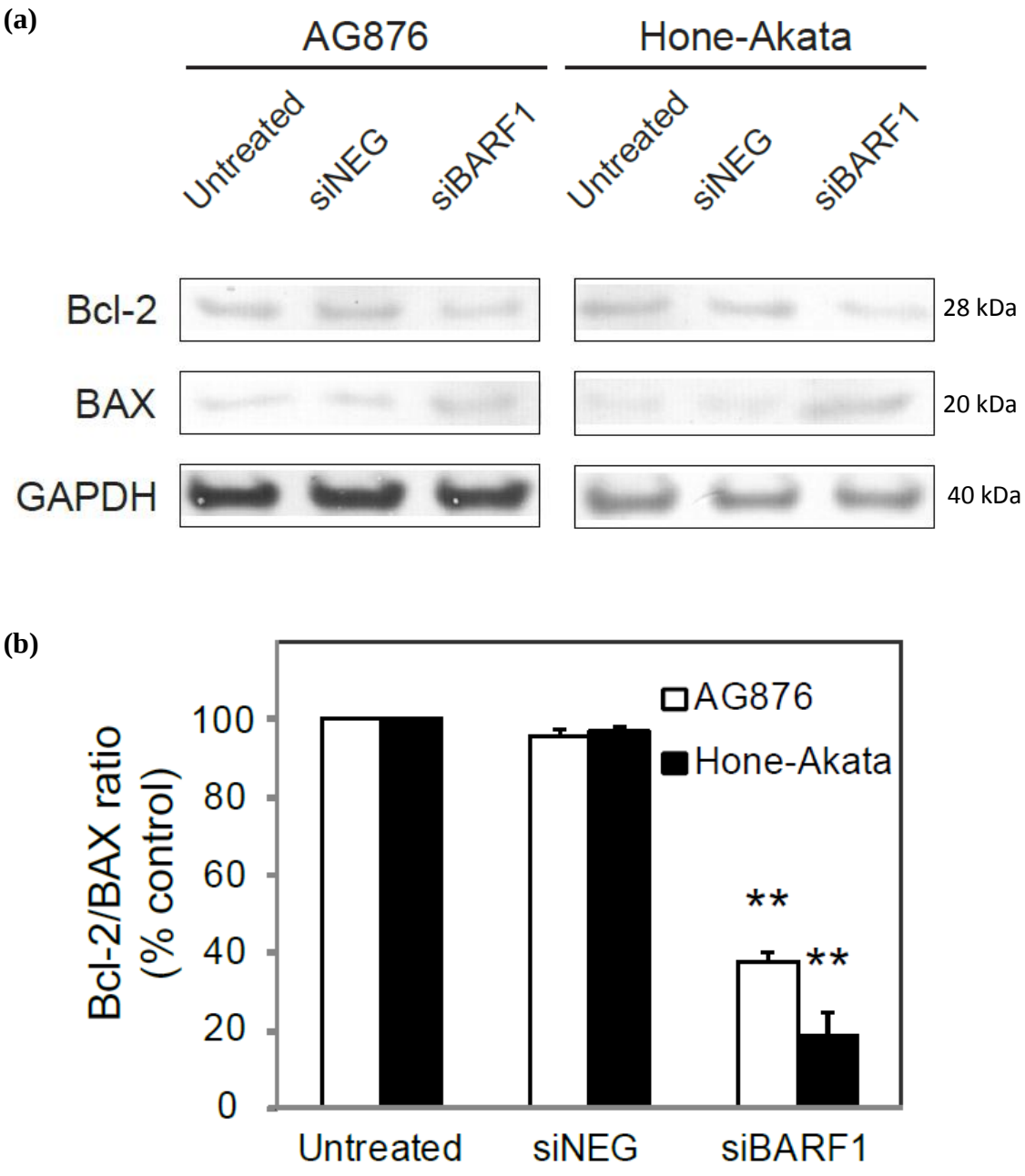

Figure 4.19. Analysis of Bcl-2 and BAX protein expression in control and siBARF1-transfected AG876 and Hone-Akata cells. (a) Detection of Bcl-2 and BAX protein expression using Western blot. (b) Bcl-2/BAX protein ratio analyzed by densitometry. Representative data from three independent experiments are shown as mean ± SD ($^{**}p<0.001$, significant difference from untreated and siNEG-treated controls).

4.8. Downregulation of BARF1 induces caspase dependent apoptosis

4.8.1. Flow cytometry analysis of MMP

To investigate the involvement of caspases, we used a broader caspase inhibitor, z-VAD-fmk to examine its ability to prevent apoptosis caused by BARF1 silencing. Analysis of mitochondrial membrane potential collapse by flow cytometry revealed that pretreatment with the broad caspase inhibitor, z-VAD-fmk at 50 uM rescued the apoptosis in siBARF1-2-treated cells (Figures 4.20 and 4.21).

Pretreatment with z-VAD-fmk caspase inhibitor followed by siBARF1-2 transfection decreased the percentage of cells with only JC-1 monomers to 18.7% and 10% in AG876 and Hone-Akata cells respectively when compared with siBARF1-2-transfected cells (Figure 4.21). The above results reveal that siBARF1-2-induced apoptosis in both AG876 and Hone-Akata cells is caspase-dependent.

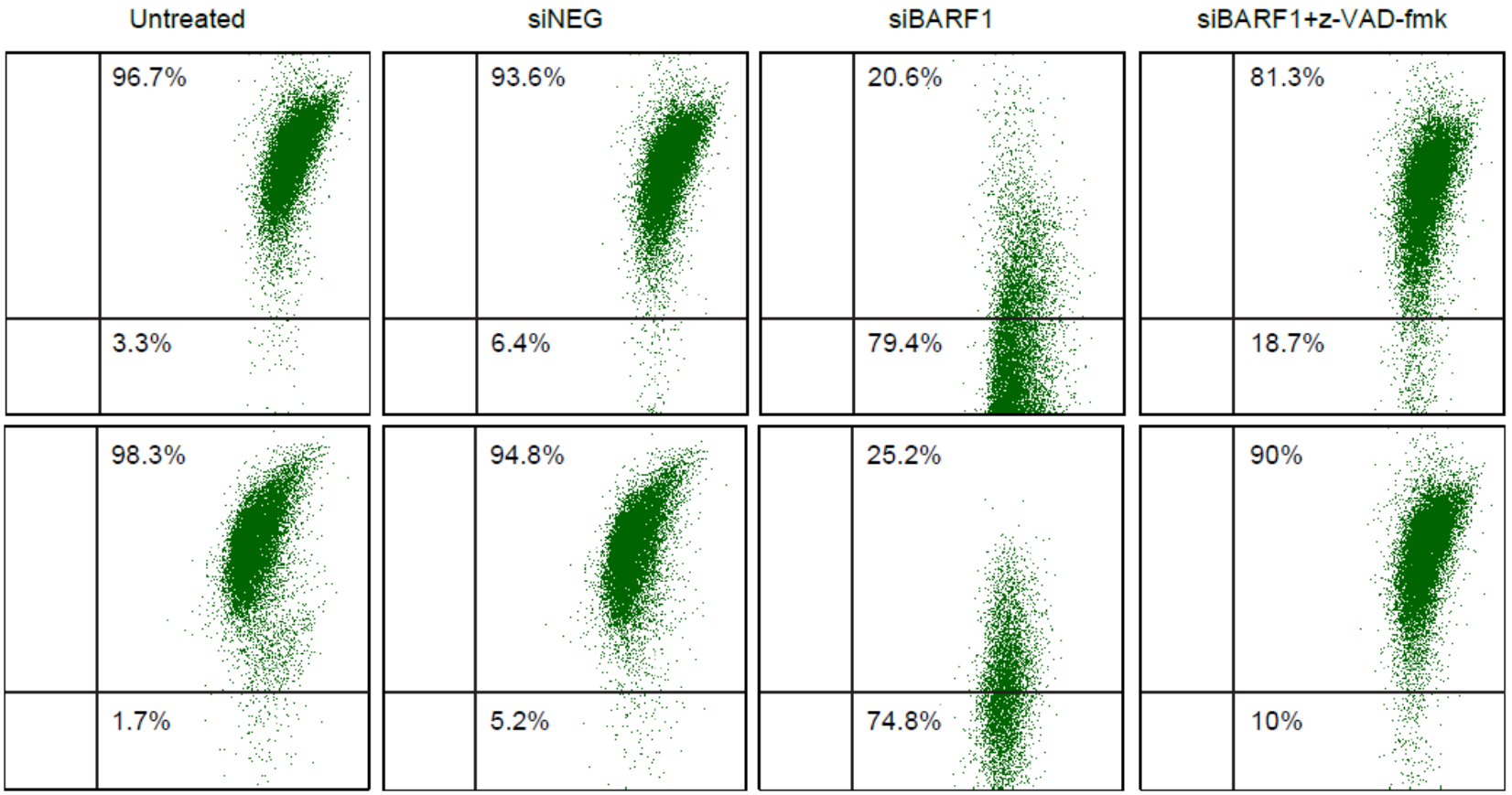

Figure 4.20. MMP analysis of siBARF1-transfected AG876 and Hone-Akata cells pre-treated with z-VAD-fmk caspase inhibitor by flow cytometry. Representative data from three independent experiments are shown as mean ± SD ($^{**}p<0.001$, significant difference from siBARF1-treated cells.

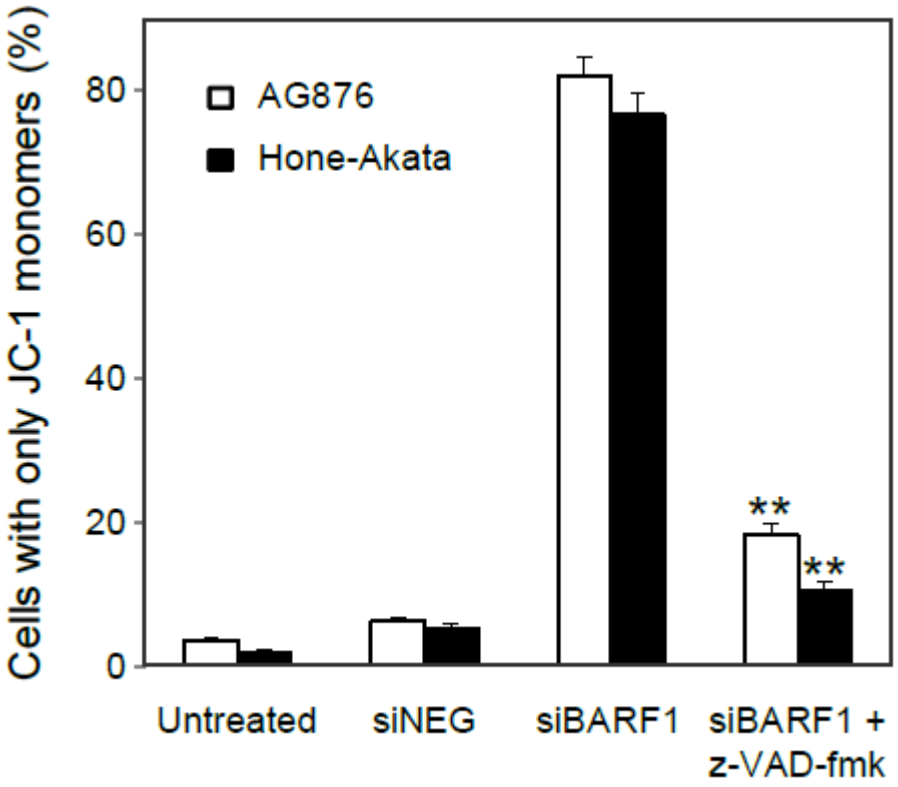

Figure 4.21. Percentage of cells with only JC-1 monomers (cells with collapsed MMP). Histograms are representative data from three independent experiments that are shown as mean ± SD ($^{**}p<0.001$, significant difference from siBARF1-treated cells).

4.9. BARF1 depletion increases cleavage of caspases 3 and 9

4.9.1. Western blot analysis

To examine the roles of activated caspase 3 and caspase 9 in siBARF1-2-induced apoptosis, western blot analysis was performed. Figure 4.22 shows that BARF1 knockdown increased cleavage of caspase 3 and caspase 9 significantly as compared to controls in both AG876 and Hone Akata cells.

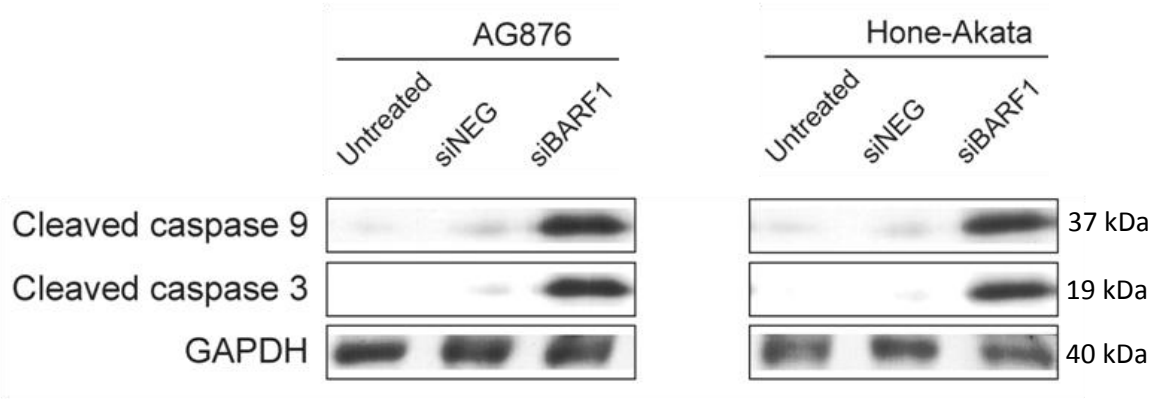

Figure 4.22. Western blot analysis of cleaved caspase 9 and cleaved caspase 3 in control and siBARF1-treated cells. GAPDH was used as the loading control. Immunoblots are representative of three experiments.

4.10. BARF1 knockdown enhances cytochrome c release from mitochondria into cytosol

4.10.1. Immunoblotting for detection of cytochrome c

Cytochrome c, which is released from the mitochondrial membrane into the cytosol facilitates cleavage of caspases (Brunelle & Letai, 2009). Therefore, using western blot analysis the levels of cytochrome c in both mitochondrial and cytosolic fractions were examined. The cytochrome c level in the cytosolic fractions of siBARF1-treated cells was found to be significantly increased as compared to control cells whereas decreased cytochrome c level in the mitochondrial fractions was detected (Figure 4.23).

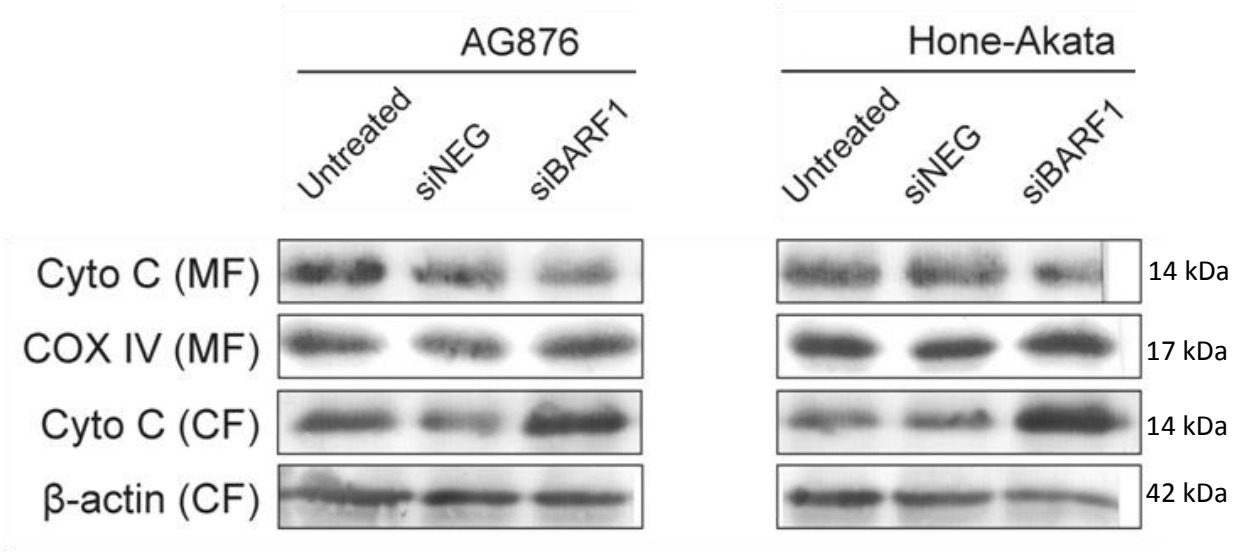

Figure 4.23. Immunoblot for detection of cytochrome c level in mitochondrial fractions (MF) and cytoplasmic fractions (CF). For loading control, cytochrome c oxidase IV was used for MF, β-actin was used for CF. Immunoblots are representative of three experiments.

4.11. BARF1 silencing induces formation of apoptosome complex

4.11.1. Immunoprecipitation for Apaf-1

Cytochrome c is released into the cytosol and binds to the cytosolic apoptotic protease-activating factor (Apaf-1) together with caspase 9 to form the apoptosome (Hajra & Liu, 2004). Immunoprecipitation of caspase 9 with anti-caspase 9 antibody was performed followed by western blot detection with anti Apaf-1 antibody to check the formation of apoptosome complex in BARF1-silenced AG876 and Hone-Akata cells. Western blot results revealed that Apaf-1 was significantly immunoprecipitated with caspase 9 in BARF1-transfected cells as compared to controls (Figure 4.24).

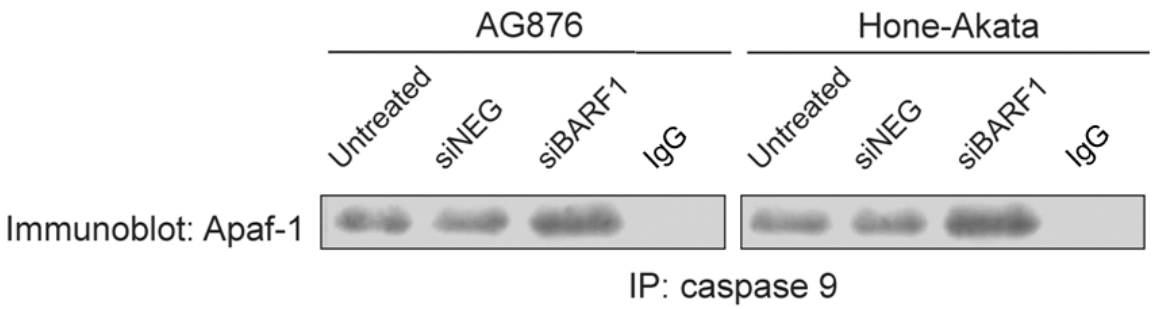

Figure 4.24. Immunoprecipitation for Apaf-1 from cell lysates. Cell lysates were immunoprecipitated with anti-caspase 9 antibody and immunoblotted for Apaf-1. Normal rabbit IgG was added to cell lysates as negative control. Immunoblots are representative of three experiments.

CHAPTER 5: DISCUSSION

The Epstein-Barr virus encoded BARF1 is expressed in NPC, EBV-associated GC, B cell lymphoma as well as in nasal NK/T-cell lymphoma and exhibits oncogenic activity (Xue et al., 2002; Zhang et al., 2006; Decaussin et al., 2000; Seto et al., 2005; Zur Hausen et al., 2000). Although BARF1 is able to induce malignant transformation in rodent cells and human B cell lines (Wei and Ooka, 1989; Wei et al., 1994), immortalization can only be achieved in primary monkey epithelial cells (Wei et al., 1997). Interestingly, in this EBV-induced immortalization, BARF1 expression was detected but LMP1 was absent (Danve et al., 2001). Previous studies on BARF1 suggest its role in promoting cell growth (Wei et al., 1997; Sakka et al., 2013) as well as in providing protection against apoptosis (Wang et al., 2006). However, the anti-apoptotic mechanism of BARF1 remains unclear. Hence, we sought to assess the effects of BARF1 depletion in EBV-associated malignant cells and unravel the molecular mechanism by which BARF1 elicits its function.

In this chapter, the approaches and considerations that were taken into account in designing RNAi experiments are discussed (Section 5.1). The findings of this study are discussed next in Sections 5.2-5.6 and the limitations of the current study are described in Section 5.7. Discussed further in Section 5.8 is how findings of this study are consistent with other published roles of BARF1 and most importantly how the results have contributed to new knowledge on the roles of BARF1. Lastly, implications of the findings and suggestions on future research are discussed in Section 5.9.

5.1. RNAi experimental design

RNAi has been used extensively to explore molecular mechanisms of gene functions and also employed as treatment in viral diseases (Gitlin et al., 2002). In RNAi experiments, sequence-specific off-target effects occur when siRNA is processed by RISC and leads to the downregulation of unintended targets. Studies have reported that changes in gene expression resulting from off-target effects may induce measurable phenotypes that may give rise to 'false positives'. Using high concentration of siRNA duplexes (~100 nM) may contribute to off-target effects.

In this study, approaches that are believed to minimize downregulation of unintended targets while preserving high on-target silencing have been employed. These approaches include the use of a reduced siRNA concentration as well as the use of chemically modified siRNAs that were designed using a more rigorous bioinformatics platform provided by Ambion, USA. Besides that, a few published guidelines on RNAi experimental design and execution, including important control methods (Steitz, 2004; Duxbury and Whang, 2004; Sandy et al., 2005) were followed to ensure a valid and successful RNAi experiment.

Researches on siRNA off-target effects have also shown that a combination of bioinformatics, chemical modification and the use of multiple siRNA sequences targeting the gene of interest may significantly reduce unintended gene silencing (Sandy et al., 2005). Different siRNAs to the same gene with comparable gene silencing efficacy should induce similar changes in gene expression profiles or phenotypes. Any changes induced by one siRNA and not the other(s) may be attributed to off-target effects. In this study, both siBARF1-2 and siBARF1-3 induced downregulation of BARF1 gene expression and exhibited similar effects in inhibition of cell proliferation in siBARF1-transfected AG876 and Hone-Akata cells.

5.2. siRNA-mediated BARF1 downregulation inhibits cell proliferation in AG876 and Hone-Akata cells

In this study, the effect of RNAi-mediated knockdown of BARF1 related to cell proliferation and apoptosis in EBV-associated malignant cells was assessed. Data from preliminary experiment confirmed that AG876 and Hone-Akata cell lines express BARF1 (Figure 4.1). We also confirmed that there were no mutations on BARF1 genes in both AG876 and Hone-Akata cell lines. This was especially critical in designing siRNA sequences that are specific to the mRNA target. Based on these confirmations, the two cell lines were therefore chosen to evaluate the knockdown effect of BARF1-specific siRNAs.

Transfection of BARF1 siRNA into AG876 and Hone-Akata cell lines efficiently downregulated both BARF1 mRNA (Figures 4.5 and 4.6) and protein expressions from the cell lysate (Figure 4.7). In this study, the secreted form of BARF1 protein from the concentrated culture media could not be detected. This may be due to the fact that in this small scale experiment, we were only able to perform medium concentration by a maximum of 1000 fold, unlike by 3000 or 6000 fold as published recently by Chang et al. 2013. However, it is believed that the downregulation of BARF1 protein observed in the cell lysate of siBARF1-transfected cells reflects a general and overall BARF1 protein depletion in these cells. Implications of the failure to detect secreted BARF1 protein to this study require further investigations. Validation in more cell lines will shed light in understanding this observation. Experiments in which BARF1 is overexpressed and detected through immunofluorescence would be able to provide understanding regarding BARF1 secretion in the cell lines used in this study.

Next, results from trypan blue exclusion and WST-1 assays revealed that BARF1 knockdown in these cells led to inhibition of cell proliferation (Figures 4.8-4.11). Our findings confirmed the growth-inhibitory effects of BARF1 siRNA reported very recently in EBV-positive gastric carcinoma cell line by Chang et al (Chang et al., 2013). Under microscope, cells appeared rounded (data not shown) and growth of cells treated with siBARF1 was inhibited, suggesting apoptosis.

5.3. Silencing of BARF1 induces apoptosis-mediated cell death in AG876 and Hone-Akata cells

Apoptosis is a physiologic process by which cells undergo controlled cell death accompanied by nuclear condensation and fragmentation before loss of membrane integrity (Steller, 1995). The externalization of phosphatidylserine (PS) following the loss of plasma membrane asymmetry is one of the earliest events in apoptosis (Martin et al., 1995; Balasubramanian et al., 2007). Phosphatidylserine is redistributed from the inner-to-outer plasma membrane (PM) leaflet, where it functions as a ligand for phagocyte recognition and the suppression of inflammatory responses (Fadok et al., 1992; Franz et al., 2007).

Poly-(ADP-ribose) polymerase-1 (PARP-1) is involved in various cellular processes including DNA repair, recombination, genomic stability, transcription regulation, and cell death. Cleavage of PARP-1 by caspases is one hallmark of apoptosis and caspase activation (Kaufmann et al., 1993; Chaitanya et al., 2010).

To ascertain the mode of cell death, we conducted flow cytometry analysis of PS externalization using annexin V-FITC as well as PARP cleavage detection. Results from these tests (Figures 4.12 and 4.13) indicate that apoptosis was induced in BARF1-silenced AG876 and Hone-Akata cells.

5.4. Depletion of BARF1 induces apoptosis by collapsing mitochondrial membrane potential in AG876 and Hone Akata cells

Next aim was to investigate the molecular mechanisms by which apoptosis is mediated in these BARF1-downregulated cells. The two major routes of apoptosis are the death receptor (extrinsic) pathway and the mitochondrial (intrinsic) pathway; both converge on a common execution phase. In the latter, mitochondria plays a central role in the commitment of cells to apoptosis (Fulda and Debatin, 2006). Many apoptotic stimuli cause either functional or morphological mitochondrial alterations such as collapse of the transmembranal potential or swelling. Opening of the mitochondrial permeability transition pore has been demonstrated to induce depolarization of the transmembrane potential, release of apoptogenic factors and loss of oxidative phosphorylation.

In response to apoptotic stimuli, loss of mitochondrial membrane potential is required for mitochondrial-mediated apoptosis (Gottlieb et al., 2003; Ly et al., 2003). In the present study, using flow cytometry analysis, it is demonstrated that the apoptosis in siBARF1-treated cells was accompanied by a collapse in mitochondrial membrane potential (Figure 4.14).

5.5. BARF1 downregulation alters the expression of apoptotic molecules in AG876 and Hone-Akata cells

Bcl-2 family members are critical regulators of the apoptotic pathway. In the mitochondrial-dependent pathway, interaction between mitochondria and the Bcl-2 family members initiates the release of cytochrome c from the mitochondria.

The mechanisms that regulate mitochondrial apoptosis involve pro-apoptotic proteins (e.g., BAX, Bak, Bim) and anti-apoptotic proteins (e.g., Bcl-2, Bcl-xL) of the Bcl-2 family (Oltvai et al., 1993; Korsmeyer, 1999). The ratio of the anti-apoptotic Bcl-2 to the pro-apoptotic BAX provides a major checkpoint in mammalian cell death pathway (Gross et al., 1999). Overexpression of apoptosis-preventing Bcl-2 protein contributes to tumorigenesis in many types of cancers and BAX counteracts this apoptosis-inhibiting effect of Bcl-2 (Reed, 1996). In this study, it has been shown that BARF1 silencing decreased the Bcl-2/BAX ratio (Figures 4.17-4.19).

The upregulation of several pro-apoptotic proteins (BAX, p21, p27, IGFBP-2, IGFBP-3 and IGFBP-4) and the downregulation of anti-apoptotic proteins (Bcl-2, cIAP-2, survivin) in cells with BARF1 depletion were also observed (Figure 4.16).

In this study, the upregulation of both p21 and p27 in BARF1 depleted cells may have been a mechanism by which these cells undergo apoptosis or inhibiton of cell proliferation. Further investigation on the cell cycle arrest/machinery is needed to reveal if BARF1 play any roles in regulating cell cycle and also to ascertain the involvement of both p21 and p27 in the this possible role. Besides that, upregulation of IGFBP-2, 3 and 4 observed in this study raises the possibility of the involvement of other pathways that may have modulated pro-apoptotic and growth inhibitory effects in BARF1-depleted cancer cells. It was also observed that BARF1 silencing downregulated the expression

survivin and cIAP-2. Downregulation of these proteins may have contributed to the apoptosis induction in BARF1-silenced cells.

5.6. Silencing of BARF1 induces caspase-dependent apoptosis in AG876 and Hone-Akata cells

In this study, it has been demonstrated that pre-treatment with z-VAD-fmk caspase inhibitor rescued the siBARF1-mediated apoptosis in AG876 and Hone-Akata cells (Figures 4.20 and 4.21). This indicates that apoptosis mediated by BARF1 downregulation is caspase-dependent.

Apoptotic cell death is often mediated by a caspase cascade. Cytochrome c is released from mitochondria following the collapse of mitochondrial membrane potential. In the cytosol, in the presence of modest levels of dATP or ATP, cytochrome c binds to Apaf-1 and caspase 9 to form the large heptameric complex, apoptosome (Ledgerwood and Morison, 2009; Bratton and Salvesen, 2010). Apoptosome assembly triggers effector caspase activation (caspase 3) which leads to cell death (Ferraro and Cecconi, 2009).

Using western blot analysis, a significant increase in active caspase 3 and active caspase 9 expressions in BARF1-silenced cells has been shown (Figure 4.22). Furthermore, cytochrome c has been shown to be released from mitochondria into cytosol in these cells (Figure 4.23).

We have also demonstrated that a significant level of Apaf-1 was immunoprecipitated with caspase 9 in BARF1-silenced cells (Figure 4.24), indicating the activation of apoptosome complex formation.

5.7. Limitations of study

Although the siRNA-knockdown approach used in this study has allowed for the elucidation and better understanding of BARF1 function, several limitations using this technology exist. The transduction of siRNA into cells led to only a transient knockdown of BARF1 gene. As modified siRNAs seem to be relatively resistant to degradation, the transient nature of the knockdown is determined by the rate of cell growth and the dilution of the siRNAs below a crucial threshold level that is necessary to maintain the inhibition of gene expression. In actively dividing cells, the duration of silencing is directly related to the number of cell doublings. For example, in AG876 and Hone-Akata cells, which double approximately every 24 hours, the maximum amount of silencing is seen ~72 hours post-transfection and lasts for only several more days (data not presented). Another factor that could limit siRNA-mediated silencing is the half-life of the protein. It might be difficult to effectively silence genes that encode proteins with long half-lives by transient transfection of siRNA.

The introduction of siRNAs into AG876 and Hone-Akata cells has been accomplished by the transfection of the siRNAs using lipid-based reagent. Each cell type was optimized with respect to the number of cells plated and the cells:siRNA:lipid-carrier ratio for efficient transfection. This involved the use of a high amount of siRNAs that had to be chemically synthesized, which remains a costly process.

Although a transient gene silencing was sufficient for our study, a stable silencing approach would be better to be applied in downstream experiments to further explore BARF1 function or signalling pathways. To achieve a long-term and stable gene silencing, the vector-based short hairpin RNAs (shRNAs) could be employed. shRNAs are introduced into the nuclei of target cells using either bacterial or viral

vectors that, in some cases, can stably integrate into the genome. shRNAs are transcribed by either RNA polymerase II or III, depending on the promoter driving their expression. These initial precursors are processed by Drosha and its dsRNA-binding partner DGCR8, resulting in species known as pre-shRNAs, before being exported to the cytoplasm by Exportin-5. The pre-shRNA is then cleaved by Dicer and TRBP/PACT, removing the hairpin and creating a 20–25 nt double-stranded siRNA with 2 nt 3' overhangs at each end. This active siRNA is then loaded onto the RISC complex followed by target mRNA recognition and degradation. shRNA expression could also be controlled using inducible promoters (Li et al., 2002).

Findings from this study should be validated using more cell lines especially in gastric carcinoma cell lines as BARF1 is also implicated to play a role in anti-apoptotic regulation in EBV-driven GC. The anti-proliferative and apoptotic effects of BARF1-depletion could also be tested *in vivo* using mouse models.

5.8. Roles of BARF1

In NPC, BARF1 has been shown to function as oncogene, in line with the widely researched LMP1 (Zheng et al., 2007). Interestingly, in EBV-driven GC, BARF1 is expressed in the absence of LMP1 raising the possibility that BARF1 may be the main EBV oncogene in GC (Zur Hausen et al., 2000). Several functions have been attributed to BARF1; from oncogenic to antiapoptotic and immune modulation.

BARF1 was first suggested to play a role in immortalization of monkey epithelial cells three decades ago (Griffin and Karran, 1984). Later it was shown that BARF1 could also immortalize human epithelial cells (Song et al., 2004). BARF1 is able to immortalize rodent cells (BALB/c3T3 and NIH3T3) and BARF1-transfected

cells induced tumour formation in newborn rodents (Wei and Ooka, 1989). Monkey kidney epithelial cells that were immortalized by BARF1 were tumorigenic in severe combined immunodeficiency mice but not in nude mice (Guo et al., 2001). The N-terminal of BARF1 was found to be responsible for malignant transformation in rodent fibroblasts as well as for the upregulation of the antiapoptotic Bcl-2 (Sheng et al., 2001).

Further studies demonstrated the ability of BARF1 to induce cell immortalization or malignant transformation and to activate several cellular genes, including Bcl-2 (de Turenne-Tessier et al., 2005; Ooka, 2005). However, Wei et al in 1997 reported that immortalization can only be achieved in primary monkey epithelial cells. These findings indicate that the function of BARF1 may be cell type specific.

Introduction of BARF1 into h-Ras-expressing epithelial cells resulted in cells becoming tumorigenic, suggesting that h-Ras synergizes with BARF1. Activations of telomerase and other signal pathways, including c-myc were observed in BARF1-immortalized and transformed PATAS cells (Jiang et al., 2009). These findings suggest that transforming function of BARF1 may be partly mediated by activation of pro-oncogenic cellular pathways. To fully define the oncogenic role of BARF1, pathways mediating epithelial cell transformation and carcinogenesis by BARF1 should be explored.

In GC cell lines, introduction of BARF1 led to deregulation of genes involved in cell proliferation, mitosis and cell cycle regulation. BARF1 was found to induce overexpression of cyclin D1, a positive regulator of cell cycle (Wiech et al., 2008). These findings suggest a possible role of BARF1 in regulation of the cell cycle in malignant cells. In this study, antibody array data revealed that in BARF1-depleted cells, p21 and p27 were upregulated. p21 and p27 are cell cycle inhibitors that suppress tumours by promoting cell cycle arrest in response to various stimuli (Abbas and Dutta,

2009). Hence, further investigation on cell cycle machinery in BARF1-depleted cells would be able to uncover the roles of BARF1 in cell cycle regulation. Data from antibody array also showed an upregulation of IGFBP-2, 3 and 4. Studies on IGF and IGFBP signalling pathways may help to further elucidate underlying mechanisms of how BARF1 elicits its functions in EBV-associated cancers.

Although BARF1 is thought to function as a survival factor by suppressing apoptosis pathway, the molecular mechanism by which BARF1 exerts in providing protection against apoptosis is poorly understood. Findings of this study have provided knowledge on the molecular mechanism by which BARF1 elicits its biological effects, which has not been documented before. These findings are summarized in Figure 5.1.

This study has demonstrated for the first time that siRNA targeting EBV-encoded BARF1 efficiently suppressed BARF1 mRNA expression in AG876 and Hone-Akata cell lines. In these cells, BARF1 depletion resulted in induction of apoptosis-mediated cell death by collapsing the mitochondrial membrane potential. BARF1 silencing also resulted in the upregulation of several pro-apoptotic proteins (BAX, p21, p27) and the downregulation of anti-apoptotic proteins (Bcl-2, cIAP-2, survivin). We have also demonstrated that apoptosis mediated by BARF1 downregulation is caspase-dependent through modulation of Bcl-2/BAX ratio. Induction of apoptosis by silencing BARF1 expression also led to the formation of apoptosome complex. Implications of the findings from this study are discussed in the next section.

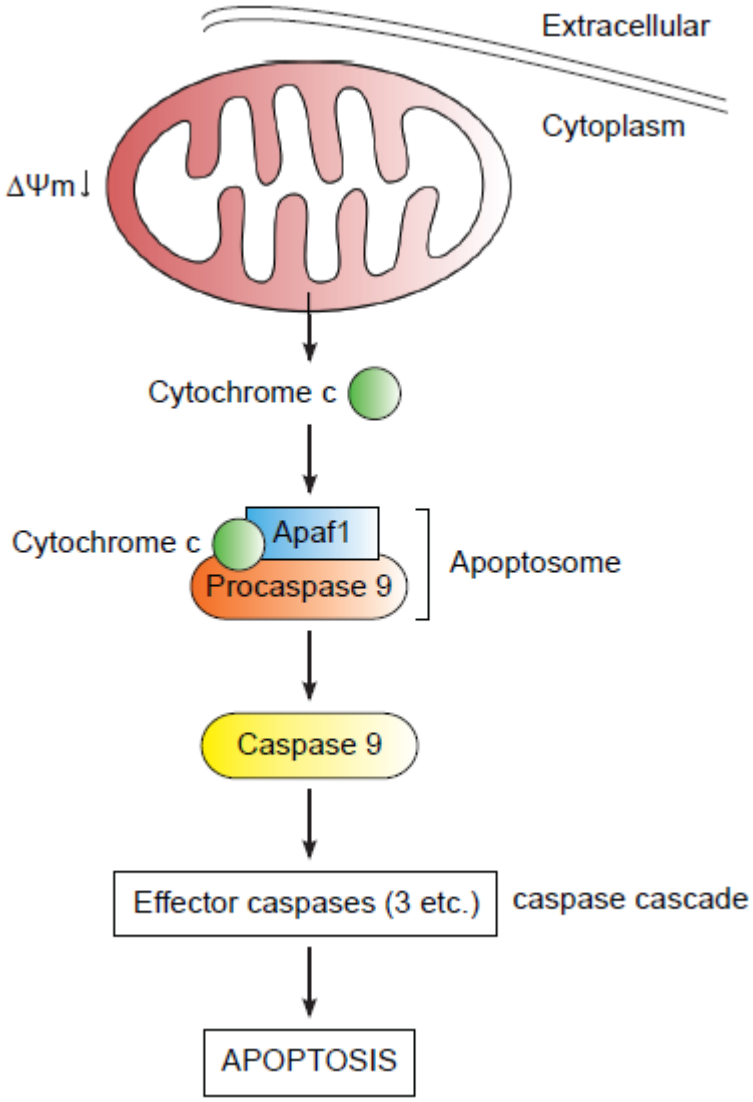

Figure 5.1. Schematic diagram of proposed molecular mechanisms in the regulation of caspase-dependent mitochondrial-mediated apoptosis in BARF1-silenced AG876 and Hone-Akata cells.

5.9. Implications and future directions

By understanding the regulation of the complex signaling pathways in tumours, especially the regulation of apoptosis, rationally designed anticancer strategies could be developed. Thus far, knowledge of the intrinsic and extrinsic apoptotic pathways as well as the other signalling modulators such as the p53, NF- κB, and the PI3K/Akt pathways have led to the discovery of many novel agents that are effective when used as single agents or in combination with conventional cytotoxic therapy or radiation. Further understanding of the different signaling pathways that control apoptosis in the different tumour types will help with the discovery of novel agents specific to the targeted tumour.

Over the years, studies to understand the mechanisms controlling tumour cell proliferation and cell death have identified key molecular pathways involved in cancer formation, progression and treatment resistance. One of the most important discoveries made in cancer research has been the fact that anticancer chemotherapy kills cancer cells by activating the intrinsic and/or extrinsic apoptosis pathway. Although most findings support a role of the CD95 system in anticancer drug-induced apoptosis, most cytotoxic drugs are shown to initiate cell death by triggering the mitochondrial cytochrome c/Apaf-1/caspase-9-dependent pathway. Collectively, these data point to a key role of the mitochondrial pathway in chemotherapy-induced apoptosis, whereas the CD95 system may amplify killing by cytotoxic drugs under certain conditions (Los and Gibson, 2005).

Nevertheless, apoptosis does not represent the sole killing mechanism by which cancers are eradicated, and other methods of cell death, for example, necrosis,

autophagy, or mitotic catastrophe have also to be considered. Further insight into the complex signaling network activated in response to anticancer therapy using cancer cell lines, primary tumour cells and animal models are necessary to see to what extent the current knowledge can be exploited for the design of apoptosis-based cancer therapies. These studies may eventually allow the identification of novel therapeutic targets thereby providing the basis for tailored, individual tumour therapy.

The effectiveness of siBARF1 when used as single agent or in combination with conventional cytotoxic therapy or radiation in treatment of EBV-associated malignancies could be explored. Of late, antiviral RNA interference (RNAi) using short-interfering RNA (siRNA) has been developed as a novel strategy in treatment of diseases and tested in clinical trials. siRNAs have been demonstrated to selectively silence not only endogenous genes in mammalian cells but also viral genes in virus-associated diseases (Ge et al., 2003; Qin et al., 2003). Combination therapy with siRNA may significantly enhance the sensitivity of cancer cells to the anticancer therapy and thereby help prevent the development of chemo/radio resistance resulting from low-dose chemo/radio therapy. In combination therapy, the effect of the multiple modalities is considered to be additive if the combined effect is equal to the sum of the effect of the individual modalities. If the combined effect is greater than the predicted effect of the multiple individual modalities, this interaction is considered to be synergistic. It is also possible that the multiple modalities interact in an antagonistic fashion (Lu et al., 2012). Hence, a valid statistical analysis method should be applied in order to determine the synergistic therapeutic effects. Most importantly, the assessments of no off-target effect and minimal induction of interferon are the prerequisite for the application of RNAi-based combination therapeutics in clinical field trials.

CHAPTER 6: CONCLUSION

The EBV-encoded BARF1 is a candidate oncogene and studies have shown its function in immortalization and transformation in EBV-driven carcinogenesis. Moreover, BARF1 is thought to function as a survival factor by suppressing apoptosis pathway. To date, the molecular mechanism by which BARF1 elicits protection against apoptosis remains to be clarified. Hence, this study was undertaken to unravel this mechanism.

Data presented in this thesis shows that siRNA against the viral oncogene BARF1 is proven to be able to efficiently suppress the BARF1 mRNA expression in EBV-positive malignant cells. This study shows for the first time that siRNA against BARF1 is able to induce apoptosis-mediated cell death in EBV-positive malignant cells. Furthermore, this study concludes that the siRNA-mediated BARF1 downregulation induced caspase-dependent apoptosis via the mitochondrial apoptotic pathway through modulation of Bcl-2/BAX ratio.

Findings of this study have provided understanding of molecular mechanisms in the regulation of apoptosis in BARF1-silenced AG876 and Hone-Akata cells. However, to fully define the intracellular signalling pathways in BARF1-depleted cells, further studies of changes in protein expression and activities are needed.

Thus far, advances and understanding of the apoptotic pathway have led to better and more innovative treatments against cancer and other diseases. The siRNAs designed against BARF1 in this study may have the potential to be exploited for the design of apoptosis-based therapies in EBV-associated malignancies. Future studies will be directed towards investigation of the effects of BARF1 siRNA *in vivo* as well as the value of BARF1 siRNA in treatment of EBV-associated malignancies.

The effectiveness of siBARF1 when used as single agent or in combination with conventional cytotoxic therapy or radiation could also be explored. Despite the great therapeutic potential of RNAi by regulating many disease-related genes, many barriers prevent its practical applications. Most importantly, an efficient delivery system of siRNA to the targeted site needs to be developed and the specific targeting needs to be validated.

REFERENCES

Abbas, T., & Dutta, A. (2009). p21 in cancer: intricate networks and multiple activities. *Nature Reviews Cancer*, *9*(6), 400–414.

Abdel-Hamid, M., Chen, J. J., Constantine, N., Massoud, M., & Raab-Traub, N. (1992). EBV strain variation: geographical distribution and relation to disease state. *Virology*, *190*(1), 168–175.

Akkiprik, M., Feng, Y., Wang, H., Chen, K., Hu, L., Sahin, A, et al. (2008). Multifunctional roles of insulin-like growth factor binding protein 5 in breast cancer. *Breast Cancer Research: BCR*, *10*(4), 212.

Alfieri, C., Birkenbach, M., & Kieff, E. (1991). Early events in Epstein-Barr virus infection of human B lymphocytes. *Virology*, *181*(2), 595–608.

Allday, M. J., Crawford, D. H., & Griffin, B. E. (1989). Epstein-Barr virus latent gene expression during the initiation of B cell immortalization. *The Journal of General Virology*, *70 (Pt 7)*, 1755–1764.

Allday, M. J., & Farrell, P. J. (1994). Epstein-Barr virus nuclear antigen EBNA3C/6 expression maintains the level of latent membrane protein 1 in G1-arrested cells. *Journal of Virology*, *68*(6), 3491–3498.

Amon, W., & Farrell, P. J. (2005). Reactivation of Epstein-Barr virus from latency. *Reviews in Medical Virology*, *15*(3), 149–156.

Araujo, I., Foss, H. D., Bittencourt, A., Hummel, M., Demel, G., Mendonca, N., et al. (1996). Expression of Epstein-Barr virus-gene products in Burkitt's lymphoma in Northeast Brazil. *Blood*, *87*(12), 5279–5286.

Armstrong, A. A., Alexander, F. E., Cartwright, R., Angus, B., Krajewski, A. S., Wright, D. H., et al. (1998). Epstein-Barr virus and Hodgkin's disease: further evidence for the three disease hypothesis. *Leukemia*, *12*(8), 1272–1276.

Auer, H., Lyianarachchi, S., Newsom, D., Klisovic, M. I., Marcucci, G., Marcucci, U., & Kornacker, K. (2003). Chipping away at the chip bias: RNA degradation in microarray analysis. *Nature Genetics*, *35*(4), 292–293.

Balasubramanian, K., Mirnikjoo, B., & Schroit, A. J. (2007). Regulated externalization of phosphatidylserine at the cell surface: implications for apoptosis. *The Journal of Biological Chemistry*, *282*(25), 18357–18364.

Bartel, D. P. (2004). MicroRNAs: genomics, biogenesis, mechanism, and function. *Cell*, *116*(2), 281–297.

Baumforth, K. R., Young, L. S., Flavell, K. J., Constandinou, C., & Murray, P. G. (1999). The Epstein-Barr virus and its association with human cancers. *Molecular Pathology: MP*, *52*(6), 307–322.

Bejarano, M. T., & Masucci, M. G. (1998). Interleukin-10 Abrogates the Inhibition of Epstein-Barr Virus–Induced B-Cell Transformation by Memory T-Cell Responses. *Blood*, *92*(11), 4256–4262.

Beurel, E., & Jope, R. S. (2006). The Paradoxical Pro- and Anti-apoptotic Actions of GSK3 in the Intrinsic and Extrinsic Apoptosis Signaling Pathways. *Progress in Neurobiology*, *79*(4), 173–189.

Bouvier, G., Hergenhahn, M., Polack, A., Bornkamm, G. W., de Thé, G., & Bartsch, H. (1995). Characterization of macromolecular lignins as Epstein-Barr virus inducer in foodstuff associated with nasopharyngeal carcinoma risk. *Carcinogenesis*, *16*(8), 1879–1885.

Boyle, M. J., Vasak, E., Tschuchnigg, M., Turner, J. J., Sculley, T., Penny, R., et al. (1993). Subtypes of Epstein-Barr virus (EBV) in Hodgkin's disease: association between B-type EBV and immunocompromise. *Blood*, *81*(2), 468–474.

Bratton, S. B., & Salvesen, G. S. (2010). Regulation of the Apaf-1–caspase-9 apoptosome. *Journal of Cell Science*, *123*(19), 3209–3214.

Brunelle, J. K., & Letai, A. (2009). Control of mitochondrial apoptosis by the Bcl-2 family. *Journal of Cell Science*, *122*(4), 437–441.

Burkitt, D. (1958). A sarcoma involving the jaws in african children. *British Journal of Surgery*, *46*(197), 218–223.

Burkitt, D. (1972). A sarcoma involving the jaws in african children. *CA: A Cancer Journal for Clinicians*, *22*(6), 349–355.

Chaitanya, G. V., Alexander, J. S., & Babu, P. P. (2010). PARP-1 cleavage fragments: signatures of cell-death proteases in neurodegeneration. *Cell Communication and Signaling*, *8*(1), 31.

Chang, E. T., & Adami, H.-O. (2006). The Enigmatic Epidemiology of Nasopharyngeal Carcinoma. *Cancer Epidemiology Biomarkers & Prevention*, *15*(10), 1765–1777.

Chang, M. S., Kim, D. H., Roh, J. K., Middeldorp, J. M., Kim, Y. S., Kim, S., et al. (2013). Epstein-Barr Virus-Encoded BARF1 Promotes Proliferation of Gastric Carcinoma Cells through Regulation of NF-κB. *Journal of Virology*.

Chapman, A. L., & Rickinson, A. B. (1998). Epstein-Barr virus in Hodgkin's disease. *Annals of Oncology: Official Journal of the European Society for Medical Oncology / ESMO*, *9 Suppl 5*, S5–16.

Cheng, E. H., Kirsch, D. G., Clem, R. J., Ravi, R., Kastan, M. B., Bedi, A., et al. (1997). Conversion of Bcl-2 to a Bax-like death effector by caspases. *Science (New York, N.Y.)*, *278*(5345), 1966–1968.

Cheng, E. H., Wei, M. C., Weiler, S., Flavell, R. A., Mak, T. W., Lindsten, T., & Korsmeyer, S. J. (2001). BCL-2, BCL-X(L) sequester BH3 domain-only molecules preventing BAX- and BAK-mediated mitochondrial apoptosis. *Molecular Cell*, *8*(3), 705–711.

Chen, X., Liu, H., Focia, P. J., Shim, A. H.-R., & He, X. (2008). Structure of macrophage colony stimulating factor bound to FMS: diverse signaling assemblies of class III receptor tyrosine kinases. *Proceedings of the National Academy of Sciences of the United States of America*, *105*(47), 18267–18272.

Cohen, J. I., & Lekstrom, K. (1999). Epstein-Barr virus BARF1 protein is dispensable for B-cell transformation and inhibits alpha interferon secretion from mononuclear cells. *Journal of Virology*, *73*(9), 7627–7632.

Coqueret, O. (2003). New roles for p21 and p27 cell-cycle inhibitors: a function for each cell compartment? *Trends in Cell Biology*, *13*(2), 65–70.

Cryns, V., & Yuan, J. (1998). Proteases to die for. *Genes & Development*, *12*(11), 1551–1570.

Danial, N. N., & Korsmeyer, S. J. (2004). Cell death: critical control points. *Cell*, *116*(2), 205–219.

Danve, C., Decaussin, G., Busson, P., & Ooka, T. (2001). Growth Transformation of Primary Epithelial Cells with a NPC-Derived Epstein–Barr Virus Strain. *Virology*, *288*(2), 223–235.

Dave, R. S., & Pomerantz, R. J. (2003). RNA interference: on the road to an alternate therapeutic strategy! *Reviews in Medical Virology*, *13*(6), 373–385.

Dawson, C. W., Eliopoulos, A. G., Dawson, J., & Young, L. S. (1995). BHRF1, a viral homologue of the Bcl-2 oncogene, disturbs epithelial cell differentiation. *Oncogene*, *10*(1), 69–77.

Decaussin, G., Sbih-Lammali, F., Turenne-Tessier, M. de, Bouguermouh, A., & Ooka, T. (2000). Expression of BARF1 Gene Encoded by Epstein-Barr Virus in Nasopharyngeal Carcinoma Biopsies. *Cancer Research*, *60*(19), 5584–5588.

De Turenne-Tessier, M., Jolicoeur, P., Middeldorp, J. M., & Ooka, T. (2005). Expression and analysis of the Epstein-Barr virus BARF1-encoded protein from a tetracycline-regulatable adenovirus system. *Virus Research*, *109*(1), 9–18.

Devi, B. C. R., Pisani, P., Tang, T. S., & Parkin, D. M. (2004). High Incidence of Nasopharyngeal Carcinoma in Native People of Sarawak, Borneo Island. *Cancer Epidemiology Biomarkers & Prevention*, *13*(3), 482–486.

Dorsett, Y., & Tuschl, T. (2004). siRNAs: applications in functional genomics and potential as therapeutics. *Nature Reviews. Drug Discovery*, *3*(4), 318–329.

Durai, R., Yang, S. Y., Sales, K. M., Seifalian, A. M., Goldspink, G., & Winslet, M. C. (2007). Increased apoptosis and decreased proliferation of colorectal cancer cells

using insulin-like growth factor binding protein-4 gene delivered locally by gene transfer. *Colorectal Disease*, *9*(7), 625–631.

Duxbury, M. S., & Whang, E. E. (2004). RNA interference: a practical approach. *Journal of Surgical Research*, *117*(2), 339–344.

Dykxhoorn, D. M., Novina, C. D., & Sharp, P. A. (2003). Killing the messenger: short RNAs that silence gene expression. *Nature Reviews. Molecular Cell Biology*, *4*(6), 457–467.

Elbashir, S. M., Lendeckel, W., & Tuschl, T. (2001). RNA interference is mediated by 21- and 22-nucleotide RNAs. *Genes & Development*, *15*(2), 188–200.

Eliopoulos, A. G., Gallagher, N. J., Blake, S. M., Dawson, C. W., & Young, L. S. (1999). Activation of the p38 mitogen-activated protein kinase pathway by Epstein-Barr virus-encoded latent membrane protein 1 coregulates interleukin-6 and interleukin-8 production. *The Journal of Biological Chemistry*, *274*(23), 16085–16096.

Enari, M., Sakahira, H., Yokoyama, H., Okawa, K., Iwamatsu, A., & Nagata, S. (1998). A caspase-activated DNase that degrades DNA during apoptosis, and its inhibitor ICAD. *Nature*, *391*(6662), 43–50.

Epstein, M., Achong, B., & Barr, Y. (1964). Virus particles in cultured lymphoblasts from Burkitt's lymphoma. *The Lancet*, *283*(7335), 702–703.

Epstein, M., Henle, G., Achong, B., & Barr, Y. (1965). Morphological and biological studies on a virus in cultured lymphoblasts from burkitt's lymphoma, *121*(5), 761–770.

Fadok, V. A., Voelker, D. R., Campbell, P. A., Cohen, J. J., Bratton, D. L., & Henson, P. M. (1992). Exposure of phosphatidylserine on the surface of apoptotic lymphocytes triggers specific recognition and removal by macrophages. *Journal of Immunology (Baltimore, Md.: 1950)*, *148*(7), 2207–2216.

Ferraro, E., & Cecconi, F. (2009). The apoptosome: the executioner of mitochondria-mediated apoptosis. In John Wiley & Sons, Ltd (Ed.), *Encyclopedia of Life Sciences*. Chichester, UK: John Wiley & Sons, Ltd. Fiorini, S., & Ooka, T.

(2008). Secretion of Epstein-Barr Virus-encoded BARF1 oncoprotein from latently infected B cells. *Virology Journal*, *5*(1), 70.

Fire, A., Xu, S., Montgomery, M. K., Kostas, S. A., Driver, S. E., & Mello, C. C. (1998). Potent and specific genetic interference by double-stranded RNA in Caenorhabditis elegans. *Nature*, *391*(6669), 806–811.

Franz, S., Herrmann, K., Fürnrohr, B. G., Führnrohr, B., Sheriff, A., Frey, B., … Herrmann, M. (2007). After shrinkage apoptotic cells expose internal membrane-derived epitopes on their plasma membranes. *Cell Death and Differentiation*, *14*(4), 733–742.

Fries, K. L., Miller, W. E., & Raab-Traub, N. (1996). Epstein-Barr virus latent membrane protein 1 blocks p53-mediated apoptosis through the induction of the A20 gene. *Journal of Virology*, *70*(12), 8653–8659.

Frommer, K. W., Reichenmiller, K., Schutt, B. S., Hoeflich, A., Ranke, M. B., Dodt, G., & Elmlinger, M. W. (2006). IGF-independent effects of IGFBP-2 on the human breast cancer cell line Hs578T. *Journal of Molecular Endocrinology*, *37*(1), 13–23.

Fukuda, S., & Pelus, L. M. (2006). Survivin, a cancer target with an emerging role in normal adult tissues. *Molecular Cancer Therapeutics*, *5*(5), 1087–1098.

Fulda, S., & Debatin, K.-M. (2006). Extrinsic versus intrinsic apoptosis pathways in anticancer chemotherapy. *Oncogene*, *25*(34), 4798–4811.

Ge, Q., McManus, M. T., Nguyen, T., Shen, C.-H., Sharp, P. A., Eisen, H. N., & Chen, J. (2003). RNA interference of influenza virus production by directly targeting mRNA for degradation and indirectly inhibiting all viral RNA transcription. *Proceedings of the National Academy of Sciences of the United States of America*, *100*(5), 2718–2723.

Gilligan, K., Sato, H., Rajadurai, P., Busson, P., Young, L., Rickinson, A., et al. (1990). Novel transcription from the Epstein-Barr virus terminal EcoRI fragment, DIJhet, in a nasopharyngeal carcinoma. *Journal of Virology*, *64*(10), 4948–4956.

Gires, O., Kohlhuber, F., Kilger, E., Baumann, M., Kieser, A., Kaiser, C., et al. (1999). Latent membrane protein 1 of Epstein-Barr virus interacts with JAK3 and activates STAT proteins. *The EMBO Journal*, *18*(11), 3064–3073.

Gitlin, L., Karelsky, S., & Andino, R. (2002). Short interfering RNA confers intracellular antiviral immunity in human cells. *Nature*, *418*(6896), 430–434.

Glaser, R., Zhang, H. Y., Yao, K. T., Zhu, H. C., Wang, F. X., Li, G. Y., et al. (1989). Two epithelial tumor cell lines (HNE-1 and HONE-1) latently infected with Epstein-Barr virus that were derived from nasopharyngeal carcinomas. *Proceedings of the National Academy of Sciences of the United States of America*, *86*(23), 9524–9528.

Gottlieb, E., Armour, S. M., Harris, M. H., & Thompson, C. B. (2003). Mitochondrial membrane potential regulates matrix configuration and cytochrome c release during apoptosis. *Cell Death & Differentiation*, *10*(6), 709–717.

Graber, T. E., & Holcik, M. (2011). Distinct roles for the cellular inhibitors of apoptosis proteins 1 and 2. *Cell Death & Disease*, *2*(3), 135.

Griffin, B. E., & Karran, L. (1984). Immortalization of monkey epithelial cells by specific fragments of Epstein–Barr virus DNA. *Nature*, *309*(5963), 78–82.

Grimberg, A. (2000). P53 and IGFBP-3: apoptosis and cancer protection. *Molecular Genetics and Metabolism*, *70*(2), 85–98.

Gross, A., McDonnell, J. M., & Korsmeyer, S. J. (1999). BCL-2 family members and the mitochondria in apoptosis. *Genes & Development*, *13*(15), 1899–1911.

Guo, X., Sheng, W., & Zhang, Y. (2001). Malignant transformation of monkey kidney epithelial cell induced by EBV BARF1 gene and TPA. *Chinese journal of experimental and clinical virology*, *15*(4), 321–323.

Hajra, K. M., & Liu, J. R. (2004). Apoptosome dysfunction in human cancer. *Apoptosis: An International Journal on Programmed Cell Death*, *9*(6), 691–704.

Haldar, S., Jena, N., & Croce, C. M. (1995). Inactivation of Bcl-2 by phosphorylation. *Proceedings of the National Academy of Sciences*, *92*(10), 4507–4511.

Helminen, M., Lahdenpohja, N., & Hurme, M. (1999). Polymorphism of the interleukin-10 gene is associated with susceptibility to Epstein-Barr virus infection. *The Journal of Infectious Diseases*, *180*(2), 496–499.

Henderson, S., Huen, D., Rowe, M., Dawson, C., Johnson, G., & Rickinson, A. (1993). Epstein-Barr virus-coded BHRF1 protein, a viral homologue of Bcl-2, protects human B cells from programmed cell death. *Proceedings of the National Academy of Sciences*, *90*(18), 8479–8483.

Henkel, T., Ling, P. D., Hayward, S. D., & Peterson, M. G. (1994). Mediation of Epstein-Barr virus EBNA2 transactivation by recombination signal-binding protein J kappa. *Science*, *265*(5168), 92–95.

Hennessy, K., & Kieff, E. (1985). A second nuclear protein is encoded by Epstein-Barr virus in latent infection. *Science*, *227*(4691), 1238–1240.

Herbst, H., Stein, H., & Niedobitek, G. (1993). Epstein-Barr virus and CD30+ malignant lymphomas. *Critical Reviews in Oncogenesis*, *4*(2), 191–239.

Hoebe, E. K., Hutajulu, S. H., van Beek, J., Stevens, S. J., Paramita, D. K., Greijer, A. E., & Middeldorp, J. M. (2011). Purified Hexameric Epstein-Barr Virus-Encoded BARF1 Protein for Measuring Anti-BARF1 Antibody Responses in Nasopharyngeal Carcinoma Patients. *Clinical and Vaccine Immunology : CVI*, *18*(2), 298–304.

Hoebe, E. K., Le Large, T. Y. S., Greijer, A. E., & Middeldorp, J. M. (2013). BamHI-A rightward frame 1, an Epstein–Barr virus-encoded oncogene and immune modulator. *Reviews in Medical Virology*, *23*(6), 367–383.

Hoebe, E. K., Le Large, T. Y. S., Tarbouriech, N., Oosterhoff, D., De Gruijl, T. D., Middeldorp, J. M., & Greijer, A. E. (2012). Epstein-Barr Virus-Encoded BARF1 Protein is a Decoy Receptor for Macrophage Colony Stimulating Factor and Interferes with Macrophage Differentiation and Activation. *Viral Immunology*, *25*(6), 461–470.

Ho, J. W., Ho, F. C., Chan, A. C., Liang, R. H., & Srivastava, G. (1998). Frequent detection of Epstein-Barr virus-infected B cells in peripheral T-cell lymphomas. *The Journal of Pathology*, *185*(1), 79–85.

Ho, J. W., Liang, R. H., & Srivastava, G. (1999). Differential cytokine expression in EBV positive peripheral T cell lymphomas. *Molecular Pathology*, *52*(5), 269–274.

Houali, K., Wang, X., Shimizu, Y., Djennaoui, D., Nicholls, J., Fiorini, S., et al. (2007). A new diagnostic marker for secreted epstein-barr virus–encoded lmp1 and barf1 oncoproteins in the serum and saliva of patients with nasopharyngeal carcinoma. *Clinical Cancer Research*, *13*(17), 4993–5000.

Hsu, M. M., Huang, S. C., Lynn, T. C., Hsieh, T., & Tu, S. M. (1982). The survival of patients with nasopharyngeal carcinoma. *Otolaryngology--Head and Neck Surgery: Official Journal of American Academy of Otolaryngology-Head and Neck Surgery*, *90*(3 Pt 1), 289–295.

Imbeaud, S., Graudens, E., Boulanger, V., Barlet, X., Zaborski, P., Eveno, E., et al. (2005). Towards standardization of RNA quality assessment using user-independent classifiers of microcapillary electrophoresis traces. *Nucleic Acids Research*, *33*(6), e56–e56.

Izumi, K. M., & Kieff, E. D. (1997). The Epstein-Barr virus oncogene product latent membrane protein 1 engages the tumor necrosis factor receptor-associated death domain protein to mediate B lymphocyte growth transformation and activate NF-kappaB. *Proceedings of the National Academy of Sciences of the United States of America*, *94*(23), 12592–12597.

Jacque, J.-M., Triques, K., & Stevenson, M. (2002). Modulation of HIV-1 replication by RNA interference. *Nature*, *418*(6896), 435–438.

Jiang, R., Cabras, G., Sheng, W., Zeng, Y., & Ooka, T. (2009). Synergism of BARF1 with Ras induces malignant transformation in primary primate epithelial cells and human nasopharyngeal epithelial cells. *Neoplasia*, *11*(9), 964–973.

Joutel, A., & Tournier-Lasserve, E. (1998). Notch signalling pathway and human diseases. *Seminars in Cell & Developmental Biology*, *9*(6), 619–625.

Kapadia, S. B., Brideau-Andersen, A., & Chisari, F. V. (2003). Interference of hepatitis C virus RNA replication by short interfering RNAs. *Proceedings of the National Academy of Sciences*, *100*(4), 2014–2018.

Karlin, S., Blaisdell, B. E., & Schachtel, G. A. (1990). Contrasts in codon usage of latent versus productive genes of Epstein-Barr virus: data and hypotheses. *Journal of Virology*, *64*(9), 4264–4273.

Kaufmann, S. H., Desnoyers, S., Ottaviano, Y., Davidson, N. E., & Poirier, G. G. (1993). Specific proteolytic cleavage of poly(ADP-ribose) polymerase: an early marker of chemotherapy-induced apoptosis. *Cancer Research*, *53*(17), 3976–3985.

Khanna, R., Burrows, S. R., Kurilla, M. G., Jacob, C. A., Misko, I. S., Sculley, T. B., et al. (1992). Localization of Epstein-Barr virus cytotoxic T cell epitopes using recombinant vaccinia: implications for vaccine development. *The Journal of Experimental Medicine*, *176*(1), 169–176.

Khvorova, A., Reynolds, A., & Jayasena, S. D. (2003). Functional siRNAs and miRNAs exhibit strand bias. *Cell*, *115*(2), 209–216.

Komano, J., Maruo, S., Kurozumi, K., Oda, T., & Takada, K. (1999). Oncogenic role of Epstein-Barr virus-encoded RNAs in Burkitt's lymphoma cell line Akata. *Journal of Virology*, *73*(12), 9827–9831.

Komano, J., Sugiura, M., & Takada, K. (1998). Epstein-Barr virus contributes to the malignant phenotype and to apoptosis resistance in Burkitt's lymphoma cell line Akata. *Journal of Virology*, *72*(11), 9150–9156.

Korsmeyer, S. J. (1999). BCL-2 gene family and the regulation of programmed cell death. *Cancer Research*, *59*(7 Supplement), 1693s–1700s.

Kume, T., Oshima, K., Shinohara, T., Takeo, H., Yamashita, Y., Shirakusa, T., & Kikuchi, M. (1999). Low rate of apoptosis and overexpression of bcl-2 in Epstein-Barr virus-associated gastric carcinoma. *Histopathology*, *34*(6), 502–509.

Kwong, Y. L., Chan, A. C., Liang, R., Chiang, A. K., Chim, C. S., Chan, T. K., et al. (1997). CD56+ NK lymphomas: clinicopathological features and prognosis. *British Journal of Haematology*, *97*(4), 821–829.

Lacour, S., Micheau, O., Hammann, A., Drouineaud, V., Tschopp, J., Solary, E., & Dimanche-Boitrel, M.-T. (2003). Chemotherapy enhances TNF-related apoptosis-inducing ligand DISC assembly in HT29 human colon cancer cells. *Oncogene*, *22*(12), 1807–1816.

Ledgerwood, E. C., & Morison, I. M. (2009). Targeting the Apoptosome for Cancer Therapy. *Clinical Cancer Research*, *15*(2), 420–424.

Lee, Y. S., Nakahara, K., Pham, J. W., Kim, K., He, Z., Sontheimer, E. J., & Carthew, R. W. (2004). Distinct roles for Drosophila Dicer-1 and Dicer-2 in the siRNA/miRNA silencing pathways. *Cell*, *117*(1), 69–81.

Leoncini, L., Spina, D., Nyong'o, A., Abinya, O., Minacci, C., Disanto, A., et al. (1996). Neoplastic cells of Hodgkin's disease show differences in EBV expression between Kenya and Italy. *International Journal of Cancer. Journal International Du Cancer*, *65*(6), 781–784.

Levine, P. H., Ablashi, D. V., Berard, C. W., Carbone, P. P., Waggoner, D. E., & Malan, L. (1971). Elevated antibody titers to Epstein-barr virus in Hodgkin's disease. *Cancer*, *27*(2), 416–421.

Lichner, Z., Silhavy, D., & Burgyán, J. (2003). Double-stranded RNA-binding proteins could suppress RNA interference-mediated antiviral defences. *The Journal of General Virology*, *84*(Pt 4), 975–980.

Li, H., Li, W. X., & Ding, S. W. (2002). Induction and Suppression of RNA Silencing by an Animal Virus. *Science*, *296*(5571), 1319–1321.

Lin, C. T., Lin, C. R., Tan, G. K., Chen, W., Dee, A. N., & Chan, W. Y. (1997). The mechanism of Epstein-Barr virus infection in nasopharyngeal carcinoma cells. *The American Journal of Pathology*, *150*(5), 1745–1756.

Li, X.-P., Li, G., Peng, Y., Kung, H., & Lin, M. C. (2004). Suppression of Epstein-Barr virus-encoded latent membrane protein-1 by RNA interference inhibits the metastatic potential of nasopharyngeal carcinoma cells. *Biochemical and Biophysical Research Communications*, *315*(1), 212–218.

Lo, A. K. F., Huang, D. P., Lo, K. W., Chui, Y. L., Li, H. M., Pang, J. C. S., & Tsao, S.-W. (2004). Phenotypic alterations induced by the Hong Kong-prevalent Epstein-Barr virus-encoded LMP1 variant (2117-LMP1) in nasopharyngeal epithelial cells. *International Journal of Cancer*, *109*(6), 919–925.

Lu, Q. L., Elia, G., Lucas, S., & Thomas, J. A. (1993). Bcl-2 proto-oncogene expression in Epstein-Barr-virus-associated nasopharyngeal carcinoma. *International Journal of Cancer*. *53*(1), 29–35.

Lu, X.-Y., Cao, K., Li, Q.-Y., Yuan, Z.-C., & Lu, P.-S. (2012). The synergistic therapeutic effect of temozolomide and hyperbaric oxygen on glioma U251 cell lines is accompanied by alterations in vascular endothelial growth factor and multidrug resistance-associated protein-1 levels. *The Journal of International Medical Research*, *40*(3), 995–1004.

Ly, J. D., Grubb, D. R., & Lawen, A. (2003). The mitochondrial membrane potential (deltapsi(m)) in apoptosis; an update. *Apoptosis: An International Journal on Programmed Cell Death*, *8*(2), 115–128.

Lyons, S. F., & Liebowitz, D. N. (1998). The roles of human viruses in the pathogenesis of lymphoma. *Seminars in Oncology*, *25*(4), 461–475.

Mancao, C., Altmann, M., Jungnickel, B., & Hammerschmidt, W. (2005). Rescue of 'crippled' germinal center B cells from apoptosis by Epstein-Barr virus. *Blood*, *106*(13), 4339–4344.

Manero, F., Gautier, F., Gallenne, T., Cauquil, N., Grée, D., Cartron, P.-F., et al. (2006). The small organic compound HA14-1 prevents Bcl-2 interaction with Bax to sensitize malignant glioma cells to induction of cell death. *Cancer Research*, *66*(5), 2757–2764.

Martin, S. J., Reutelingsperger, C. P., McGahon, A. J., Rader, J. A., Schie, R. C. van, LaFace, D. M., & Green, D. R. (1995). Early redistribution of plasma membrane phosphatidylserine is a general feature of apoptosis regardless of the initiating stimulus: inhibition by overexpression of Bcl-2 and Abl. *The Journal of Experimental Medicine*, *182*(5), 1545–1556.

Marzo, I., Brenner, C., Zamzami, N., Jürgensmeier, J. M., Susin, S. A., Vieira, H. L., et al. (1998). Bax and adenine nucleotide translocator cooperate in the mitochondrial control of apoptosis. *Science*, *281*(5385), 2027–2031.

Middeldorp, J. M., Brink, A. A. T. P., van den Brule, A. J. C., & Meijer, C. J. L. M. (2003). Pathogenic roles for Epstein-Barr virus (EBV) gene products in EBV-associated proliferative disorders. *Critical Reviews in Oncology/hematology*, *45*(1), 1–36.

Migita, T., Narita, T., Asaka, R., Miyagi, E., Nagano, H., Nomura, K., et al. (2010). Role of Insulin-Like Growth Factor Binding Protein 2 in Lung Adenocarcinoma. *The American Journal of Pathology*, *176*(4), 1756–1766.

Miller, G., & Lipman, M. (1973). Release of Infectious Epstein-Barr Virus by Transformed Marmoset Leukocytes. *Proceedings of the National Academy of Sciences of the United States of America*, *70*(1), 190–194.

Miyashita, T., & Reed, J. C. (1995). Tumor suppressor p53 is a direct transcriptional activator of the human bax gene. *Cell*, *80*(2), 293–299.

M Los, & S Gibson. (2005). *Apoptotic Pathways as Targets for Novel Therapies in Cancer and Other Diseases* (Vol. XXVI). Retrieved from http://www.springer.com/biomed/pharmacology+%26+toxicology/book/978-0-387-23384-0

Monterroso, V., Zhou, Y., Koo, S., Glackin, C., Bujan, W., & Medeiros, L. J. (1998). Hodgkin's disease in Costa Rica: a report of 40 cases analyzed for Epstein-Barr virus. *American Journal of Clinical Pathology*, *109*(5), 618–624.

Moore, K. W., Rousset, F., & Banchereau, J. (1991). Evolving principles in immunopathology: interleukin 10 and its relationship to Epstein-Barr virus protein BCRF1. *Springer Seminars in Immunopathology*, *13*(2), 157–166.

Moorthy, R. K., & Thorley-Lawson, D. A. (1993). Biochemical, genetic, and functional analyses of the phosphorylation sites on the Epstein-Barr virus-encoded oncogenic latent membrane protein LMP-1. *Journal of Virology*, *67*(5), 2637–2645.

Muñoz, N., Davidson, R. J. L., Witthoff, B., Ericsson, J. E., & De-Thé, G. (1978). Infectious mononucleosis and Hodgkin's disease. *International Journal of Cancer*, *22*(1), 10–13.

Murray, P. G., & Young, L. S. (2002). The Role of the Epstein-Barr virus in human disease. *Frontiers in Bioscience: A Journal and Virtual Library*, *7*, d519–540.

Nakano, K., & Vousden, K. H. (2001). PUMA, a novel proapoptotic gene, is induced by p53. *Molecular Cell*, *7*(3), 683–694.

Nicholson, D. W., Ali, A., Thornberry, N. A., Vaillancourt, J. P., Ding, C. K., Gallant, M., et al. (1995). Identification and inhibition of the ICE/CED-3 protease necessary for mammalian apoptosis. *Nature*, *376*(6535), 37–43.

Niedobitek, G., Agathanggelou, A., Herbst, H., Whitehead, L., Wright, D. H., & Young, L. S. (1997). Epstein-Barr virus (EBV) infection in infectious mononucleosis: virus latency, replication and phenotype of EBV-infected cells. *The Journal of Pathology*, *182*(2), 151–159.

Niedobitek, G., & Young, L. S. (1994). Epstein-Barr virus persistence and virus-associated tumours. *Lancet*, *343*(8893), 333–335.

Novina, C. D., Murray, M. F., Dykxhoorn, D. M., Beresford, P. J., Riess, J., Lee, S.-K., et al. (2002). siRNA-directed inhibition of HIV-1 infection. *Nature Medicine*, *8*(7), 681–686.

Oda, E., Ohki, R., Murasawa, H., Nemoto, J., Shibue, T., Yamashita, T., et al. (2000). Noxa, a BH3-only member of the Bcl-2 family and candidate mediator of p53-induced apoptosis. *Science*, *288*(5468), 1053–1058.

Okada, H., & Mak, T. W. (2004). Pathways of apoptotic and non-apoptotic death in tumour cells. *Nature Reviews. Cancer*, *4*(8), 592–603.

Oltersdorf, T., Elmore, S. W., Shoemaker, A. R., Armstrong, R. C., Augeri, D. J., Belli, B. A., et al. (2005). An inhibitor of Bcl-2 family proteins induces regression of solid tumours. *Nature*, *435*(7042), 677–681.

Oltvai, Z. N., Milliman, C. L., & Korsmeyer, S. J. (1993). Bcl-2 heterodimerizes in vivo with a conserved homolog, Bax, that accelerates programmed cell death. *Cell*, *74*(4), 609–619.

Orth, K., Chinnaiyan, A. M., Garg, M., Froelich, C. J., & Dixit, V. M. (1996). The CED-3/ICE-like Protease Mch2 Is Activated during Apoptosis and Cleaves the Death Substrate Lamin A. *Journal of Biological Chemistry*, *271*(28), 16443–16446.

Oudejans, J. J., van den Brule, A. J., Jiwa, N. M., de Bruin, P. C., Ossenkoppele, G. J., van der Valk, P., et al. (1995). BHRF1, the Epstein-Barr virus (EBV) homologue of the BCL-2 protooncogene, is transcribed in EBV-associated B-cell lymphomas and in reactive lymphocytes. *Blood*, *86*(5), 1893–1902.

Pagano, J. S. (1999). Epstein-Barr virus: the first human tumor virus and its role in cancer. *Proceedings of the Association of American Physicians*, *111*(6), 573–580.

Pathmanathan, R., Prasad, U., Sadler, R., Flynn, K., & Raab-Traub, N. (1995). Clonal proliferations of cells infected with Epstein-Barr virus in preinvasive lesions related to nasopharyngeal carcinoma. *The New England Journal of Medicine*, *333*(11), 693–698.

Peter, M. E., & Krammer, P. H. (2003). The CD95(APO-1/Fas) DISC and beyond. *Cell Death & Differentiation*, *10*(1), 26–35.

Pizzo, P. A., Magrath, I. T., Chattopadhyay, S. K., Biggar, R. J., & Gerber, P. (1978). A new tumour-derived transforming strain of Epstein–Barr virus. *Nature*, *272*(5654), 629–631.

Plasterk, R. H. A. (2002). RNA silencing: the genome's immune system. *Science*, *296*(5571), 1263–1265.

Prasad, U., Singh, J., & Patmanathan, R. (1985). Fossa of Rosenmuller: the site for initial development of carcinoma of the nasopharynx. In P. H. Levine, D. V. Ablashi, G. R. Pearson, & S. D. Kottaridis (Eds.), *Epstein-Barr Virus and Associated Diseases* (pp. 200–206).

Pua, K. C., Khoo, A. S. B., Yap, Y. Y., Subramaniam, S. K., Ong, C. A., Gopala Krishnan, G., et al. (2008). Nasopharyngeal carcinoma database. *The Medical Journal of Malaysia*, *63 Suppl C*, 59–62.

Qin, X.-F., An, D. S., Chen, I. S. Y., & Baltimore, D. (2003). Inhibiting HIV-1 infection in human T cells by lentiviral-mediated delivery of small interfering RNA against CCR5. *Proceedings of the National Academy of Sciences*, *100*(1), 183–188.

Radkov, S. A., Bain, M., Farrell, P. J., West, M., Rowe, M., & Allday, M. J. (1997). Epstein-Barr virus EBNA3C represses Cp, the major promoter for EBNA expression, but has no effect on the promoter of the cell gene CD21. *Journal of Virology*, *71*(11), 8552–8562.

Reed, J. C. (1996). Balancing cell life and death: bax, apoptosis, and breast cancer. *The Journal of Clinical Investigation*, *97*(11), 2403–2404.

Rickinson, A. B., Young, L. S., & Rowe, M. (1987). Influence of the Epstein-Barr virus nuclear antigen EBNA 2 on the growth phenotype of virus-transformed B cells. *Journal of Virology*, *61*(5), 1310–1317.

Robertson, E. S. (2005). *Epstein-Barr Virus*. Horizon Scientific Press.

Rowe, D. T. (1999). Epstein-Barr virus immortalization and latency. *Frontiers in Bioscience: A Journal and Virtual Library*, *4*, D346–371.

Rowe, D. T., & Clarke, J. R. (1989). The type-specific epitopes of the Epstein-Barr virus nuclear antigen 2 are near the carboxy terminus of the protein. *The Journal of General Virology*, *70 (Pt 5)*, 1217–1229.

Ryan, A. J., Napoletano, S., Fitzpatrick, P. A., Currid, C. A., O'Sullivan, N. C., & Harmey, J. H. (2009). Expression of a protease-resistant insulin-like growth factor-binding protein-4 inhibits tumour growth in a murine model of breast cancer. *British Journal of Cancer*, *101*(2), 278–286.

Sadler, R. H., & Raab-Traub, N. (1995). Structural analyses of the Epstein-Barr virus BamHI a transcripts. *Journal of Virology*, *69*(2), 1132–1141.

Saha, A., & Robertson, E. S. (2011). Epstein-Barr virus–associated b-cell lymphomas: pathogenesis and clinical outcomes. *Clinical Cancer Research*, *17*(10), 3056–3063.

Sakka, E., Hausen, A. zur, Houali, K., Liu, H., Fiorini, S., & Ooka, T. (2013). Cellular localization of BARF1 oncoprotein and its cell stimulating activity in human epithelial cell. *Virus Research*, *174*(1–2), 8–17.

Sall, A., Caserta, S., Jolicoeur, P., Franqueville, L., de Turenne-Tessier, M., & Ooka, T. (2004). Mitogenic activity of Epstein-Barr virus-encoded BARF1 protein. *Oncogene*, *23*(28), 4938–4944.

Sample, J., Young, L., Martin, B., Chatman, T., Kieff, E., Rickinson, A., & Kieff, E. (1990). Epstein-Barr virus types 1 and 2 differ in their EBNA-3A, EBNA-3B, and EBNA-3C genes. *Journal of Virology*, *64*(9), 4084–4092.

Sandy, P., Ventura, A., & Jacks, T. (2005). Mammalian RNAi: a practical guide. *BioTechniques*, *39*(2), 215–224.

Schlager, S., Speck, S. H., & Woisetschläger, M. (1996). Transcription of the Epstein-Barr virus nuclear antigen 1 (EBNA1) gene occurs before induction of the BCR2 (Cp) EBNA gene promoter during the initial stages of infection in B cells. *Journal of Virology*, *70*(6), 3561–3570.

Schutt, B. S., Langkamp, M., Rauschnabel, U., Ranke, M. B., & Elmlinger, M. W. (2004). Integrin-mediated action of insulin-like growth factor binding protein-2 in tumor cells. *Journal of Molecular Endocrinology*, *32*(3), 859–868.

Seto, E., Ooka, T., Middeldorp, J., & Takada, K. (2008). Reconstitution of nasopharyngeal carcinoma–type EBV infection induces tumorigenicity. *Cancer Research*, *68*(4), 1030–1036.

Seto, E., Yang, L., Middeldorp, J., Sheen, T.-S., Chen, J.-Y., Fukayama, M., et al. (2005). Epstein–Barr virus (EBV)-encoded BARF1 gene is expressed in nasopharyngeal carcinoma and EBV-associated gastric carcinoma tissues in the absence of lytic gene expression. *Journal of Medical Virology*, *76*(1), 82–88.

Sheng, W., Decaussin, G., Ligout, A., Takada, K., & Ooka, T. (2003). Malignant transformation of Epstein-Barr Virus-negative Akata cells by introduction of the BARF1 gene carried by Epstein-Barr virus. *Journal of Virology*, *77*(6), 3859–3865.

Sheng, W., Decaussin, G., Sumner, S., & Ooka, T. (2001). N-terminal domain of BARF1 gene encoded by Epstein-Barr virus is essential for malignant transformation of rodent fibroblasts and activation of BCL-2. *Oncogene*, *20*(10), 1176–1185.

Shim, A. H.-R., Chang, R. A., Chen, X., Longnecker, R., & He, X. (2012). Multipronged attenuation of macrophage-colony stimulating factor signaling by Epstein-Barr virus BARF1. *Proceedings of the National Academy of Sciences of the United States of America*, *109*(32), 12962–12967.

Shimizu, N., Tanabe-Tochikura, A., Kuroiwa, Y., & Takada, K. (1994). Isolation of Epstein-Barr virus (EBV)-negative cell clones from the EBV-positive Burkitt's lymphoma (BL) line Akata: malignant phenotypes of BL cells are dependent on EBV. *Journal of Virology*, *68*(9), 6069–6073.

Shimizu, S., Narita, M., & Tsujimoto, Y. (1999). Bcl-2 family proteins regulate the release of apoptogenic cytochrome c by the mitochondrial channel VDAC. *Nature*, *399*(6735), 483–487.

Sinclair, A. J., Brimmell, M., & Farrell, P. J. (1992). Reciprocal antagonism of steroid hormones and BZLF1 in switch between Epstein-Barr virus latent and productive cycle gene expression. *Journal of Virology*, *66*(1), 70–77.

Sinclair, A. J., Palmero, I., Peters, G., & Farrell, P. J. (1994). EBNA-2 and EBNA-LP cooperate to cause G0 to G1 transition during immortalization of resting human B lymphocytes by Epstein-Barr virus. *The EMBO Journal*, *13*(14), 3321–3328.

Song, E., Lee, S.-K., Wang, J., Ince, N., Ouyang, N., Min, J., et al. (2003). RNA interference targeting Fas protects mice from fulminant hepatitis. *Nature Medicine*, *9*(3), 347–351.

Song, J.-J., Liu, J., Tolia, N. H., Schneiderman, J., Smith, S. K., Martienssen, R. A., et al. (2003). The crystal structure of the Argonaute2 PAZ domain reveals an RNA

binding motif in RNAi effector complexes. *Nature Structural Biology*, *10*(12), 1026–1032.

Song, L.-B., Zen, M.-S., Zhang, L., Li, M.-Z., Liao, W.-T., Zheng, M.-L., et al. (2004). Effect of EBV encoded BARF1 gene on malignant transformation of human epithelial cell line HBE. *Chinese journal of cancer*, *23* (11 Suppl), 1361–1364.

Spano, J.-P., Busson, P., Atlan, D., Bourhis, J., Pignon, J.-P., Esteban, C., & Armand, J.-P. (2003). Nasopharyngeal carcinomas: an update. *European Journal of Cancer*, *39*(15), 2121–2135.

Stanley, E. R., Berg, K. L., Einstein, D. B., Lee, P. S., Pixley, F. J., Wang, Y., & Yeung, Y. G. (1997). Biology and action of colony--stimulating factor-1. *Molecular Reproduction and Development*, *46*(1), 4–10.

Steitz, J. A. (2004). RNAi: A guide to gene silencing, *RNA*, *10*(3), 350.

Steller, H. (1995). Mechanisms and genes of cellular suicide. *Science*, *267*(5203), 1445–1449.

Strockbine, L. D., Cohen, J. I., Farrah, T., Lyman, S. D., Wagener, F., DuBose, R. F., et al. (1998). The Epstein-Barr virus BARF1 gene encodes a novel, soluble colony-stimulating factor-1 receptor. *Journal of Virology*, *72*(5), 4015–4021.

Subar, M., Neri, A., Inghirami, G., Knowles, D. M., & Dalla-Favera, R. (1988). Frequent c-myc oncogene activation and infrequent presence of Epstein-Barr virus genome in AIDS-associated lymphoma. *Blood*, *72*(2), 667–671.

Suzuki, M., Youle, R. J., & Tjandra, N. (2000). Structure of Bax: coregulation of dimer formation and intracellular localization. *Cell*, *103*(4), 645–654.

Swaminathan, S., Hesselton, R., Sullivan, J., & Kieff, E. (1993). Epstein-Barr virus recombinants with specifically mutated BCRF1 genes. *Journal of Virology*, *67*(12), 7406–7413.

Swaminathan, S., Tomkinson, B., & Kieff, E. (1991). Recombinant Epstein-Barr virus with small RNA (EBER) genes deleted transforms lymphocytes and replicates in

vitro. *Proceedings of the National Academy of Sciences of the United States of America*, *88*(4), 1546–1550.

Szekely, L., Selivanova, G., Magnusson, K. P., Klein, G., & Wiman, K. G. (1993). EBNA-5, an Epstein-Barr virus-encoded nuclear antigen, binds to the retinoblastoma and p53 proteins. *Proceedings of the National Academy of Sciences of the United States of America*, *90*(12), 5455–5459.

Takada, K. (2000). Epstein-Barr virus and gastric carcinoma. *Molecular Pathology: MP*, *53*(5), 255–261.

Takada, K. (2012). Role of EBER and BARF1 in nasopharyngeal carcinoma (NPC) tumorigenesis. *Seminars in Cancer Biology*, *22*(2), 162–165.

Takada, K., & Nanbo, A. (2001). The role of EBERs in oncogenesis. *Seminars in Cancer Biology*, *11*(6), 461–467.

Tanner, J. E., Wei, M. X., Alfieri, C., Ahmad, A., Taylor, P., Ooka, T., & Menezes, J. (1997). Antibody and antibody-dependent cellular cytotoxicity responses against the BamHI A rightward open-reading frame-1 protein of Epstein-Barr virus (EBV) in EBV-associated disorders. *Journal of Infectious Diseases*, *175*(1), 38–46.

Tao, Q., Ho, F. C., Loke, S. L., & Srivastava, G. (1995). Epstein-Barr virus is localized in the tumour cells of nasal lymphomas of NK, T or B cell type. *International Journal of Cancer*, *60*(3), 315–320.

Tepper, C. G., & Seldin, M. F. (1999). Modulation of caspase-8 and FLICE-inhibitory protein expression as a potential mechanism of Epstein-Barr virus tumorigenesis in Burkitt's lymphoma. *Blood*, *94*(5), 1727–1737.

Thornberry, N. A., & Lazebnik, Y. (1998). Caspases: enemies within. *Science)*, *281*(5381), 1312–1316.

Tomita, Y., Ohsawa, M., Kanno, H., Hashimoto, M., Ohnishi, A., Nakanishi, H., & Aozasa, K. (1996). Epstein-Barr virus in Hodgkin's disease patients in Japan. *Cancer*, *77*(1), 186–192.

Tsuchiyama, J., Yoshino, T., Mori, M., Kondoh, E., Oka, T., Akagi, T., et al. (1998). Characterization of a novel human natural killer-cell line (NK-YS) established from natural killer cell lymphoma/leukemia associated with Epstein-Barr virus infection. *Blood*, *92*(4), 1374–1383.

Vasef, M. A., Ferlito, A., & Weiss, L. M. (1997). Nasopharyngeal carcinoma, with emphasis on its relationship to Epstein-Barr virus. *The Annals of Otology, Rhinology, and Laryngology*, *106*(4), 348–356.

Wang, L., Tam, J. P., & Liu, D. X. (2006). Biochemical and functional characterization of Epstein–Barr virus-encoded BARF1 protein: interaction with human hTid1 protein facilitates its maturation and secretion. *Oncogene*, *25*(31), 4320–4331.

Wang, Q., Tsao, S. W., Ooka, T., Nicholls, J. M., Cheung, H. W., Fu, S., et al. (2006). Anti-apoptotic role of BARF1 in gastric cancer cells. *Cancer Letters*, *238*(1), 90–103.

Wei, M. C., Zong, W. X., Cheng, E. H., Lindsten, T., Panoutsakopoulou, V., Ross, A. J., et al. (2001). Proapoptotic BAX and BAK: a requisite gateway to mitochondrial dysfunction and death. *Science*, *292*(5517), 727–730.

Wei, M. X., Moulin, J.-C., Decaussin, G., Berger, F., & Ooka, T. (1994). Expression and tumorigenicity of the Epstein-Barr virus BARF1 gene in human Louckes B-lymphocyte cell line. *Cancer Research*, *54*(7), 1843–1848.

Wei, M. X., & Ooka, T. (1989). A transforming function of the BARF1 gene encoded by Epstein-Barr virus. *The EMBO Journal*, *8*(10), 2897–2903.

Wei, M. X., Turenne-Tessier, M. de, Decaussin, G., Benet, G., & Ooka, T. (1997). Establishment of a monkey kidney epithelial cell line with the BARF1 open reading frame from Epstein-Barr Virus, *14*(25), 3073–3081.

Weiss, L. M., Jaffe, E. S., Liu, X. F., Chen, Y. Y., Shibata, D., & Medeiros, L. J. (1992). Detection and localization of Epstein-Barr viral genomes in angioimmunoblastic lymphadenopathy and angioimmunoblastic lymphadenopathy-like lymphoma. *Blood*, *79*(7), 1789–1795.

Weiss, L. M., & Movahed, L. A. (1989). In situ demonstration of Epstein-Barr viral genomes in viral-associated B cell lymphoproliferations. *The American Journal of Pathology*, *134*(3), 651–659.

Wensing, B., & Farrell, P. J. (2000). Regulation of cell growth and death by Epstein-Barr virus. *Microbes and Infection / Institut Pasteur*, *2*(1), 77–84.

Wiech, T., Nikolopoulos, E., Lassman, S., Heidt, T., Schöpflin, A., Sarbia, M., et al. (2008). Cyclin D1 expression is induced by viral BARF1 and is overexpressed in EBV-associated gastric cancer. *Virchows Archiv: An International Journal of Pathology*, *452*(6), 621–627.

Williams, A. C., Smartt, H., H-Zadeh, A. M., MacFarlane, M., Paraskeva, C., & Collard, T. J. (2006). Insulin-like growth factor binding protein 3 (IGFBP-3) potentiates TRAIL-induced apoptosis of human colorectal carcinoma cells through inhibition of NF-κB. *Cell Death & Differentiation*, *14*(1), 137–145.

Xue, S., Labrecque, L. G., Lu, Q.-L., Ong, S. K., Lampert, I. A., Kazembe, P., et al. (2002). Promiscuous expression of Epstein-Barr virus genes in Burkitt's lymphoma from the central African country Malawi. *International Journal of Cancer*, *99*(5), 635–643.

Yates, J. L., & Guan, N. (1991). Epstein-Barr virus-derived plasmids replicate only once per cell cycle and are not amplified after entry into cells. *Journal of Virology*, *65*(1), 483–488.

Yin, Q., & Wan, Y. (2002). RNA-mediated gene regulation system: now and the future (Review). *International Journal of Molecular Medicine*, *10*(4), 355–365.

Yoshinouchi, M., Yamada, T., Kizaki, M., Fen, J., Koseki, T., Ikeda, Y., et al. (2003). In vitro and in vivo growth suppression of human Papillomavirus 16-positive cervical cancer cells by E6 siRNA. *Molecular Therapy*, *8*(5), 762–768.

Young, L. S., Dawson, C. W., Brown, K. W., & Rickinson, A. B. (1989). Identification of a human epithelial cell surface protein sharing an epitope with the C3d/Epstein-Barr virus receptor molecule of B lymphocytes. *International Journal of Cancer*, *43*(5), 786–794.

Young, L. S., & Rickinson, A. B. (2004). Epstein-Barr virus: 40 years on. *Nature Reviews Cancer*, *4*(10), 757–768.

Yuzawa, S., Opatowsky, Y., Zhang, Z., Mandiyan, V., Lax, I., & Schlessinger, J. (2007). Structural basis for activation of the receptor tyrosine kinase KIT by stem cell factor. *Cell*, *130*(2), 323–334.

Zamzami, N., Susin, S. A., Marchetti, P., Hirsch, T., Gómez-Monterrey, I., Castedo, M., & Kroemer, G. (1996). Mitochondrial control of nuclear apoptosis. *The Journal of Experimental Medicine*, *183*(4), 1533–1544.

Zarate-Osorno, A., Roman, L. N., Kingma, D. W., Meneses-Garcia, A., & Jaffe, E. S. (1995). Hodgkin's disease in Mexico. Prevalence of Epstein-Barr virus sequences and correlations with histologic subtype. *Cancer*, *75*(6), 1360–1366.

Zhang, C. X., Decaussin, G., Daillie, J., & Ooka, T. (1988). Altered expression of two Epstein-Barr virus early genes localized in BamHI-A in nonproducer Raji cells. *Journal of Virology*, *62*(6), 1862–1869.

Zhang, J., Chen, H., Weinmaster, G., & Hayward, S. D. (2001). Epstein-Barr virus BamHI-A rightward transcript-encoded RPMS protein interacts with the CBF1-associated corepressor CIR to negatively regulate the activity of EBNA2 and NotchIC. *Journal of Virology*, *75*(6), 2946–2956.

Zhang, Q., Soderland, C., & Steinle, J. J. (2013). Regulation of retinal endothelial cell apoptosis through activation of the IGFBP-3 receptor. *Apoptosis : An International Journal on Programmed Cell Death*, *18*(3), 361–368.

Zhang, Y., Li, T., Fu, L., Yu, C., Li, Y., Xu, X., et al. (2004). Silencing SARS-CoV Spike protein expression in cultured cells by RNA interference. *FEBS Letters*, *560*(1-3), 141–146.

Zhang, Y., Ohyashiki, J. H., Takaku, T., Shimizu, N., & Ohyashiki, K. (2006). Transcriptional profiling of Epstein–Barr virus (EBV) genes and host cellular genes in nasal NK/T-cell lymphoma and chronic active EBV infection. *British Journal of Cancer*, *94*(4), 599–608.

Zheng, H., Li, L. L., Hu, D. S., Deng, X. Y., & Cao, Y. (2007). Role of Epstein-Barr virus encoded latent membrane protein 1 in the carcinogenesis of nasopharyngeal carcinoma. *Cellular & Molecular Immunology*, *4*(3), 185–196.

Zimber-Strobl, U., Kempkes, B., Marschall, G., Zeidler, R., Van Kooten, C., Banchereau, J., et al. (1996). Epstein-Barr virus latent membrane protein (LMP1) is not sufficient to maintain proliferation of B cells but both it and activated CD40 can prolong their survival. *The EMBO Journal*, *15*(24), 7070–7078.

Zimmermann, K. C., & Green, D. R. (2001). How cells die: apoptosis pathways. *The Journal of Allergy and Clinical Immunology*, *108*(4 Suppl), S99–103.

Zur Hausen, A., Brink, A. A. T. P., Craanen, M. E., Middeldorp, J. M., Meijer, C. J. L. M., & Brule, A. J. C. van den. (2000). Unique transcription pattern of Epstein-Barr virus (EBV) in EBV-carrying gastric adenocarcinomas: expression of the transforming BARF1 gene. *Cancer Research*, *60*(10), 2745–2748.